THE DESIGN OF A LAUNCH AND RECOVERY VEHICLE FOR AUVS (LARVA)

by
© Peter Seifert, B.Eng.

A thesis submitted to the School of Graduate Studies

in partial fulfillment of the requirements for the degree of

Master of Engineering

Faculty of Engineering and Applied Science

Memorial University of Newfoundland

02 June 2022

St. John's Newfoundland and Labrador Canada

Abstract

The engineering problem presented in this paper is the design of LARVA, a new launch and recovery vessel for the *Memorial Explorer* AUV. The solution detailed in this report is one which is modelled after a heavy lift vessel. It is a 19ft long, unmanned vessel and is capable of launching or recovering the AUV by ballasting itself to a 3.7ft draft and raising itself back up. The innovative aspects of this design is that it was designed to be used with a readily available boat trailer for launch and recovery with a slipway. The concept solution was analyzed using hydrostatics analysis software to assess its stability and to aid in the process of positioning and sizing the ballast tanks. A motion tracking system was used during model testing to assess its seakeeping ability in offshore waves and an analysis of variance test (ANOVA) was conducted to: capture the dependency between the input parameters, reduce the number of runs required, and to generate a response surface characterizing the heaving motions.

Acknowledgement

I would like to thank my thesis advisor Dr. Dan Walker of the Faculty of Engineering and Applied Sciences at Memorial University of Newfoundland for his guidance, patience, and understanding throughout my degree. Dr. Walker's door was always open whenever I needed help and always took the time out of his day to make sure I had a clear understanding of what I needed to do and how to do it. He also gave up his own personal time to help build the model that was used for model testing, for which I am very grateful for.

Table of Contents

List of Tables

List of Figures

List of Symbols, Nomenclature, or Abbreviations

ANOVA – Analysis of Variance

AUV – Autonomous Underwater Vehicle

COB – Center of Buoyancy

COG – Center of Gravity

DOF – Degrees of Freedom

EPS – Extruded Polystyrene

GUI – Graphical User Interface

IR – Infrared Red

LARVA – Launch and Recovery Vehicle for AUVs

LCG – Longitudinal Center of Gravity

MOCAP – Motion Capture

MUN – Memorial University of Newfoundland

QNS - Qualitative Navigation System

ROV – Remotely Operated Vehicle

VCG – Vertical Center of Gravity

° – Degrees

ft – feet

θ – Angle of rotation about the y-axis [degrees]

ϕ – Angle of rotation about the x-axis [degrees]

ψ – Angle of rotation about the z-axis [degrees]

List of Appendicies

1. Introduction

1.1. REALM Project and MUN Explorer

The ocean covers over 70% of the earth's surface and has a large impact on land-based ecosystems; for instance, the seafloor and large groups of organisms living in hydrothermal vent areas produce a substantial amount of carbon dioxide [1]. Given the impact of CO_2 has on climate change, it is vital for us to understand such significant sources of the gas. Yet, even though the ocean and its inhabitants play a vital role for Earth, we have not been able to explore the full depths of the ocean and its resources.

Through the use of underwater robots, it is possible to gain a better understanding of how to utilize the ocean's resources efficiently for human welfare. To date, this has typically been done through the use of Remotely Operated Vehicles (ROVs) which are tethered and require a human operator. Recently, technological advances have led to the development of Autonomous Underwater Vehicles (AUVs) which operate autonomously giving rise to a few advantages such mobility and (generally) a greater operating depth at the cost of limited mission time.

AUVs are playing a crucial role in exploring the resources located in deep ocean environments. They are employed for the use of oceanographic observations, bathymetric surveys, ocean floor analysis, military applications, or the location and recovery of lost man-made objects [2].

`

Figure 1.1 depicts the *Memorial Explorer* AUV being developed at Memorial University of Newfoundland. Its payload consists of an R2Sonic 2024 multibeam sensor and an Edgetech 2200-M combined system featuring a 100/400 kHz side-scan sonar system and a 1-6 kHz sub-bottom profiler. The AUV utilizes a Qualitative Navigation System (QNS) which allows localization and path following along a trained route without the necessity of a globally referenced position estimate [3].

Figure 1.1: *Memorial Explorer* AUV [4].

1.2. Need identification

Because the *Memorial Explorer* is a large AUV, it cannot be launched or recovered easily. The method of launch and recovery used by the REALM project involves the use of a boom truck. This is problematic because the cost of hiring a boom truck is roughly $1000 per day, and cost close to $20,000 in 2013. However, the high cost of launch and recovery is not the only problem encountered with the large AUV. In most rural areas, the marine infrastructure is inadequate to handle high loads on the wharfs. Because of the need for a boom truck to perform launch and recovery from shore, the possible locations for surveying are greatly restricted.

For ship-based operations, launching and recovering the AUV is much more complicated. The method of launching and recovering an AUV off a ship normally includes the use of a commercial system. A launch and recovery system that will work with an AUV of equivalent size of the *Memorial Explorer* will cost roughly $650,000. These systems also have a freeboard restriction of about 2-3 meters which places a restriction on the ship that can be used with these commercial systems. Another problem with these systems is that for large AUVs, the systems are placed near the stern of the ship where there is a much greater chance of damaging or completely destroying the AUV with the ship's propeller.

Finally, AUVs cannot determine their GPS co-ordinates while submerged due to the inability of the signal to penetrate water. This is problematic for a number of reasons:

- It is difficult to track the AUV while underwater;
- Any points of interest mapped (such as underwater installations, marine habitats, or undocumented shipwrecks) will not have GPS locations associated with them; and

- Should the AUV suffer a navigation system failure underwater, it will not be able to signal its location when it surfaces.

Therefore, it is clear that the lack of localization and the launch and recovery of large AUVs from either a ship or shore is problematic. While there are current solutions to these problems, they present their own set of unique problems. As AUVs gain popularity for exploratory missions, military applications and other uses, a new method of launch and recovery as well as GPS tracking needs to be explored.

1.3. Research and Commercial Applications

A marine reserve is an important tool for promoting and conserving biodiversity. The establishment of a network of marine reserves will be essential for conservation and fisheries management. Therefore, marine habitat mapping is essential to establish individual marine reserves. Furthermore, these maps can be used to estimate important resources within the protected area, which can lead to models and predictions of marine life distribution and abundances in different areas [5]. However, in order to achieve the necessary resolution, an AUV or ROV is needed to get close to the seabed. Not only does the AUV or ROV need to get high resolution data, it also needs to maintain an accurate record of its position for post-processing of the data.

The search for hydrocarbons has led oil companies into increasingly deep water. Oil is now being produced from fields in 1000+ meters of depth. Traditional hydrographic surveying methods involve taking these surveys from a ship. The problem with this method is that the water column between the surface and seabed significantly reduces the resolution of the data. In deep water AUVs offer the ability to obtain high resolution hydrographic data. This application presents another need for an effective launch and recovery system.

2. Design Concept

2.1. Concept Solution

Based upon the requirements of the missions undertaken by the *Memorial Explorer* AUV, the solution to the launch & recovery and localization problems had to meet the following requirements. A launch and recovery system should:

- be capable to operate from shore in rural communities with minimal marine infrastructure;
- be able to operate on a a ship with minimal third-party equipment;
- maintain an accurate position of the AUV while surveying;
- be able to operate in the same conditions as the AUV;
- remain stable for all conditions during all operations.
- be designed for ease of construction using readily available technology; and,
- remain structurally sound for all conditions of operation.

2.2. Design Drivers

Two of the main factors behind the design of the vessel were the ability to launch and recover the AUV from the vessel and being able to use existing marine infrastructure in rural communities or existing equipment onboard ships to launch and recover the LARVA.

For shore-based launching sites, the idea was to use existing slipways in local marinas and if the LARVA could be designed to use existing boat trailers, the LARVA could be launched with ease using these slipways. Additionally, the LARVA could be transported easily via trucks to and from the site. Therefore, the overall dimensions and hull shape of the LARVA was chosen to loosely conform to that of a boat which would fit on a commercially available trailer.

For ship-based launching and recovering, the idea was to use existing fast-rescue craft davits to lower and raise the vessel (with the AUV already loaded onto the LARVA). The advantage of this is that ships do not need to be retrofitted with another launch and recovery system.

2.3. Scope of Design

Due to time and budget constraints, the scope of this project has been limited to proving the concept design and determining its feasibility. This project focuses on the design of the LARVA and does not focus on the methods of launching the vessel since it was designed to utilize existing equipment. This project does not deal with the details of recovering the AUV such as lining up the AUV with the LARVA or the process in which the AUV mates with it. Additionally, due to limited time in the tow tank, only two operating conditions could be chosen. This is further discussed in Section 5.

The focus of this project is on the design of the hull and superstructure, ballasting design, hydrostatics, and seakeeping abilities. Once the concept design has been proven, then future work can be done to optimize the design in areas such as hydrodynamics, structural components of the vessel, and autonomizing the recovery process of the AUV.

3. Designing the LARVA

3.1. Hull Design

Since the main purpose of the LARVA is to launch and recover the AUV, the process by which this happens was the main driving factor behind the design. The hull was designed to be long, wide, and open to accommodate the AUV, with an open transom to allow the AUV to enter and exit the LARVA. Additionally, the LARVA was designed with no over-head obstacles so in the event the LARVA suffers a failure while carrying the AUV, the AUV would not be trapped in the LARVA and would float under its own buoyancy to be recovered via other means. Finally, since the LARVA does not have any means of self-propulsion in the initial design, it will be towed.

Since the LARVA will be utilizing existing boat trailers, the shape of the hull had to resemble that of a conventional small boat that would normally be launched using such a trailer. Additionally, since the LARVA will be towed using a vehicle along public roadways, the beam could not exceed eight feet to avoid it being designated as an oversized load. Based upon the requirements outlined, a planing hull shape with relatively flat bottoms and a hard chine was chosen. While this would increase the drag at non-planing speeds, the advantages of this hull shape in regards to it being large, open, lightweight, easy buildablity, and an availability of commercial trailers outweigh the disadvantage of increased drag.

As stated in the scope of design (Section 2.3), the main purpose of this experiment is to provide proof of concept by analyzing the seakeeping abilities of the concept. As there was no plan to assess other aspects of the hull performance, a simplified hullform could be used. Therefore, the LARVA was designed using “developable” surfaces (i.e. surfaces with curvature in one direction for ease of building). For the purpose of the experiments, the model was designed based upon a full-scale prototype manufactured using 3/16” 6061 aluminum.

Figure 3.1 shows the hull design and Table 3.1 contains the particulars for the LARVA. The three states referred to in Table 3.1 refer to the three states of operation: operating without the AUV (State 1 or following state) , launching the AUV (State 2 or launching state), and in transit with the AUV (State 3 or in transit state).

Table 3.1: LARVA particulars.

Length [m]	5.91
Breath [m]	2.26
Draft (State 1) [m]	0.31
Displacement (State 1) [MT]	1.11
Draft (State 2) [m]	1.17
Displacement (State 2) [MT]	3.82
Draft (State 3) [m]	0.47
Displacement (State 3) [MT]	1.80

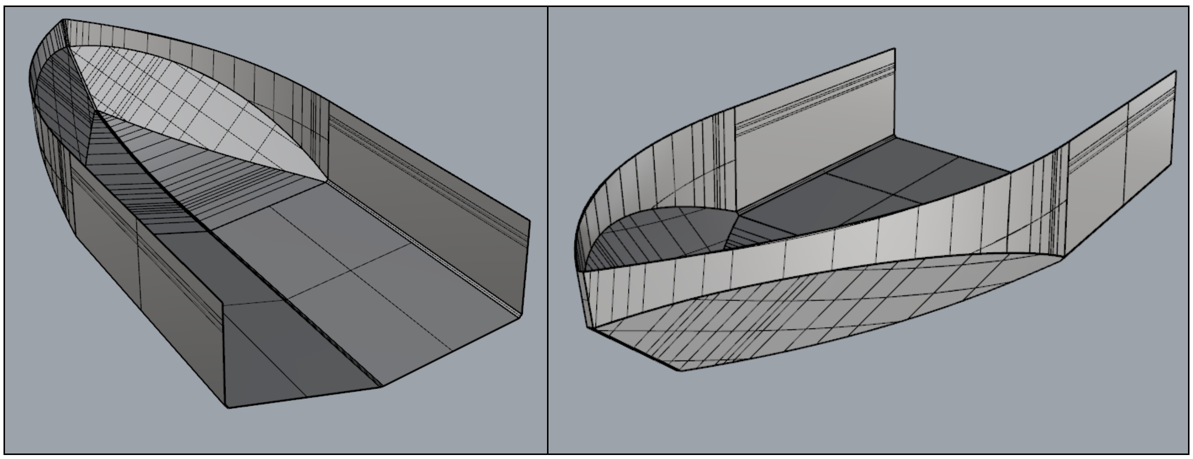

Figure 3.1: Hull design showing open transom, “developable” surfaces, and planing hull form.

3.2. Ballast Tanks Design

3.2.1. Ballasting target goals, placement, and sizing & design considerations

The LARVA must be able to support the full dry weight of the AUV which is 686 kg. As the LARVA must submerge to launch and recover the AUV and fully surface to transport the vehicle, it must have a large capacity to ballast and deballast. Due to the small, compact nature of the LARVA and the requirement for no overhead obstacles, the most suitable place for such a ballast tank was underneath the deck. Figure 3.2 shows a sectioned view of the LARVA, highlighting the locations of each individual floodable ballast tank. The deck and hull were designed to be watertight to act as a ballast tank. This tank is the largest tank and thus is the main source of buoyancy. In order to ballast itself down to launching draft, the LARVA required additional floodable ballast and therefore tanks were placed at both the bow and the stern.

The two primary design drivers behind the placement, size, and shape of the ballast tanks were 1) to provide adequate stability for the LARVA in all conditions and 2) to provide enough ballast capacity to increase the draft to launch the AUV. Since the tanks would be ballasted with water, free surface effects could negatively affect the stability. To minimize or eliminate the free surface effect, the tanks were designed to operate either empty or pressed full. In any case where the tank could not be designed to be either completely empty or pressed (i.e. only a portion of the tank is flooded), foam would be used to fill the rest of the tank. This ensured there was no free surface effect generated from the ballast tank and mitigates the consequence of uncontrolled flooding of all ballast tanks.

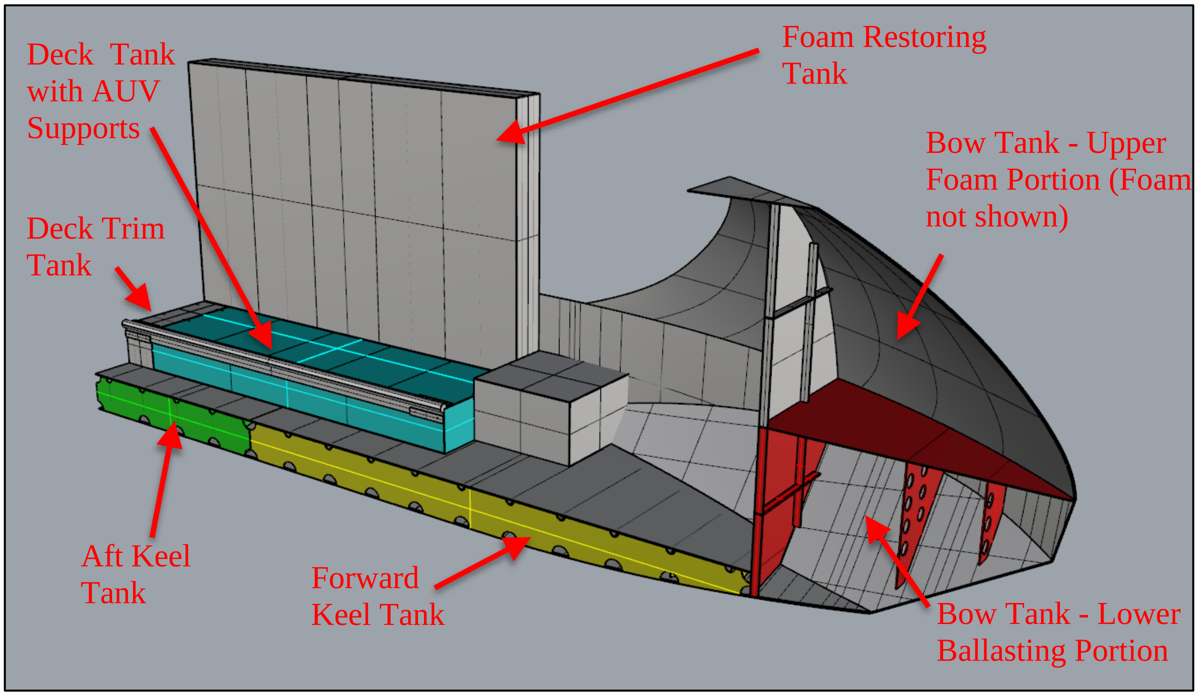

Figure 3.2: Sectioned view showing the location of all floodable ballast tanks. Each colored portion represents a single floodable ballast tank.

3.2.2. Bow tank

The bow of the vessel is designed with two sections, an upper section filled with foam, and a lower one which is the floodable ballast tank. The upper foam part is designed to provide additional buoyancy and stability for the vessel at launching draft. The lower part (the ballast tank) is designed to be floodable. Structural members designed using aluminum ¼” 6061 are added to the bulkhead for reinforcement as well as having transverse framing inside the bulkhead. The transverse frames are positioned to provide structural reinforcement to the outer hull and to the top plate of the tank. The frames are aluminum 6061 and 3/16” thick with lightening holes of 2.5” in diameter. In addition to the lightening holes, a small portion of the bottom of the frames are removed to allow the ballast water to flow freely to the lowest part where the ballast pump would be positioned.

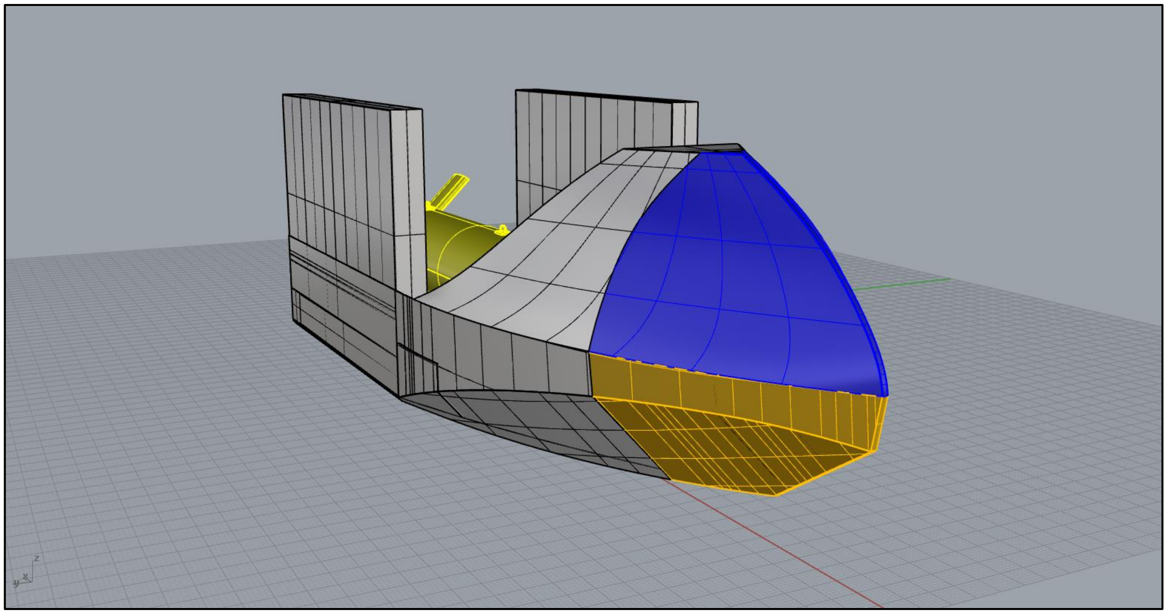

Figure 3.3: View of the bow showing the upper foam portion and the lower ballasting portion. The blue portion is the foam section and the gold portion is the ballast tank portion.

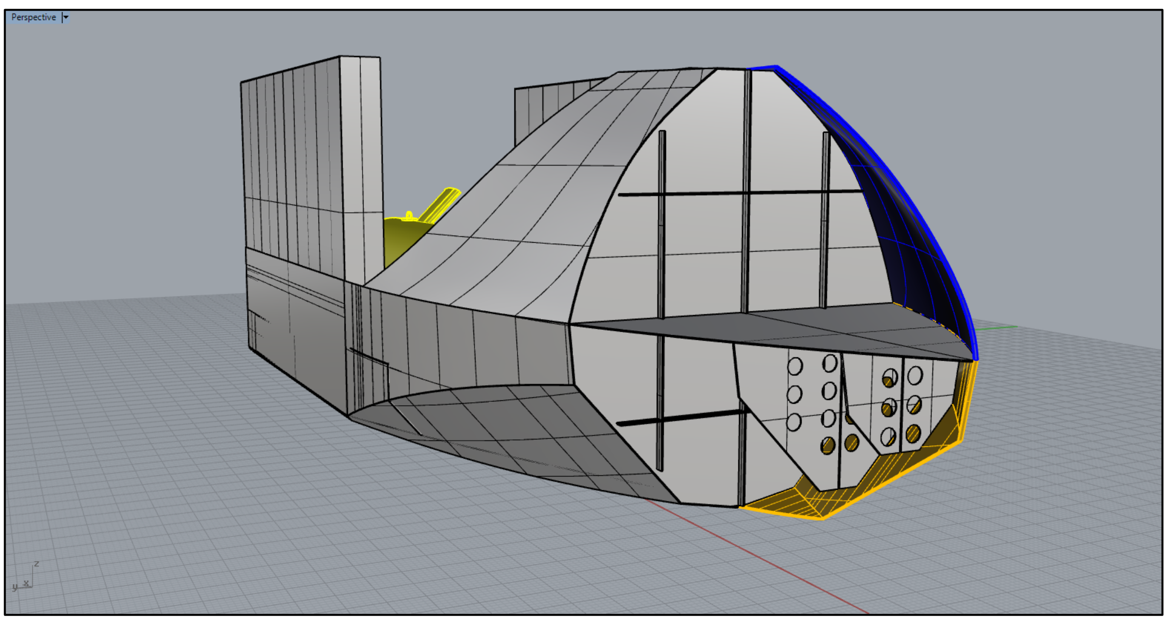

Figure 3.4: View with side shell removed showing structural members along the bulkhead and transverse framing within the lower ballasting portion.

3.2.3. Deck tanks and foam restoring tanks

The deck tanks act as both ballast tanks and support rails for the AUV. They are positioned at the stern, extend towards midship, and are positioned on either side of the centerline. Figure 3.2 shows the deck tanks with AUV supports and the foam restoring tanks. They are designed using aluminum 6061 and are 3/16" thick with stiffeners placed along the top and sides of the tanks which are also aluminum 6061 and 3/16" thick. The frames are positioned for structural support for the AUV and for equipment or personnel walking on top of the tanks.

Since these tanks sit on the deck and will be fully submerged at launch draft, additional foam tanks are needed along the port and starboard sides to provide additional buoyancy and stability while in the launching state. These tanks are designed to be tall and with a small waterplane area to help mitigate wave induced motions. These tanks also have stiffeners of 3/16" aluminum 6061 inside of them for added structural support.

During the initial stability analyses, the trim of the vessel was excessive in all three operation conditions. To reduce the trim, a small foam tank is placed at the stern, just behind the deck tank and can be seen in Figure 3.2 and Figure 3.5.

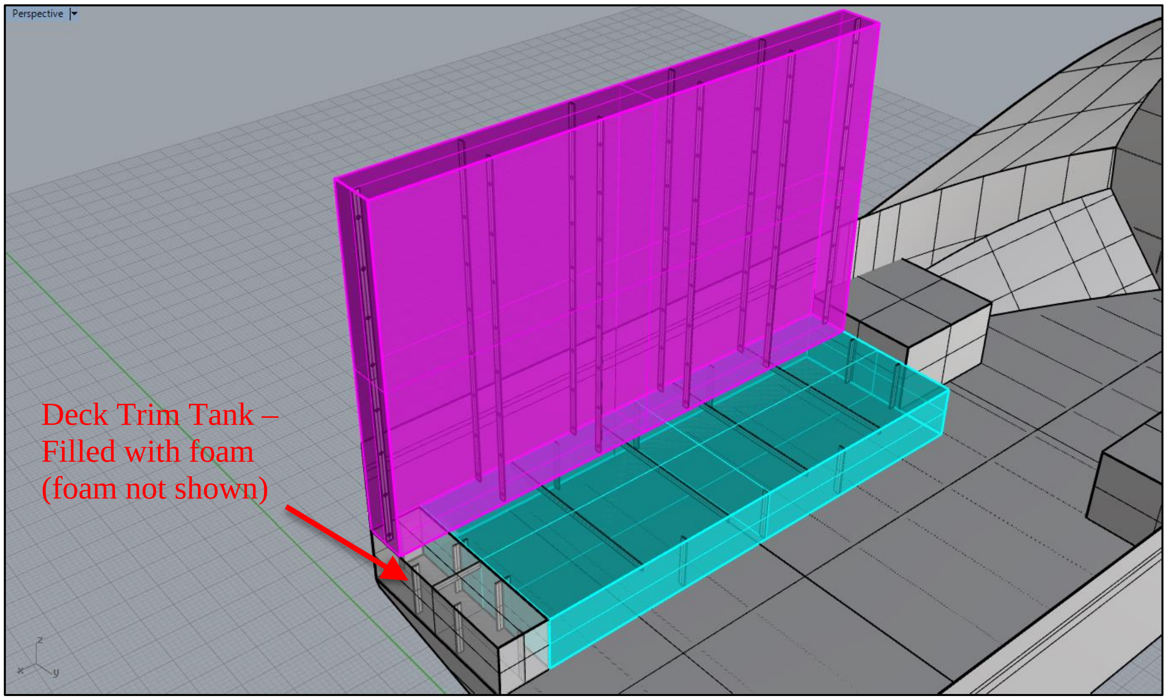

Figure 3.5: Stiffeners for the deck tank and foam tanks can be seen through the transparent shells of the tanks.

3.2.4. Keel Tank

The keel tank is divided into two sections, forward and aft (highlighted yellow and green respectively in Figure 3.2 and Figure 3.6). The tank is separated for controlling the trim of the LARVA while ballasting. When the LARVA is being ballasted, either up or down, it is needs to be at level trim and heel. Where the undivided keel tank was so large, any initial trim would cause the incoming water to pool at one end of the tank due to the free surface, further increasing the trim. With the keel tank sectioned, the trim of the LARVA can be better controlled.

To support the weight of the AUV, frames are added in the keel tank to support the deck. The transverse framing for both forward and aft keel tanks are 3/16” aluminum 6061 and spaced 12” apart with a 1/4” thick central stringer running the length of each tank.

Another concern with the keel tank is the entrapment of water (or air) between the frames during the ballasting process. To alleviate this problem, 2” diameter holes are placed at the top and 3” holes placed at the bottom corners where the transverse frames meet the longitudinal stringer, as can be seen in Figure 3.7.

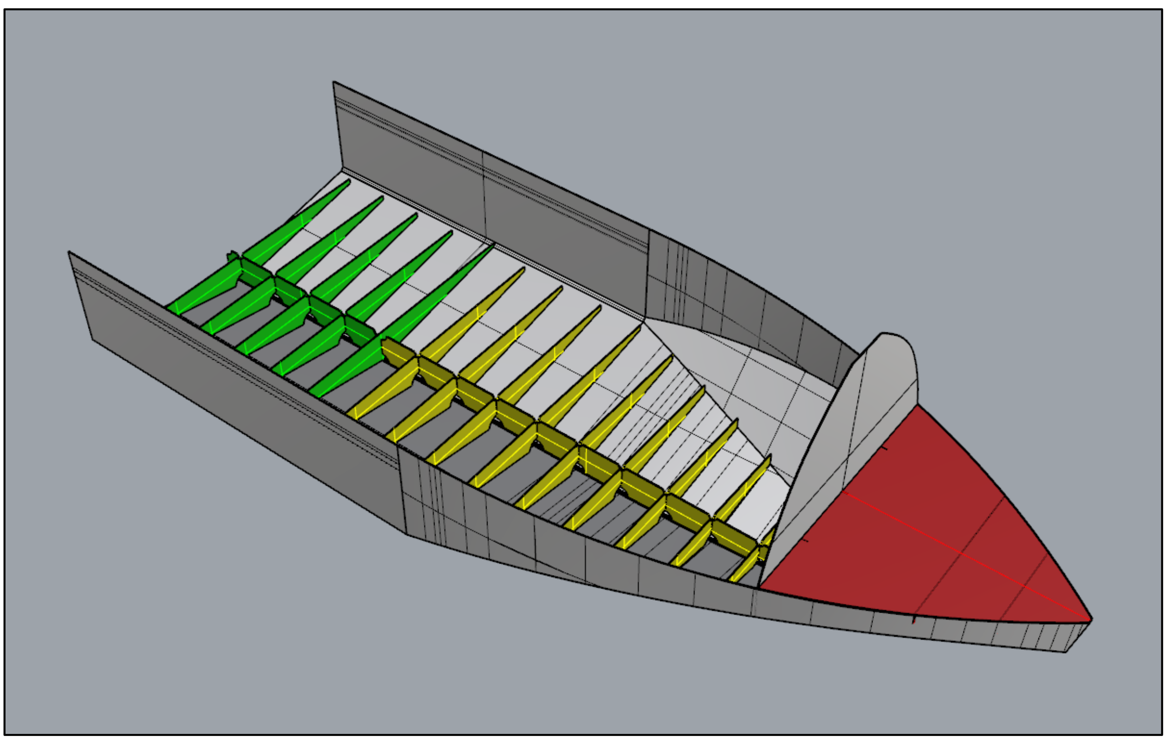

Figure 3.6: Keel tank divided into two sections. 3/16” thick aluminum 6061 transverse frames spaced 12” apart with a 1/4” thick central girder along the keel tank.

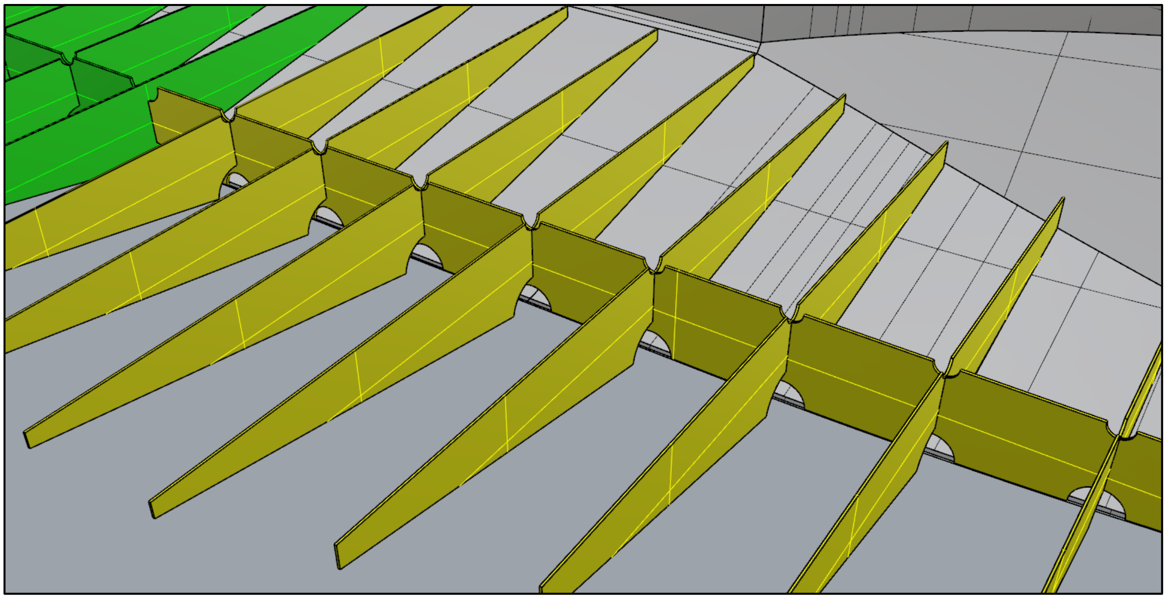

Figure 3.7: Holes placed at the transverse frame-central girder junctions to prevent entrapment of water or air during ballasting.

3.3. GHS Analysis

The hydrostatics program GHS (General Hydrostatics Software) was used to determine the final size and positioning of the tanks. To assess the stability of the vessel, the analysis had to be run for three conditions: the loaded condition (LARVA with AUV); the launching condition (LARVA lowered to launch the AUV); and the unloaded condition (LARVA without AUV). When loaded, the AUV has a significant impact on the center of gravity of the LARVA, acting to raise the center of gravity which causes the vessel to become less stable. Compounding this, any free surfaces in the ballast tanks would also further reduce stability. To prevent this additional stability loss, the tanks were designed so that in either condition, the tanks would be either completely full or empty, thus eliminating the free surface effect. The GHS input file and full outputs for each of the conditions can be found in Appendix A: GHS Analysis.

3.3.1. Loaded Condition

Figure 3.8 shows the stability of the LARVA for up to 90° of heel for the loaded condition and indicates the metacentric height is 3.75ft (1.14m). For all angles, the righting arm is positive and therefore the vessel is stable for all heel angles. Figure 3.9 shows that in its equilibrium position, the full scale LARVA has a baseline draft of 1.55ft (0.47m), trimmed by the stern by 1.84°, and has an initial heel angle of 0°.

The GZ curve in Figure 3.8 shows the righting arm increase up to about 25° of heel, then slighty decrease from angles 25° to 50°, then increase again until 72°, then decrease sharply. This is due to the shapes and locations of the tanks. As it heels to starboard, it picks up buoyancy from the tank on the deck and also loses buoyancy from the keel tank on the port side. This causes the CoB to translate to the starboard side rapidly. As it hits the angle of maximum stability, this is where the tank on the deck becomes fully submerged.

As it keeps heeling to starboard, the CoB is being rotated towards the CoG slightly faster than it is moving away due to tall, thin foam restoring tank on the starboard side. Since the CoB is moving towards the CoG slightly faster than it is moving away, the righting arm is slightly decreasing. As it hits the trough (50°) the tall starboard tank is now horizontal enough to start making the CoB move away from the CoG faster than it is being rotated towards it due to the heel. Thus the secondary increase in GZ from 50° to 72°.

The ballast tank(s) that generate the largest free-surface moment on the LARVA are the Deck tanks. The Free-surface Moment generated is 7.1 LT-ft (2.2 MT-m), and with a displacement of 3.76LT (3.82MT), the reduction in GM is 1.89ft (0.58m). Therefore, the resulting GM with the largest reduction due to free surface effect is 1.86ft (0.57m). While this was only calculated for a single tank, the ballasting operation would be such that only one tank would be slack at a time to minimize the effect of free-surface on stability.

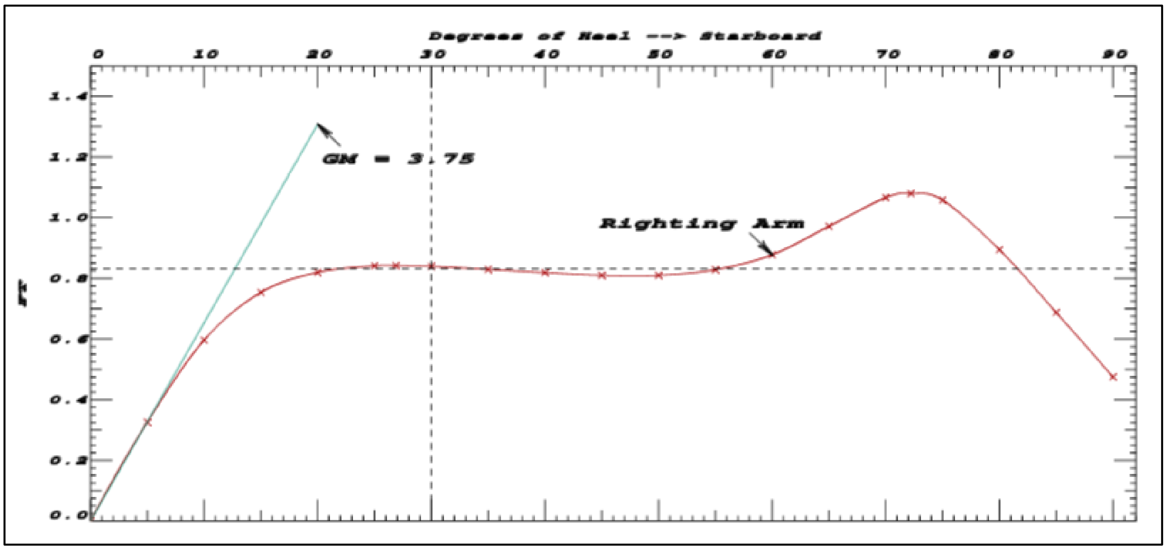

Figure 3.8: GHS righting arm diagram in the loaded condition.

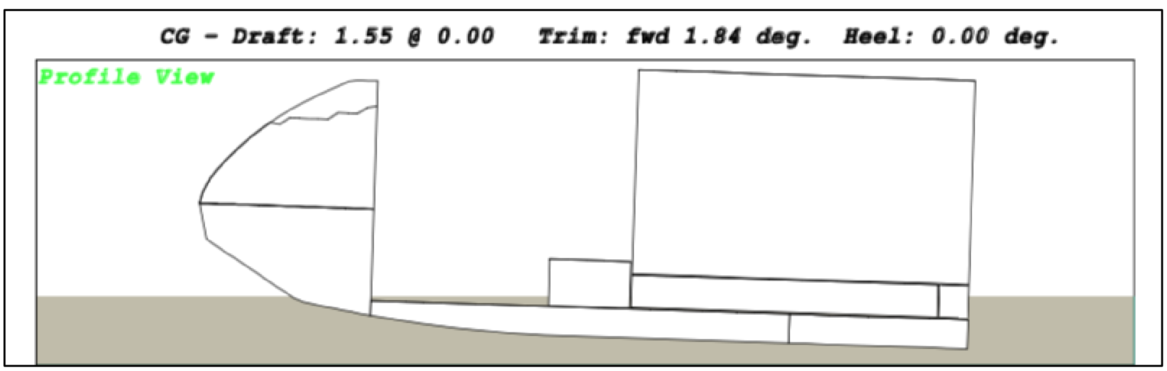

Figure 3.9: Profile view of the LARVA from GHS in the loaded condition.

3.3.2. Launching Condition

Figure 3.10 shows the stability of the LARVA for up to 90° of heel for the launching condition and shows a metacentric height of 1.11ft (0.34m). For all angles, the righting arm is positive and therefore the vessel is stable for all heel angles. Figure 3.11 shows that in its equilibrium position, the full scale LARVA has a baseline draft of 3.83ft (1.17m), trimmed by the stern by 0.81°, and has an initial heel angle of 0°.

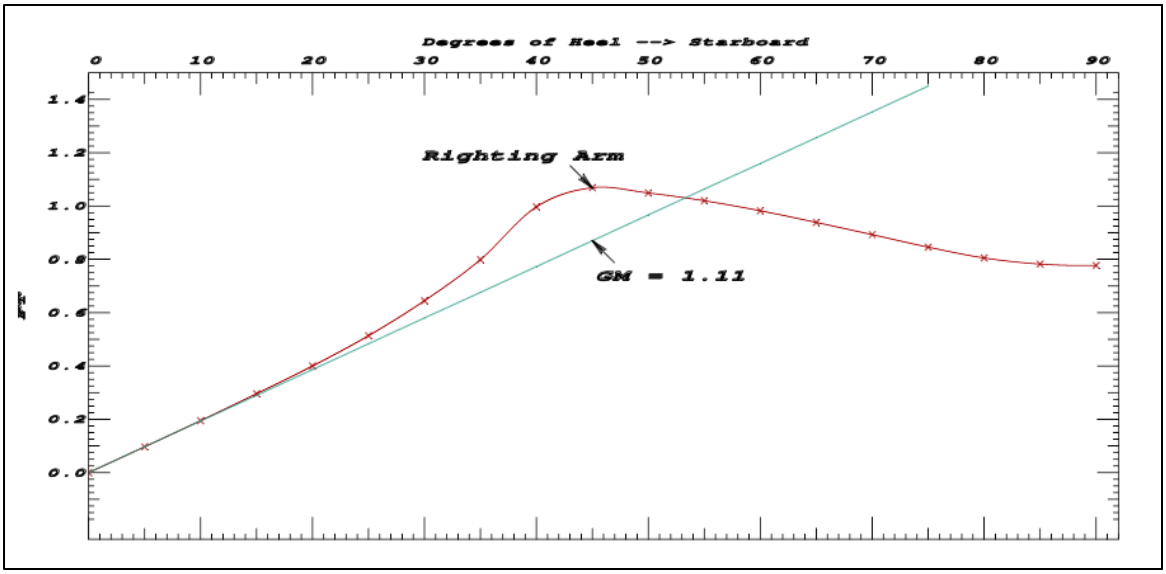

Figure 3.10: GHS righting arm diagram for the launching condition.

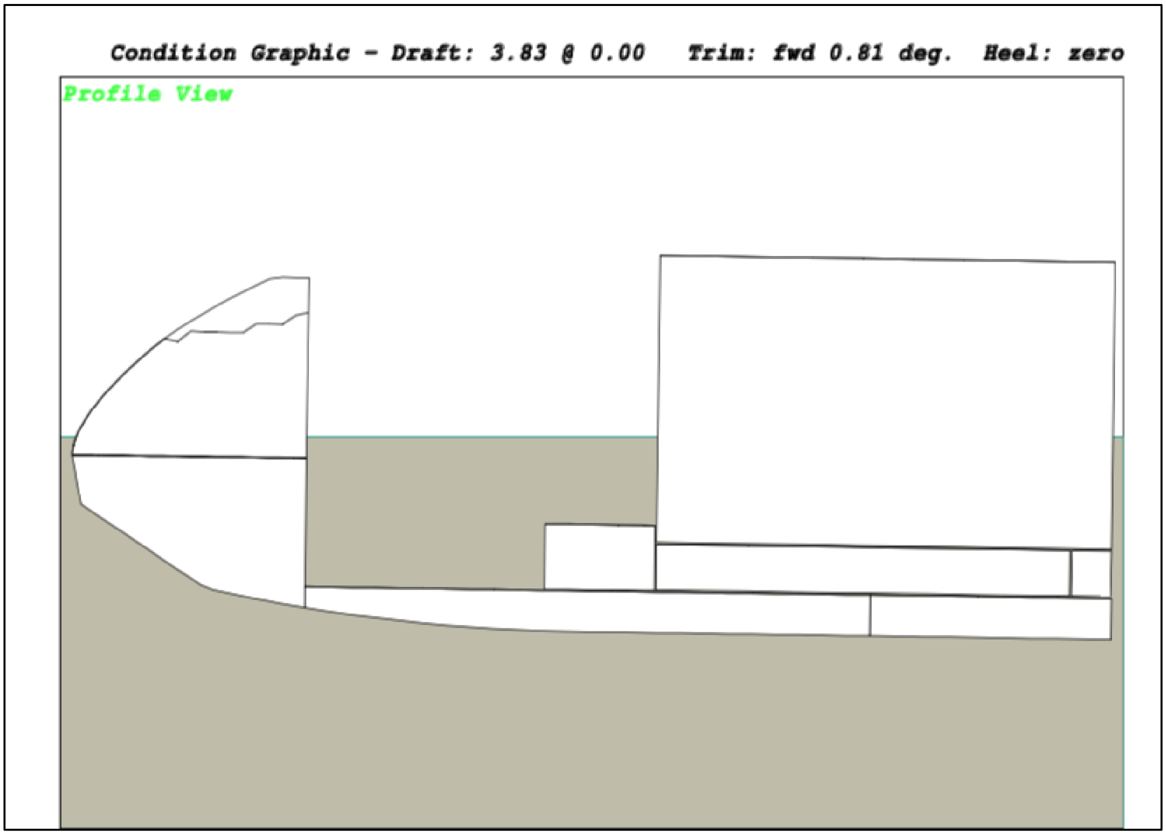

Figure 3.11: GHS profile view of the launching condition.

3.3.3. Unloaded Condition

Figure 3.12 shows the stability of the LARVA for up to 90° of heel for the unloaded condition and has a metacentric height of 4.97ft (1.51m). For all angles, the righting arm is positive and therefore the vessel is stable for all heel angles. Figure 3.13 shows that in its equilibrium position, the full scale LARVA has a baseline draft of 1.02ft (0.31m), trimmed aft by 0.62°, and has an initial heel angle of 0°.

Figure 3.12 exhibits the same secondary increase in the righting arm as shown in Figure 3.8 and shares a similar explanation even though it is more prominent in this condition.

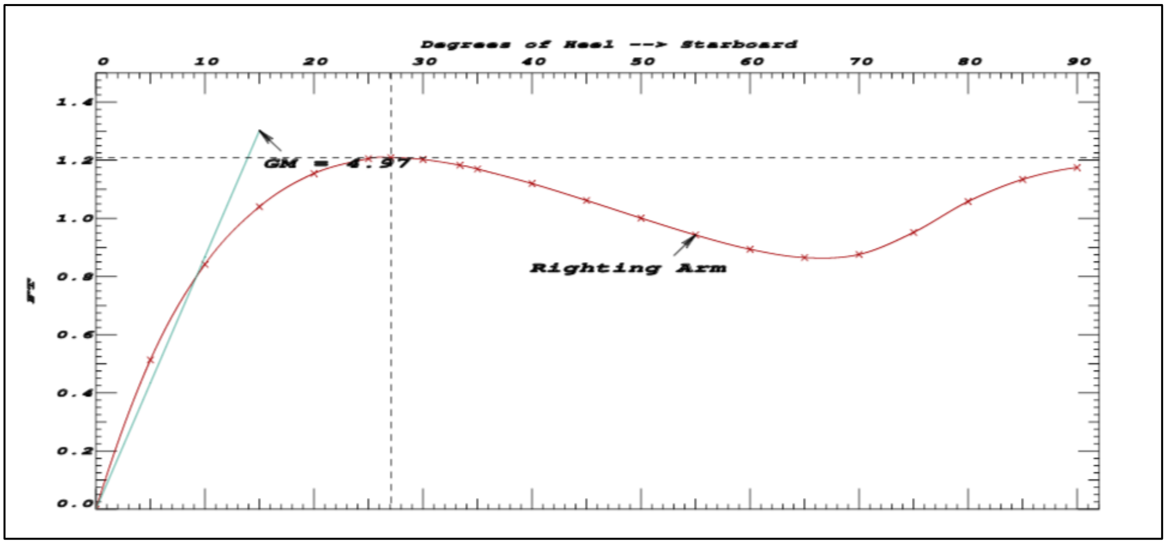

Figure 3.12: GHS righting arm diagram for the unloaded condition.

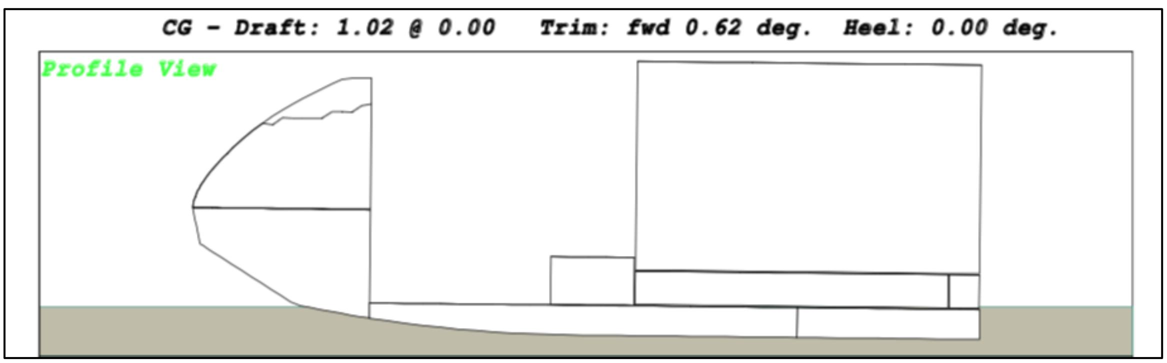

Figure 3.13: GHS profile view in the unloaded condition.

4. Experiments

4.1. The Model

To test the performance of the LARVA, an experimental program was developed for a 1:4 scale model. The model was constructed using 1/8" plywood, extruded polystyrene (EPS) foam, and glass reinforced epoxy. As stated in Section 3.1, the LARVA hullform was designed using developable plates. However, since the objective of these experiments was to assess seakeeping properties and not hydrodynamic performance, the hull curvature could be approximated as flat plates to simplify model construction. The model was constructed using flat plywood panels that were glued together using a hot glue gun. The exterior of the hull was sheathed with one layer of fibreglass cloth and the entire model coated with epoxy. The epoxy was used to both create a single skin of glass reinforced epoxy on the exterior of the hull and to seal exposed plywood to prevent it from absorbing water. Figure 4.1 shows the port side of the hull being assembled and Figure 4.2 shows the finished model floating in the trim tank.

Since all the ballast tanks were designed to be either fully pressed or empty, the two deck tanks and the bow tank were made completely out of foam which were removable. Having the foam in place would simulate the tanks completely empty and removing them simulates the tanks fully pressed. This approach eliminates the challenge of building tanks that are water tight. However the keel tank could not be simulated this way. When building the model, the keel tank was built watertight with no way to flood the tank to ballast the model. To flood the keel ballast tank, holes were drilled through the deck to allow water to enter once the tests in the dry condition were completed. This allowed the tests in the flooded condtion to be completed.

Figure 4.1: Port side of the hull being assembled. The black electrical tape was used to hold the plates in place while they are glued together.

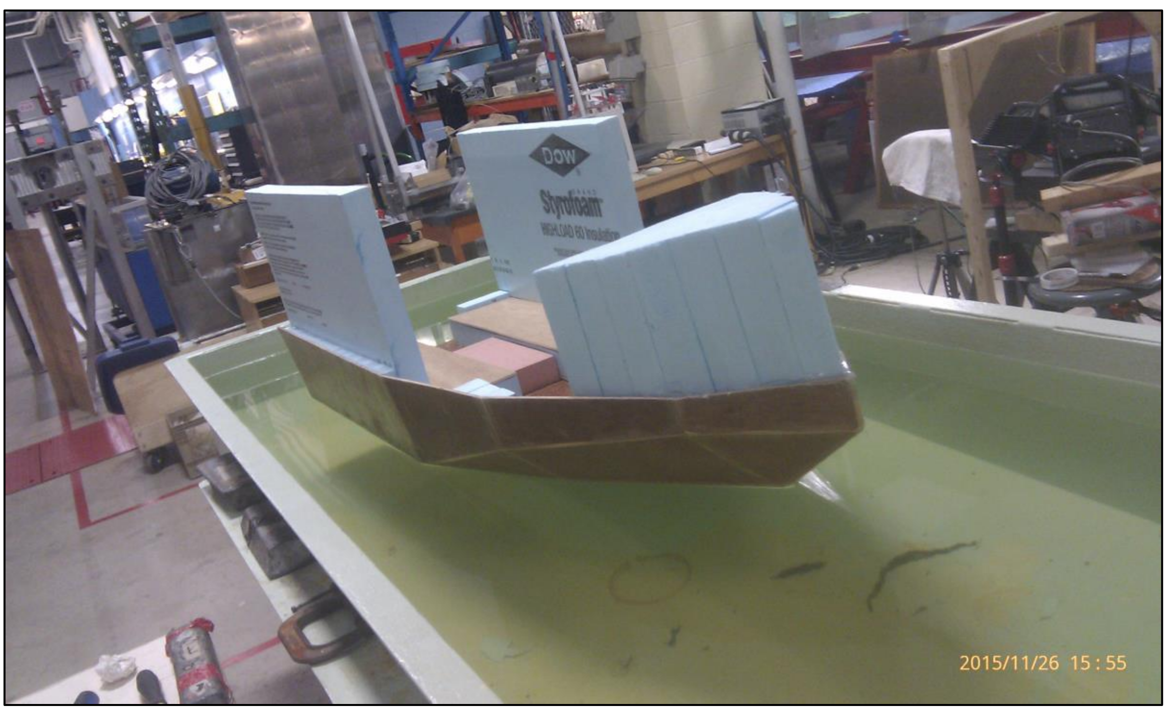

Figure 4.2: Finished model floating in the trim tank.

4.2. Ballasting

To properly ballast the scaled model, its mass properties had to be scaled appropriately from the full scale. Table 4.1 shows the mass properties for both the full scale vessel and the 1:4 scale model for the two conditions to be tested.

Table 4.1: Target mass properties for both full scale the and 1:4 scale vessels in the two conditions to be tested.

Launching					
Full Scale			Model Scale		
Weight	[MT]	3.82	Weight	[kg]	59.7
LCG	[m]	2.28	LCG	[cm]	57.1
VCG	[m]	0.48	VCG	[cm]	10.5
Draft	[m]	1.17	Draft	[cm]	26.6
Trim	[°]	0.81	Trim	[°]	0.81
I_M Pitch	[kg-m^2]	2778	I_M Pitch	[kg-m^2]	2.70
I_M Roll	[kg-m^2]	1160	I_M Roll	[kg-m^2]	1.13

Unloaded Condition					
Full Scale			Model Scale		
Weight	[MT]	1.34	Weight	[kg]	21.0
LCG	[m]	2.13	LCG	[cm]	53.3
VCG	[m]	0.66	VCG	[cm]	15.0
Draft	[m]	0.33	Draft	[cm]	6.9
Trim	[°]	1.42	Trim	[°]	1.42
I_M Pitch	[kg-m^2]	2778	I_M Pitch	[kg-m^2]	2.70
I_M Roll	[kg-m^2]	1160	I_M Roll	[kg-m^2]	1.13

To calculate the mass moment of inertia, a swing frame test was performed using the apparatus shown in Figure 4.3 along with the procedure and calculations outlined in [6] and [7]. Table 4.2 shows the target values, the obtained experimental values, and the error as a percentage of the target value. The results were considered acceptable if they were within +/- 10% of the target value. For the mass moment of inertias, the target values were very hard to accurately obtain since the calculations were very sensitive to the angle input, however, the errors obtained were only 10% for roll and 11% for pitch.

Table 4.2: Measured mass properties of the scale model in the unloaded condition.

		Measured values	Target values	Error [%]
Weight	[kg]	19.2	21.0	-9
LCG	[cm]	50.2	53.3	-6
Draft	[cm]	6.3	6.9	-9
VCG (from keel)	[cm]	15.0	15.0	0
I_{roll} [I about CG]	[kg-m^2]	1.0	1.1	-10
I_{pitch} [I about CG]	[kg-m^2]	2.4	2.7	-10

Figure 4.3: Swing frame used to calculate the vertical center of gravity and the mass moment of inertia in the roll (left) and pitch (right) configurations [7].

4.3. Experimentation Parameters and Setup

Vessel motion is affected by both the parameters of the vessel (hull shape and mass distribution) and the incident wave field (including height, frequency and wavelength). Wavelength can be correlated to wave frequency through the dispersion relationship. For deep water waves, the dispersion relationship is shown in Eq. [1] where λ is the wavelength in meters and f is the wave frequency in cycles per second.

$$\lambda = \frac{g}{2\pi f^2} \qquad [1]$$

As a result, only wave height and frequency need be considered as variables.

For any given loading condition, the vessel parameters, including hull form and mass distribution are also fixed.

Finally, other factors which could affect vessel motion include the incident wave angle and the vessel speed through the waves. Since the LARVA will be able to orient itself in any direction, only head seas (0° incident wave angle) were tested. Finally, since the LARVA will only launch while stationary, the factor of boat speed through waves was eliminated.

4.3.1. Metocean Conditions

To determine the experimental limits of the model testing, a study released by Nalcor Energy and C-CORE detailing meteorology and oceanography data for offshore Newfoundland, Canada was used. The study divides the offshore area of Newfoundland & Labrador into cells (Figure 4.4) and provides data for water depth, wind, waves, ocean currents, visibility, and ice for each cell. For the purpose of this experiment, cell #343 was selected for study, since it is close to shore where the LARVA is most likely to be used. Table 4.3 shows the significant wave height summary statistics for the cell, arranged by month. Since the *MUN Explorer* activity has normally been during summer months, the experimental limits will be chosen from between May and September. From

Table 4.3, the maximum wave height is 2.2 meters. Figure 4.5 shows a histogram of the peak spectral periods for cell #343. It can be seen that the majority of the wave periods are between 4 and 20 seconds, therefore this range will be the limits for the experiment.

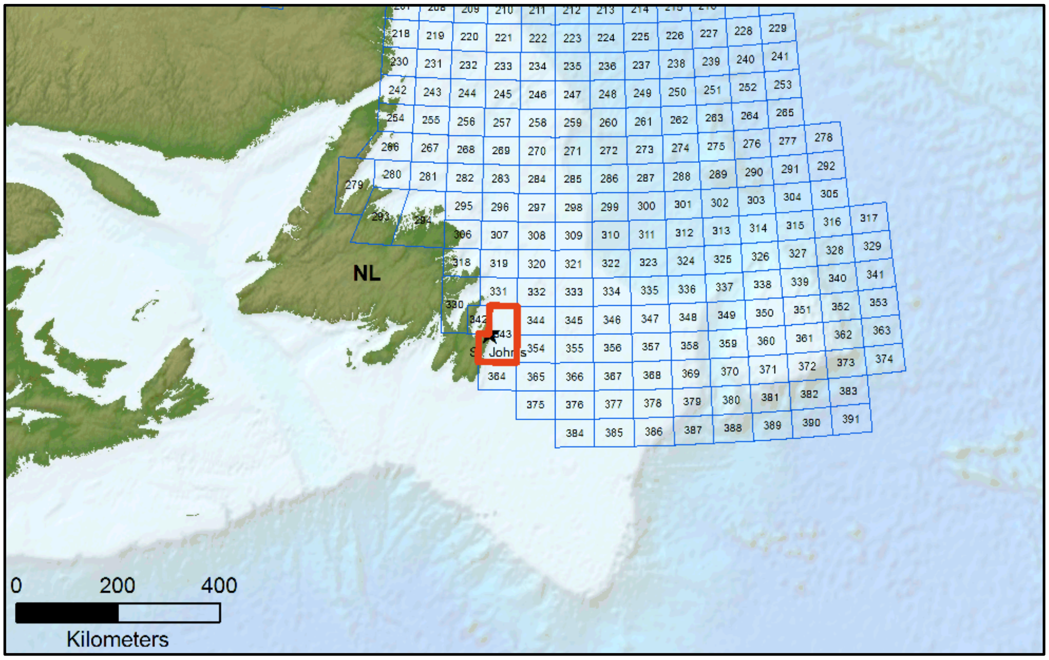

Figure 4.4: Location of Selected Region for Metocean Data [8].

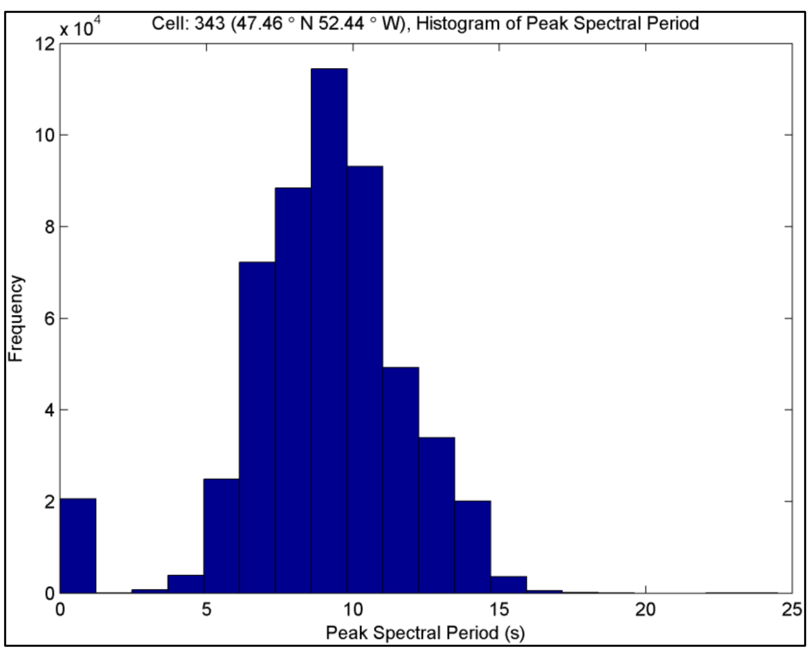

Figure 4.5: Histogram plot of Peak Spectral Period for cell #343 [8].

Table 4.3: Significant wave height summary statistics for cell #343 arranged by month [8].

Cell: 343 47.46°N 52.44°W		Summary Table - Wave												
		Jan	Feb	Mar	Apr	May	Jun	Jul	Aug	Sep	Oct	Nov	Dec	Annual
Sig. Wave Height (m)	Mean	3.3	2.7	2.2	2.4	2	1.8	1.6	1.7	2.2	2.7	3.1	3.5	2.4
	St. Dev.	1.6	1.8	1.6	1.2	0.9	0.7	0.6	0.7	0.9	1.1	1.2	1.3	1.3
	Median	3.2	2.7	2.2	2.3	1.9	1.6	1.5	1.5	2	2.5	2.8	3.3	2.2
	P90	5.2	4.8	4.3	3.9	3.1	2.6	2.3	2.5	3.3	4.1	4.6	5.3	4.1
	Max.	11.1	11.6	9.6	8.8	9.4	7.9	5.7	11.3	12.3	9.5	10.1	11.2	12.3
	Dom. Dir.	185	205	185	185	185	185	185	195	185	355	355	5	185

Since the experiments were conducted using a ¼ scale model of LARVA, wave data must be scaled as well. For wave heights and length, the scaling is directly proportional. However, for the wave period, time is scaled by the square root of the scaling factor, in accordance with Equation (4.2).

$$\begin{aligned} T_{Full} &= \sqrt{\lambda} \cdot T_{Model} \\ \sqrt{\lambda} \cdot f_{Full} &= f_{Model} \end{aligned} \tag{4.2}$$

Ideal experimental parameters are shown in Table 4.4. However, due to limitations of the experimental setup, the actual experimental parameters needed to be adjusted, since the maximum possible wave height that can be generated in the wave/towing tank is 0.3 m. The adjusted parameters are shown in Table 4.5.

Table 4.4: Ideal scaled experimental parameters.

	Wave Heights [m]		Wave Periods [s]	
Full Scale	0.5	2.2	20.0	4.0
Model Scale	0.13	0.55	10.0	2.0

Table 4.5: Adjusted experimental parameters to accommodate the experimental setup.

	Wave Heights [m]		Wave Periods [s]	
Full Scale	0.5	1.28	10.0	4.0
Model Scale	0.13	0.32	5.0	2.0

Since this is a two factor experiment, an analysis of variance (ANOVA) was conducted to capture the non-linearity and coupling of the wave height and frequency. Additionally, since there are limits imposed on the frequencies and wave heights which can be produced by the wave board in the tow tank, the best design would be an inscribed central-composite design. Table 4.6 shows the experimental conditions for each run generated using Design Expert 9 using an inscribed central-composite design and the parametres in Table 4.5. These are the parameters that were required and given to the techinican operating the wave tank.

Table 4.6: Experimental wave conditions for each run.

Run Number	Period [sec]	Height [mm]
1	0.46	291
2	0.35	223
3	0.24	291
4	0.35	125
5	0.50	223
6	0.35	320
7	0.46	154
8	0.20	223
9	0.24	291
10	0.35	320
11	0.46	154
12	0.35	223
13	0.46	291
14	0.35	223
15	0.24	154
16	0.35	223
17	0.35	125

18	0.35	223
19	0.24	154
20	0.20	223
21	0.5	223

4.3.2. Experimental Arrangement

The experimental arrangement used in the wave tank is shown in Figure 4.6. The system consisted of a wave probe to measure the incident wave height, a motion tracking system to track the vessel motion, and a soft mooring system to hold the model on station. The motion was tracked using the motion tracking system Qualisys, which uses infrared (IR) light reflected off markers covered in reflective tape that are located on the model. Three Qualisys tracking cameras triangulate the positions of the reflective markers and calculate the motion in real-time. In order to do so, a rigid body must be defined in the Qualisys tracking software. By defining a local coordinate system for the rigid-body, the motions are calculated with respect to that local origin. In the case of the LARVA model, this origin was chosen to be the center of gravity. If the system loses track of one of the reflective markers, the software cannot continue to calculate the motions of the model. Therefore, the model had to be kept in view of all three tracking cameras. To do this, a soft mooring system was employed, consisting of two soft springs at the bow and stern (shown in Figure 4.7), where springs with the lowest spring constant possible that would keep the model in the camera frame were used.

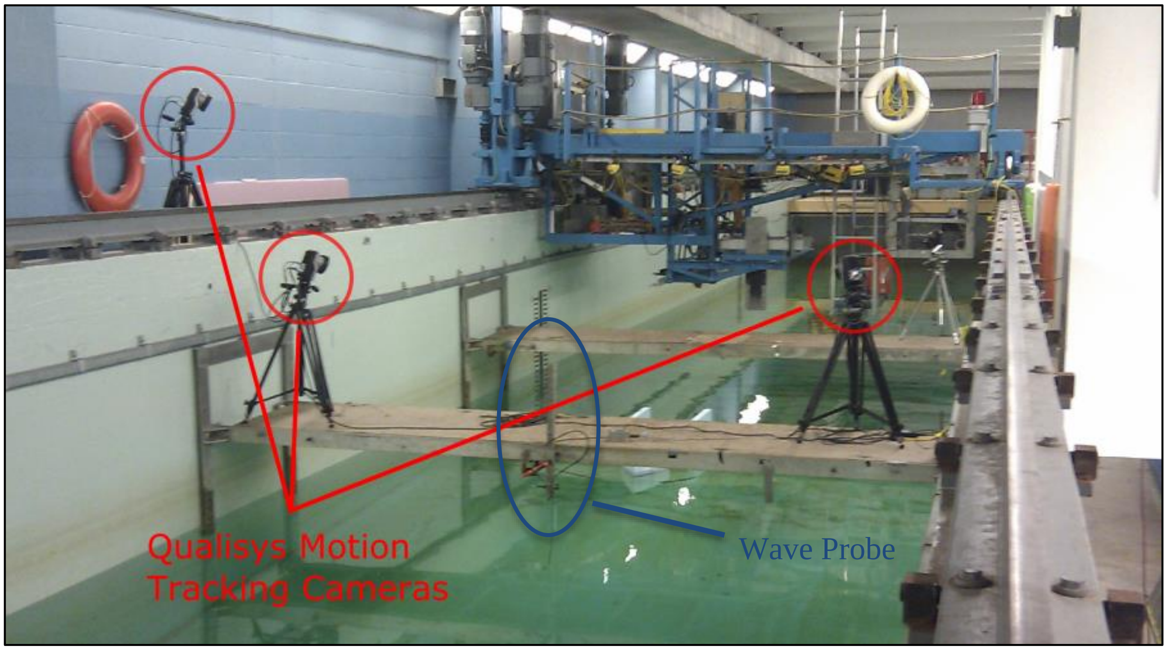

Figure 4.6: Location of the Qualisys motion tracking cameras during the experiment.

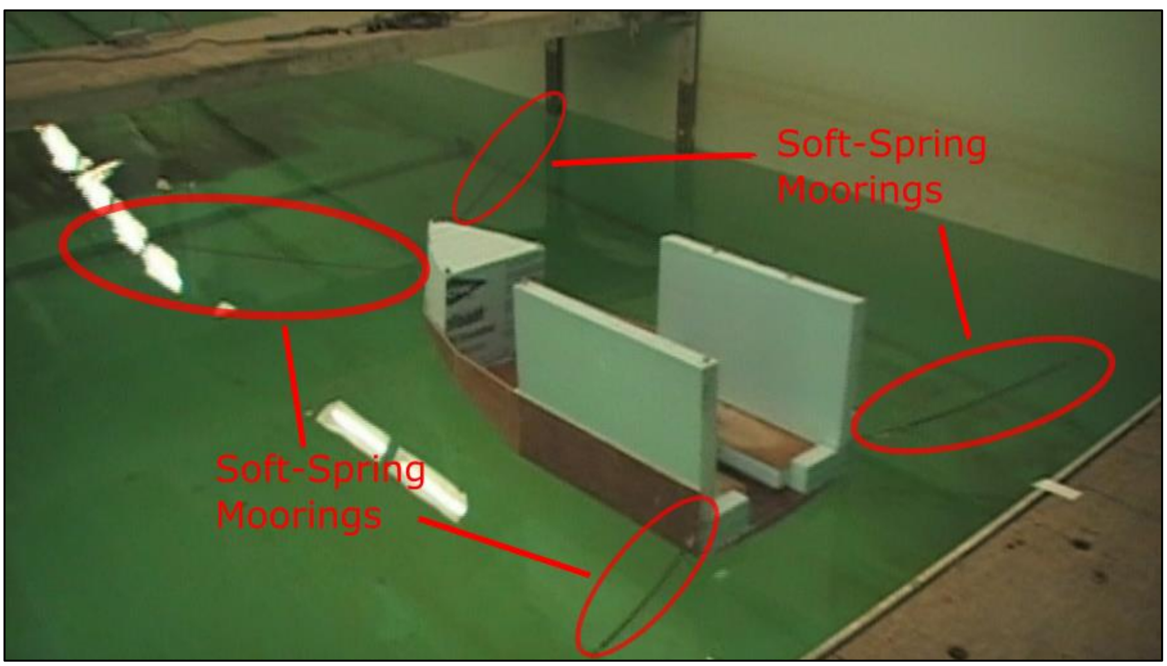

Figure 4.7: Soft-spring moorings used to keep the model within the Qualisys motion tracking camera frame.

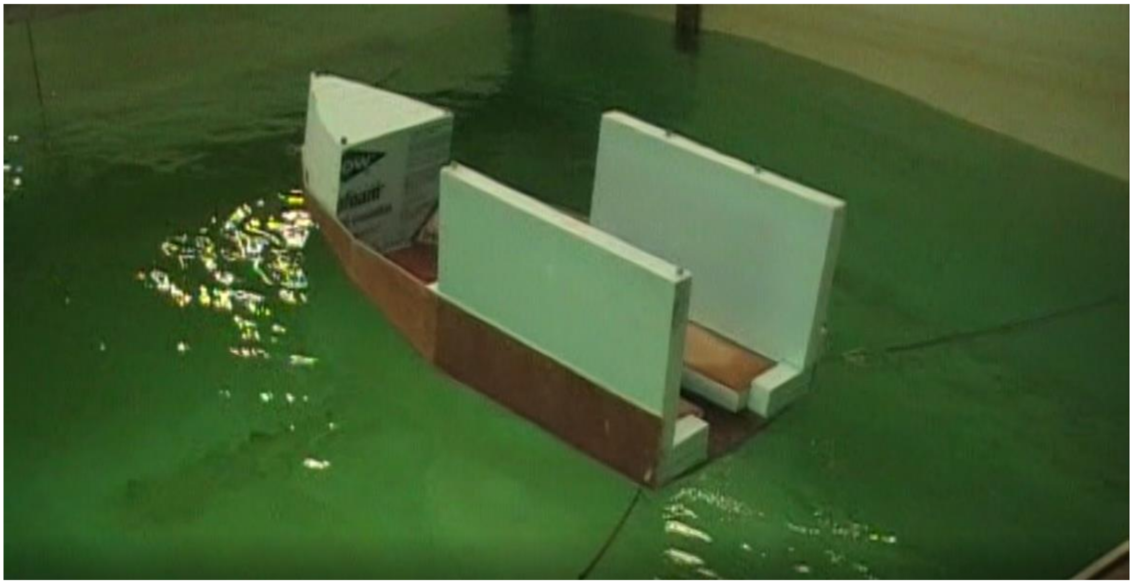

Figure 4.8: Run 5 with Larva in the Following State. Incoming wave set with a wave height of 204.02mm and a frequency of 0.507Hz.

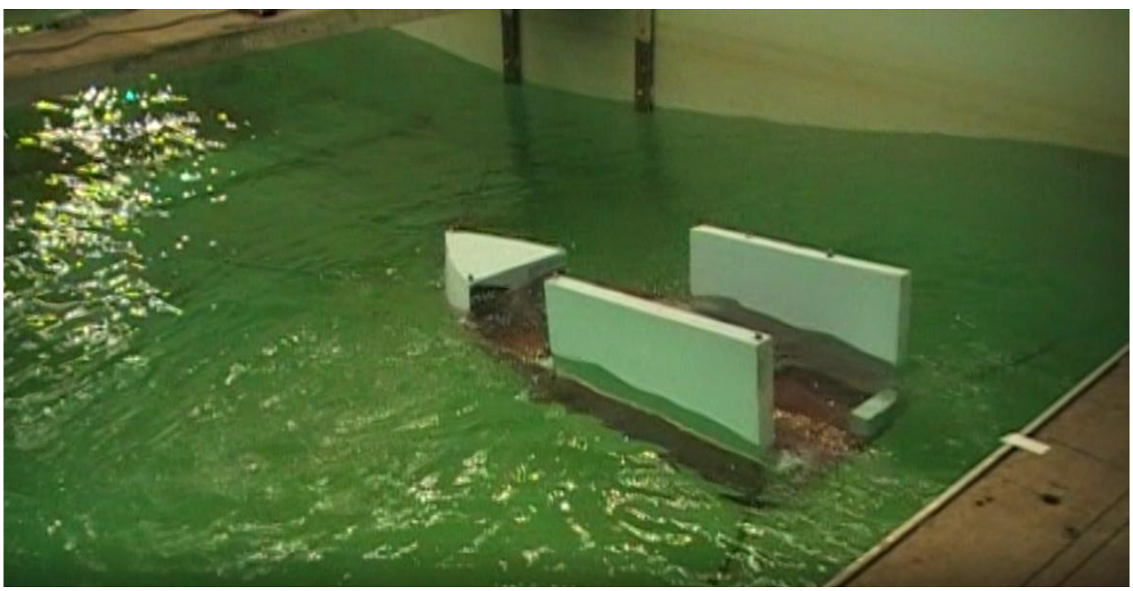

Figure 4.9: Run 13 with Larva in the Launching State. Incoming wave set with a wave height of 315.75mm and a frequency of 0.468Hz.

5. Analysis

The goal of the experimental program was to confirm that the LARVA has seakeeping characteristics appropriate for launching and recovering the *Memorial Explorer* AUV. From field observations, the *Memorial Explorer* has very little freeboard and waterplane, and is almost neutrally buoyant, which results in very small wave-induced motions. For large period waves, the *Memorial Explorer* essentially follows the surface of the wave. For short period waves, there is very little, if any, induced motion.

Since the experimental limits were set for waves with full scale wave periods between 4.0 and 10.0 seconds (2.0s to 5.0s at model scale), it was assumed, based on field observations that the motion of the *Memorial Explorer* in those conditions would be such to allow it to follow the surface. Therefore, the focus of the analysis is the rigid motion of the LARVA relative to the instantaneous wave height.

The aim and scope of this research is to provide proof-of-concept of a design for launch and recovery for the REALM project. From field observations the REALM project only required the AUV to be launched and recovered in port. Therefore it was determined that only the Launching condition was required to be analyzed in depth to ensure the wave-induced motion would not cause the LARVA to contact the AUV during launch and recovery. The Following condition was analyzed at a higher level for two reasons 1) to gain an understanding of the LARVAs seakeeping ability on its own, showing proof-of-concept for later iterations of the design, and 2) to ensure the LARVA could be maneovered easily to a wharf or mooring point without excessive wave-induced motion.

When the data was collected, the wave probe was positioned a distance ahead of the model. This resulted the data being out of phase when plotted in the time domain. To correct this, the videos of each experimental run were reviewed and the time it took the wave to reach the bow of the boat was recorded. For the transom, the phase velocity of the wave was calculated using Equation (5.1) and with a known distance from bow to transom, the time offset could be calculated. Figure 5.1 and Figure 5.2 shows the data for the same experimental trial before and after the time shift respectively.

$$c_p = \sqrt{\frac{g\lambda}{2\pi}\tanh\left(\frac{2\pi h}{\lambda}\right)} \tag{5.1}$$

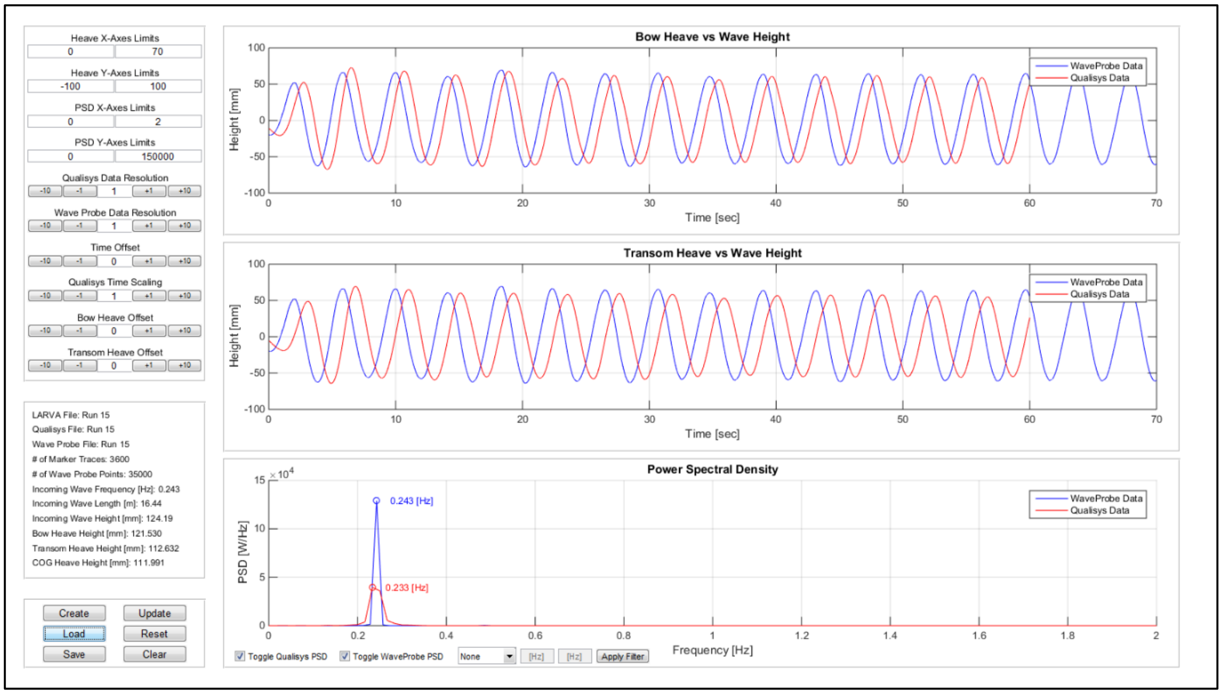

Figure 5.1: Data analysis for run 15 (0.243Hz and 124.19mm) showing the data being out of phase due to wave probe being ahead of the model.

5.1. Following Condition Analysis

For the following state, the focus of the experiments was to show that the motions of the LARVA are not so extreme such that the LARVA cannot follow the AUV. Since in this state the LARVA is just following the AUV, it is not as critical to analyze the relative heave motions since there is no danger of damaging the AUV due to excessive heaving. Therefore, there it was not necessary to conduct a full ANOVA for this condition, just confirm that the LARVA wave-induced motions were not significant.

For the first series of runs (LARVA in the following state, carrying no payload), the data showed that the LARVA response was very similar to the incoming wave. Figure 5.2, Figure 5.3, and Figure 5.4 show the LARVA response to incoming waves that have a short, medium, and long wave length and frequency respectively. The Bow Heave vs Wave Height and Transom Heave vs Wave Height plots indicate that the response amplitude was similar to the wave height and was in phase with the wave. The spectral density plot shows that the response of the LARVA COG is centered on a single frequency which is very close to the incoming wave frequency. The data shows that the response of the LARVA was similar to the incoming wave which supports what was observed during experimental trials. Therefore, it can be said that the LARVA “rode the waves” and thus does not have any extreme heaving motions.

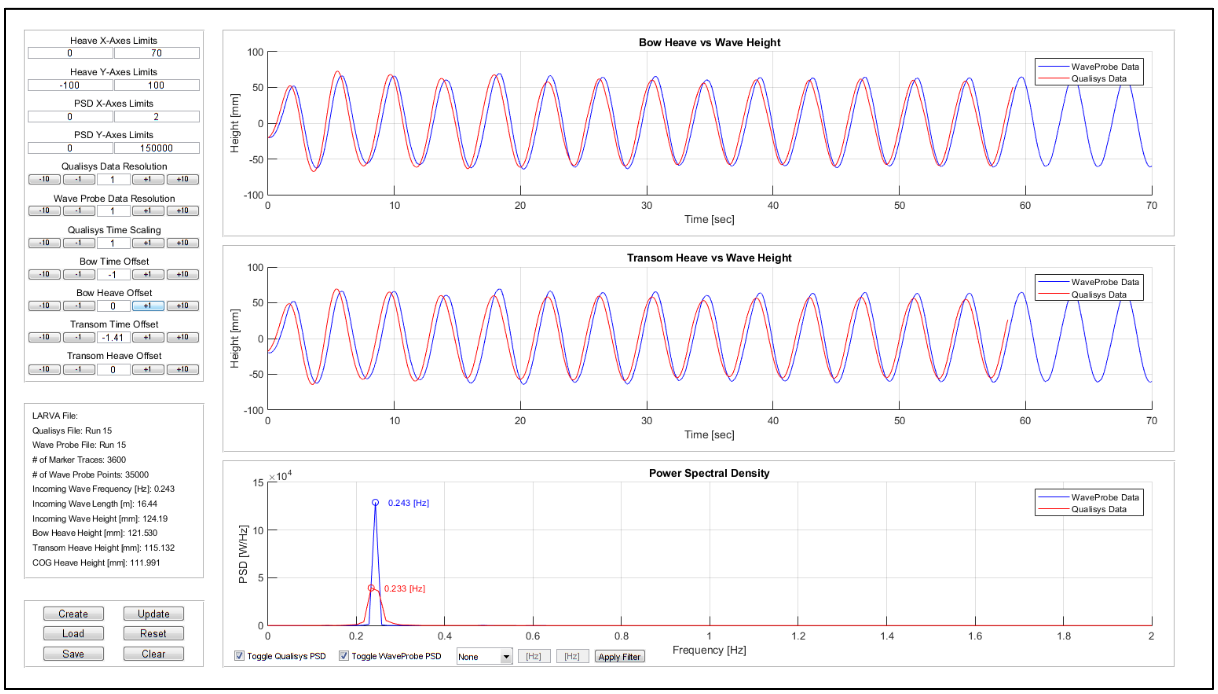

Figure 5.2: LARVA response in the following state for an incoming wave set with a small wave height (124.19mm) with a short frequency (0.243Hz).

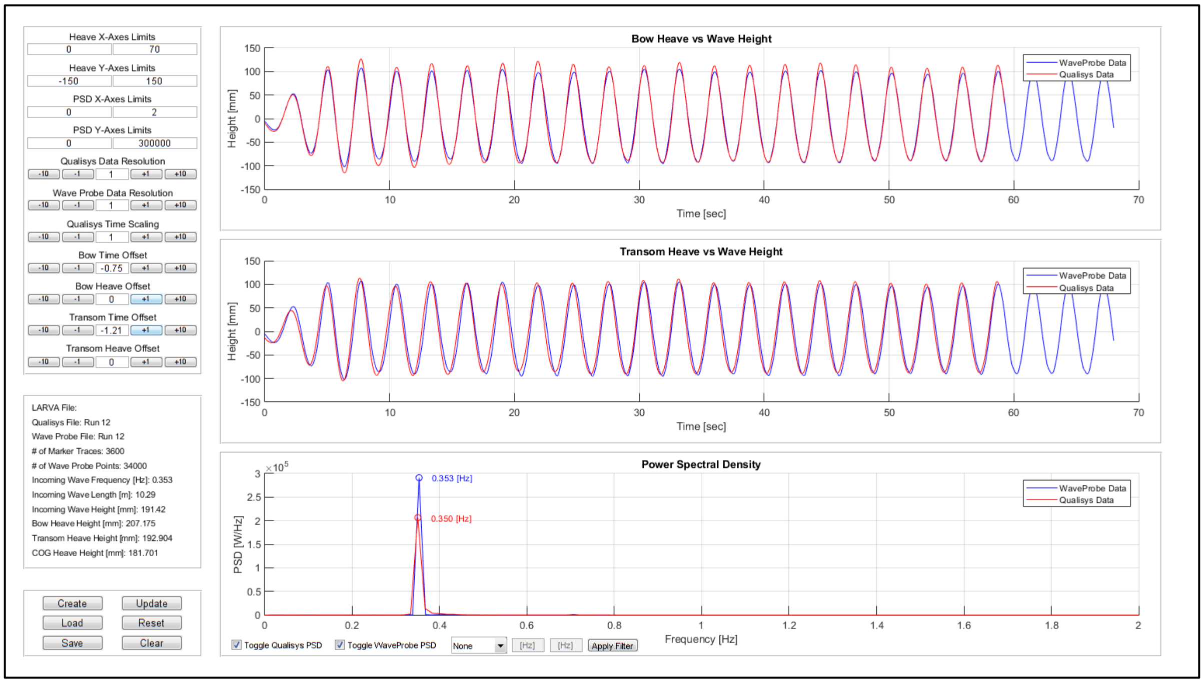

Figure 5.3: LARVA response in the following state for an incoming wave set with a medium wave height (191.42mm) with a medium frequency (0.353Hz).

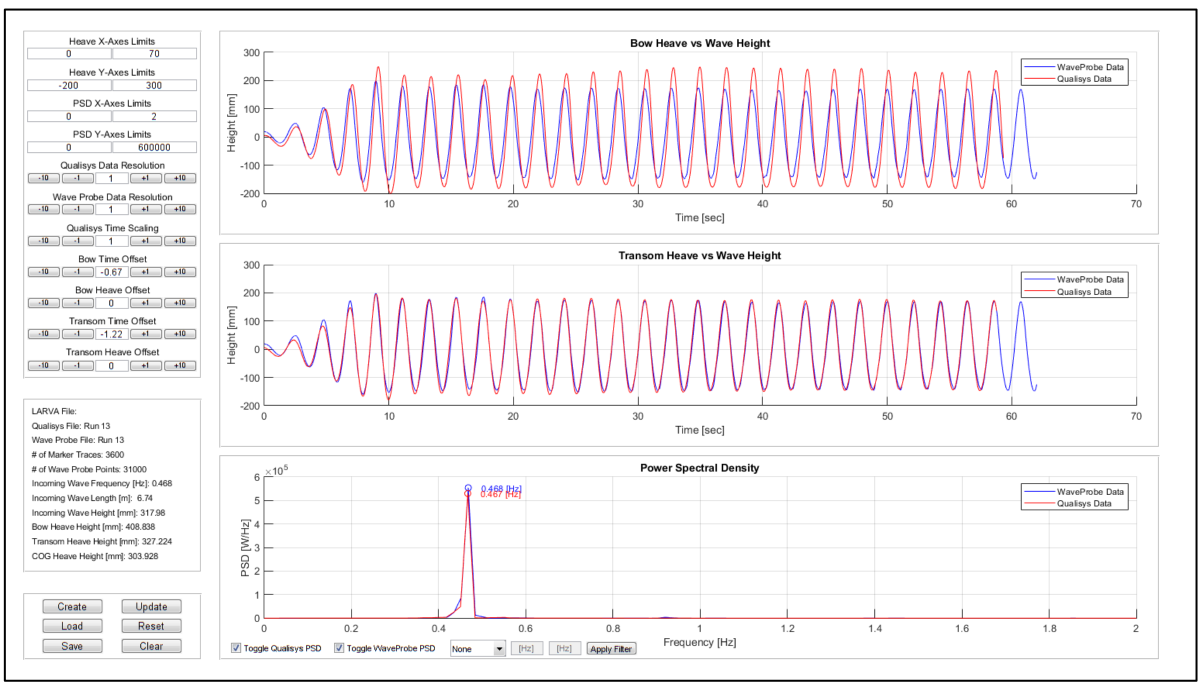

Figure 5.4: LARVA response in the following state for an incoming wave set with a large wave height (317.98mm) with a large frequency (0.468Hz).

5.2. Launching Condition Analysis

For the launching condition, the purpose of the experiments was to determine if the vertical motion of the LARVA relative to the AUV will impact and potentially damage the AUV during launch or recovery. Since the AUV motion can be assumed equal to the incoming wave, the relative heaving response of the LARVA at the transom, COG, and bow are of interest. Excessive relative heave at any of these points could result in the LARVA slamming against the AUV while launching or recovering and resulting in damage to the LARVA, AUV, or both.

Figure 5.5, Figure 5.6, and Figure 5.7 show the LARVA response in the launching state to incoming waves that have a short, medium, and long wave length and frequency respectively. The Bow Heave vs Wave Height and Transom Heave vs Wave Height plots indicate that the response amplitude was similar to the wave height and was in phase with the wave. The spectral density plot shows that the response of the LARVA COG is centered on a single frequency which is very close to the incoming wave frequency.

Once the response of the LARVA was determined to be in phase with the wave, the next step was to perform an Analysis of Variance (ANOVA) to generate a response surface method for relative heaving over the entire design space. To analyze the relative heaving motions, Design Expert 9 was used to visualize the data by fitting a polynomial to the relative heaving height. Additionally, the polynomial could be used for predicting the response of the LARVA for wave heights and frequencies which were not tested within the testing domain.

At full scale, the draft of the AUV is approximately 660mm and in the launching condition, the depth of the deck is 933mm. Therefore, the safe distance between the deck and the AUV is 273mm at full scale. At model scale, the safe distance between the deck and AUV is 68.25mm. Therefore, relative heave with an absolute value greater than 68.25mm would result in the AUV colliding with the deck, and would not be acceptable.

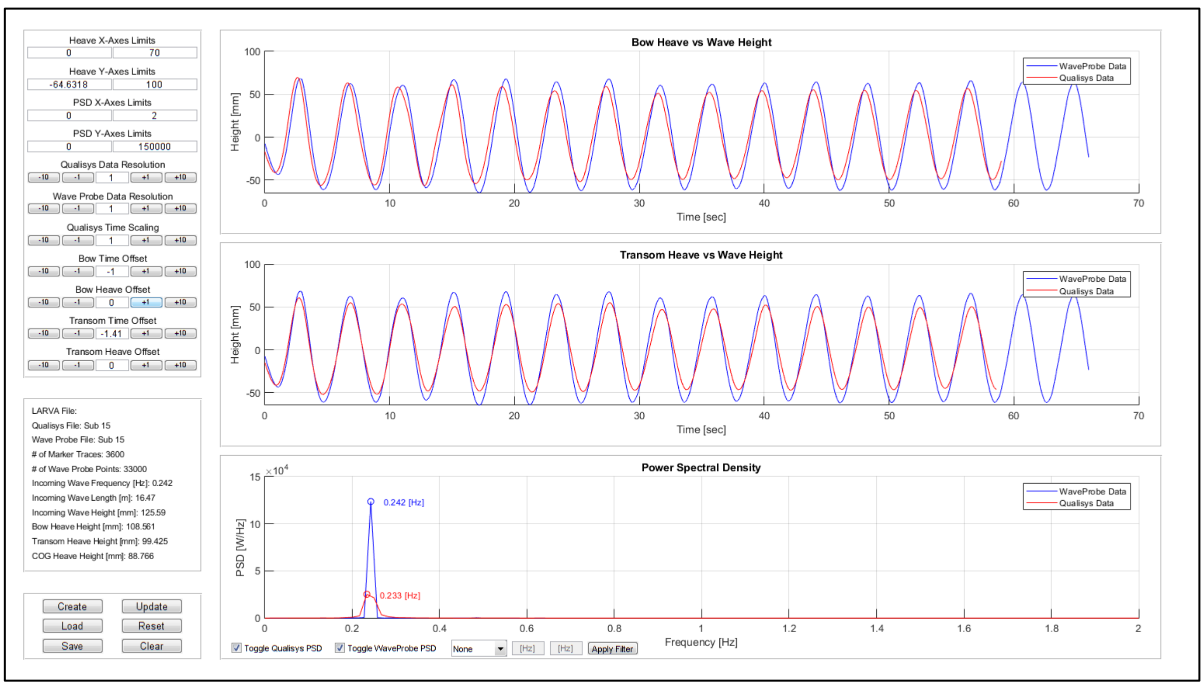

Figure 5.5: LARVA response in the launching state for an incoming wave set with a small wave height (125.59mm) with a short frequency(0.242Hz).

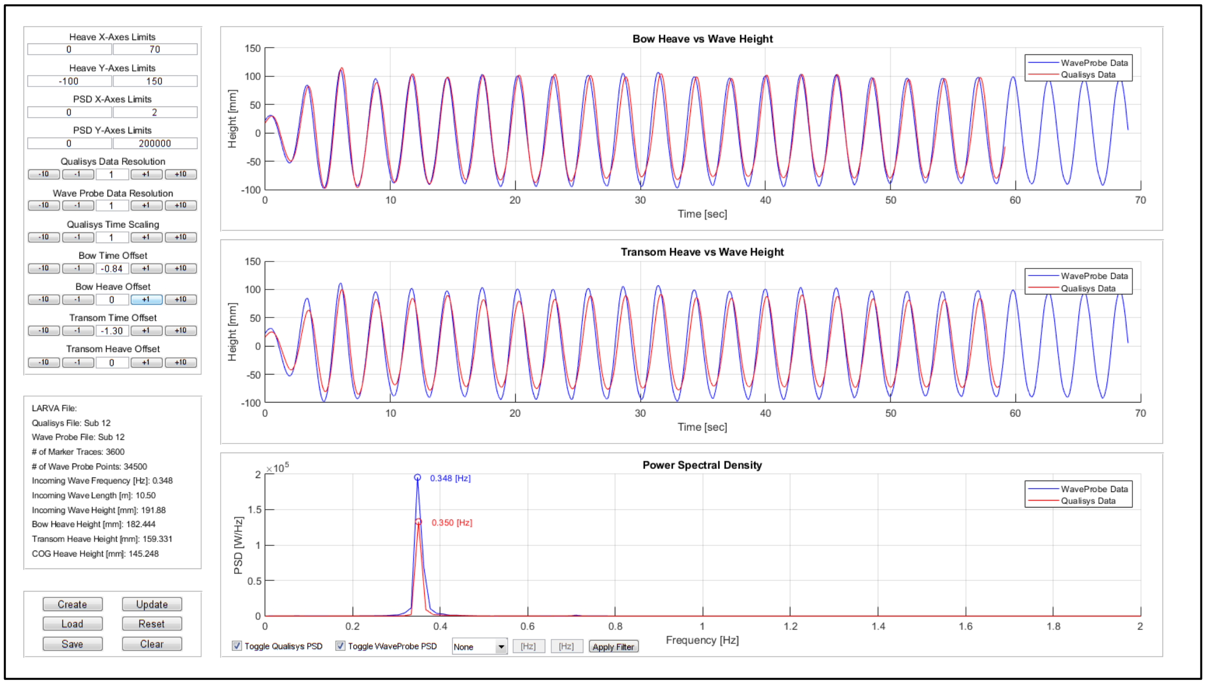

Figure 5.6: LARVA response in the launching state for an incoming wave set with a medium wave height (191.88mm) with a medium frequency (0.348Hz).

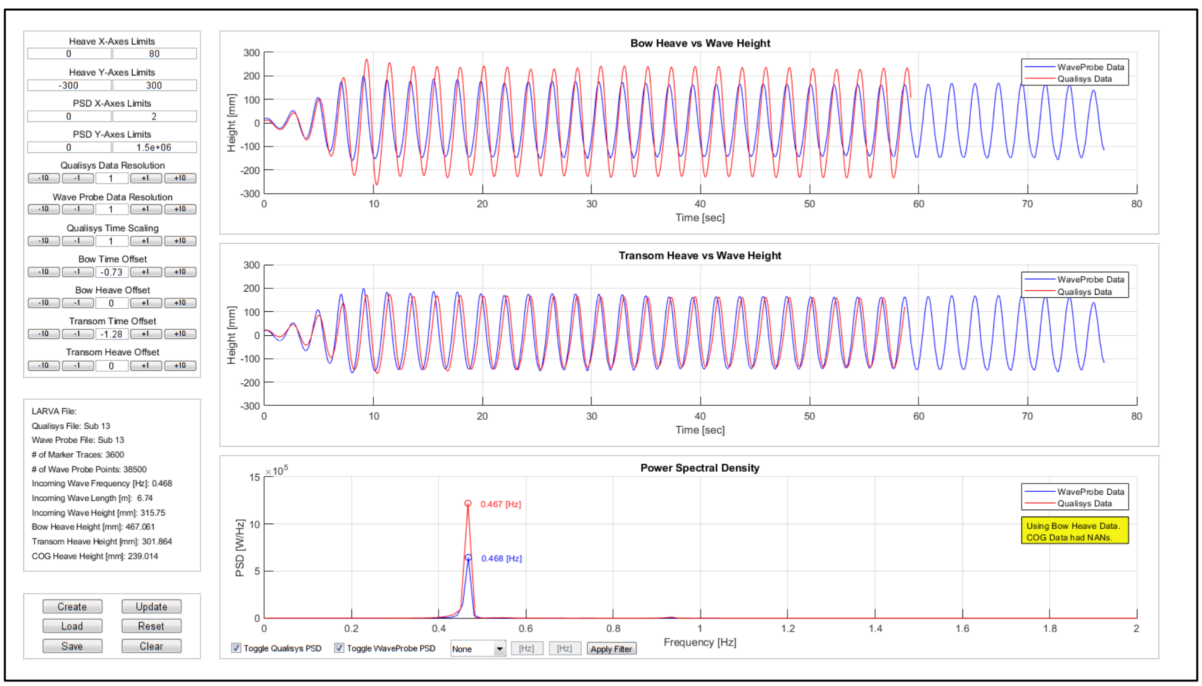

Figure 5.7: LARVA response in the launching state for an incoming wave set with a large wave height (315.75mm) with a large frequency (0.468Hz).

5.2.1. Relative Bow Heaving

Equation (5.2) is the resultant polynomial from the ANOVA that describes the relative heaving at the bow as a function of wave height and wave frequency. The full ANOVA can be found in Appendix D: ANOVA Analysis of Relative Heaving in the Launching State.

$$\begin{aligned}\ln(Relative\ Heave + 18.74) = 1.39E3 * A^3 + 0.002AB^2 + 0.95A^2B \\ - 7.79B^2 - 1584.42A^2 - 1.69AB + 0.47B + 696.7A \\ - 105.36\end{aligned} \tag{5.2}$$

Where: *Relative Heave* = Relative heave in millimeters
A = Wave frequency in Hz
B = Wave height in millimeters

Figure 5.8 shows a surface plot of the fitted polynomial (equation (5.2)) for the relative bow heave heights. It shows that for the majority of the design space, there were very small amounts of relative heaving, indicating that the bow "rode the waves" as it did for the following state (Section 5.1). For cases of high frequency and large waves, the relative heaving is showing an increasing trend. Even though the trend is increasing, this particular scenario is at the extremities of both the wave height and frequency, and thus, should not be encountered very often. Overall, the relative heave at the bow is less than the limit of 68.25mm and is therefore acceptable.

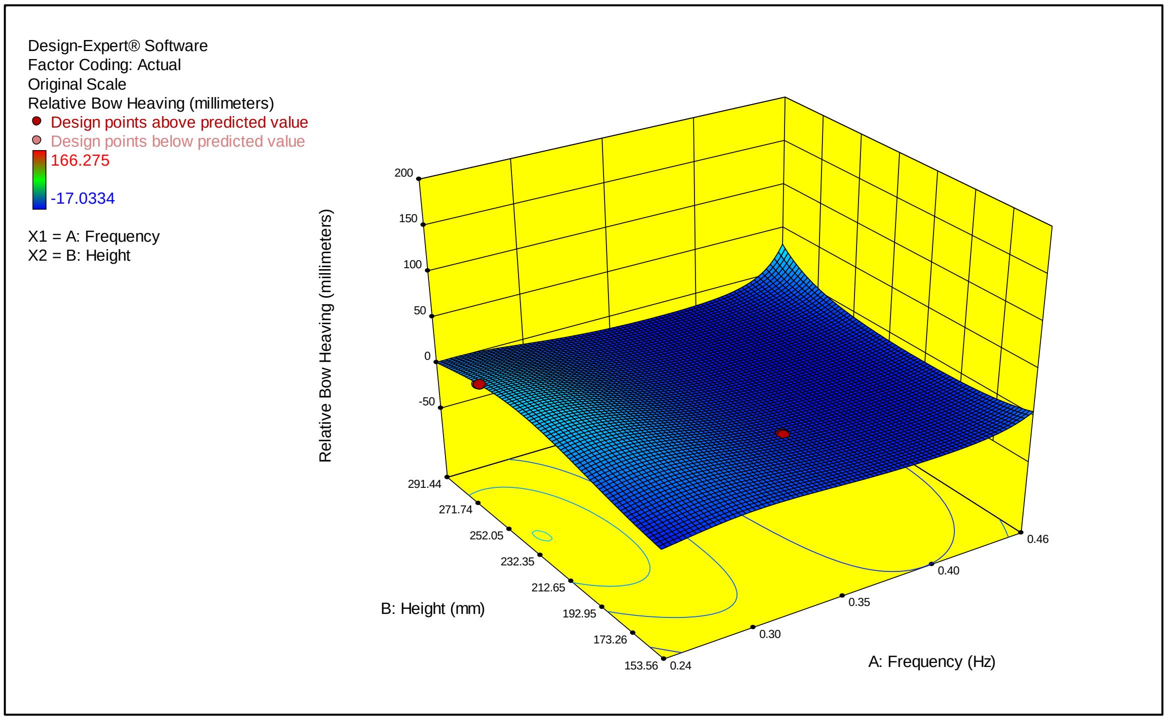

Figure 5.8: Surface plot of equation (5.2) showing the relative bow heave heights for the launching state.

5.2.2. COG Relative Heaving

Equation (5.3) is the resultant polynomial from the ANOVA that describes the relative heaving at the COG as a function of wave height and wave frequency. The full ANOVA can be found in Appendix D: ANOVA Analysis of Relative Heaving in the Launching State.

$$\begin{aligned} &Relative\ Heave \\ &\quad = 8700.04A^3 - 3.32E(-5)B^3 + 0.015AB^2 + 0.016B^2 \\ &\quad - 9044.75A^2 - 7.88AB - 1.76B + 3822.05A \\ &\quad - 344.67 \end{aligned} \tag{5.3}$$

Where: *Relative Heave* = Relative heave in millimeters
A = Wave frequency in Hz
B = Wave height in millimeters

Figure 5.9 shows a surface plot of the fitted polynomial for the relative COG heave heights. It shows that for all scenarios, the COG did not tend to “ride the waves” as in the following state (Section 5.1). In fact, there was a lack of heaving where the COG did not respond to the incoming wave resulting in a negative relative heave. For low frequencies, the COG tended to have the most response (least relative heave) to the incoming wave, with the response decreasing (increasing magnitude of relative heave) as the wave height decreases. For higher frequency waves, there was a decrease in response (increase in relative heave magnitude) and appears to be insensitive to the wave height. Essentially, for high frequency waves, the system did not have time to react to the incoming wave, hence resulting in a lack of heave (and thus a larger relative heave) regardless of the wave height. For lower frequencies, the system had enough time to respond which resulted in larger global heaving (lower relative heave) compared to large frequency waves, with the wave height having an influence on the response.

The maximum relative heave at the CoG is 66.28mm. Since this is less than the limit of 68.25mm, the motions are acceptable. However at his point, the safety margins are slim so it would be advisable impose a limit on the higher frequencies and/or the wave heights.

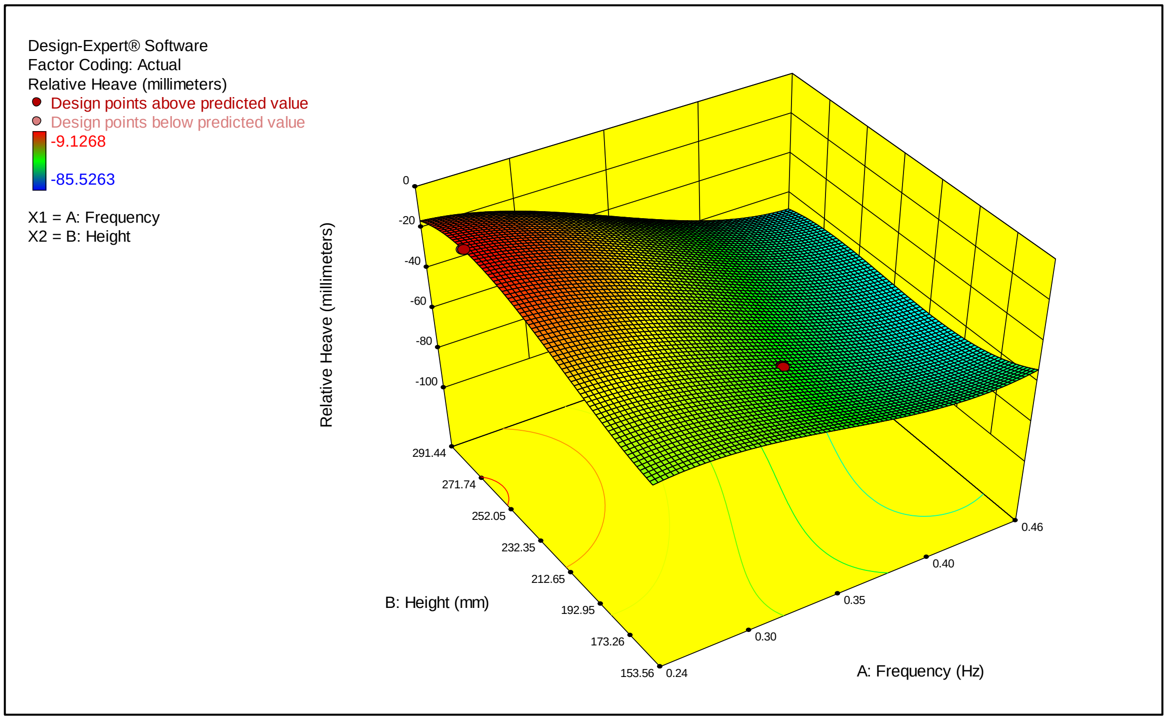

Figure 5.9: Surface plot of Equation (5.3) showing the relative COG heave heights for the launching state.

5.2.3. Transom Relative Heaving

Equation (5.4) is the resultant polynomial from the ANOVA that describes the relative heaving at the transom as a function of wave height and wave frequency. The full ANOVA can be found in Appendix D: ANOVA Analysis of Relative Heaving in the Launching State.

$$\begin{aligned} &\mathit{Relative\ Heave} \\ &\quad = 35312A^3 - 1.62E(-5)B^3 + 0.06AB^2 - 0.01B^2 \\ &\quad - 35684A^2 - 26.75AB + 7.13B + 14149A - 1978 \end{aligned} \tag{5.4}$$

Where: *Relative Heave* = Relative heave in millimeters
A = Wave frequency in Hz
B = Wave height in millimeters

Figure 5.10 shows a surface plot of the fitted polynomial for the relative transom heave heights. In general, for smaller frequencies, the magnitude of relative heave was lower. For larger frequencies, the magnitude of relative heave was larger. Based on the plot, the incoming wave height did not have as large of an influence as the wave frequency. Lower and higher wave heights tended to have less of an influence than medium wave heights. Of particular interest is that the majority of the relative heave is negative indicating that there was a lack response to the incoming wave. This is particularly evident for higher frequency waves where the system did not have enough time to respond, resulting in larger relative heaving.

The maximum relative heave is 68.98mm which is greater than the limit set forth of 68.25mm, however, this only occurs in a small section of the design space. Therefore, for the major of the design space, the motions are acceptable, however there may be a restriction imposed on operating in higher frequency waves (frequencies greater than 0.40Hz).

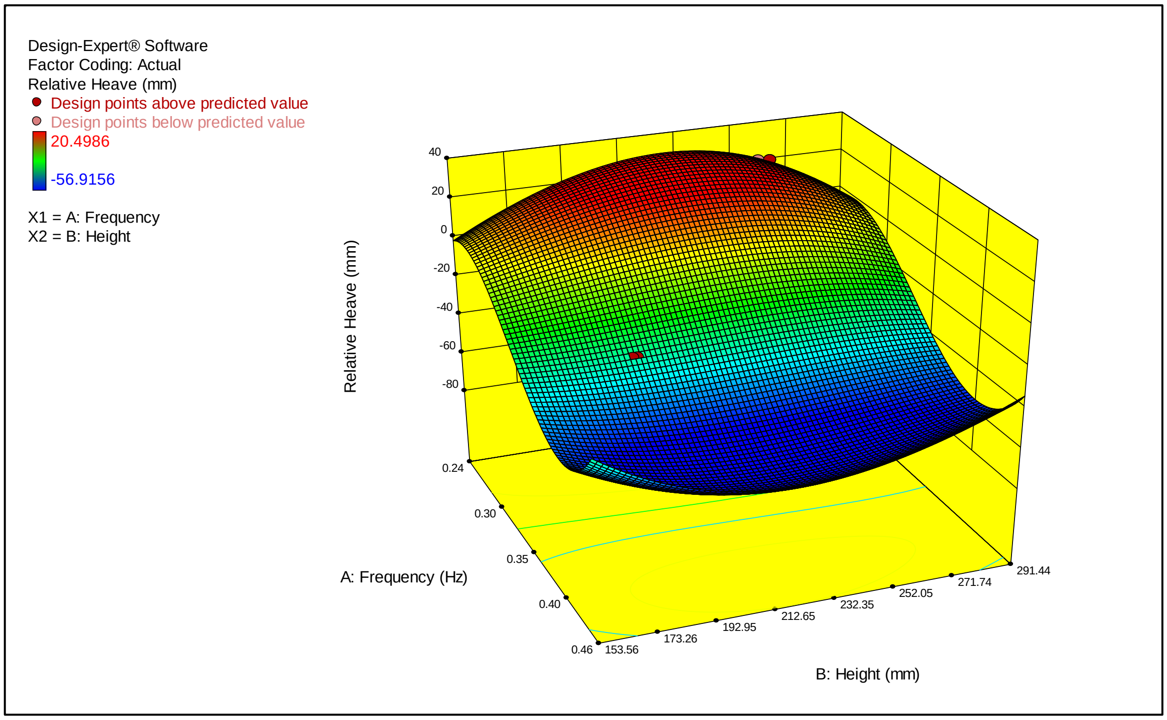

Figure 5.10: Surface plot of Equation (5.4) showing the relative transom heave heights for the launching state.

5.3. Summary

Overall, the results of the model testing seem adequate. Model testing in the following state showed that there were no extreme motions and that the LARVA rode the waves. As for the launching state, the bow tended to ride the waves and thus had very little relative heave. For small frequencies, the COG was able to respond to the incoming wave and ended up having little relative heave with the wave height having an influence on the response. However, at larger frequencies, the system did not have time to respond, resulting in negative relative heave which had little dependence on the wave height. Finally, for the transom, the response was dependent on both the frequency and wave height. For small wave frequencies, the magnitude of relative heave was smaller compared to higher wave frequencies. For the smaller frequencies, the relative heave was positive and for larger frequencies, the relative heave was negative. This is likely due to the fact that the system could not respond fast enough at the higher frequencies.

As stated in Section 5.2.2 and Section 5.2.3, there are sections of the design space where the model exhibited some large amounts of relative heave, particularly at the larger frequencies. Therefore, it is advisable to limit the wave frequency in which the LARVA can operate to 0.40Hz (model scale).

6. Conclusion

Based on the data collected from the seakeeping trials, the LARVA looks like it will be suitable as a launch and recovery platform for offshore applications where the waves are similar to the ones used in the experiments. The exception being high frequency waves as highlighted above. As previously stated, these waves have long periods and are not representative of the waves found closer inland where they tend to have a much higher frequency.

This thesis represents the first design iteration in the design of the LARVA. The next phase in the design would incorporate the refinement of the ballasting system. The restriction in high frequency waves arises as as result of the LARVA not being able to heave with the wave. To mitigate this, the next design phase would increase the launch draft of the LARVA. This would give more clearance between the AUV and the LARVA main deck which would allow the LARVA to operate in the higher frequency waves. Additonal next steps would see the incorporation of an active ballasting system, whether that be ballast pumps or the use of compressed air to clear the ballast tanks. These two steps would at the least get the LARVA operational.

Additional testing focused on the interaction between the LARVA and the AUV would also be highly beneficial. This would include numerical simulations followed by a two-body interaction experiment. This will determine the extent of the validity of the assumption that the AUV rides the waves and to see if the motions of both the LARVA and the AUV are compatible.

While this represents a first step, this design could be taken further to a fully autonomous state where it could even potentially be launched using ship davits. Of course this would require many more iterations of designs and the integration of electrical systems, but it certainly has potential and would be exciting to see built and in operational use.

7. References

[1] J. Yuh, "Design and Control of Autonomous Underwater Robots: A Survey," *Autonomous Robots,* vol. 8, pp. 7-24, 2000.

[2] F. Repoulias and E. Papdopoulos, "Trajectory Planning and Tracking Control of Underactuated," in *International Conference on Robotics and Automation*, 2005.

[3] P. King, A. Vardy, P. Vandrish and B. Anstey, "Realtime side scan image generation and registration framework," Memorial University of Newfoundland, 2012.

[4] W. Merlin, D. Mouland, W. Markuske, P. King, R. Lewis, D. Walker and G. Dinn, "High Resolution Seabed Sub-bottom Profiler for AUV," in *OMAE2011-49024*, 2011.

[5] C. Goldfinger, "Habitat Mapping and Identifying Suitable Habitat of Redfish Rocks Pilot Marine Reserve, Port Orford, Oregon," Oregon State University, 2010.

[6] D. Roy, "Balance for Measuring Moments of Inertia of Ship Models," National Research Council Canada; Institute for Marine Dynamics, 1984.

[7] W. Qui and P. Wen, *Measuring Moments of Inertia and Vertical Center of Gravity of Ship Models [Powerpoint presntation],* n.d..

[8] C-CORE, "MetOcean Climate Study Offshore Newfoundland & Labrador - Cell Report - Cell #343," Nalcor Energy Oil and Gas, 2015.

[9] Stat-Ease Inc., *Design Expert 9.0.6.2,* Minneapolis, 2015.

[10] General Hydrostatics, *GHS 14.40C,* Port Townsend, WA, USA, 2014.

Appendix A: GHS Analysis

GHS Run File

~~~
````````````````````````````````````````````````````` PREAMBLE
`````````````````````````````````````````````````````

CLEAR
READ "Full Scale Model.GF"    ```reads in hull
REPORT HSTATICS.PF  ```preview reports

WATER = SW
UNITS LT   `Units in imperial is UNITS LT (feet, tons)


`````````````````````````````````````````````````````` MACROS
``````````````````````````````````````````````````````
MACRO STATE1
	`Boat is floating at operating draft with AUV
	LOAD (AFT_KEEL) 0%
	LOAD (FORE_KEEL) 0%
	LOAD (DECK_TANKS) 0%
	LOAD (BOW_TANK) 0%
	FSMMT (AFT_KEEL) = TRUE
	FSMMT (DECK_TANKS) = TRUE
	FSMMT (BOW_TANK) = TRUE
	FSMMT (FORE_KEEL) = TRUE

	WEIGHT 1.088 6.47a 0 2.24;
	      0 9.51a 0 1.78;
	      0.686 5.18a 0 2.69
	` WEIGHTS are:
	`	HULL MATERIAL
	`	Batteries 0.232 9.51a 0 1.78;
	`	AUV
/
~~~

```
MACRO STATE2
	`Boat is lowered to deployment draft with AUV
	`Target draft is 3.75ft or larger... optimally 4ft
	LOAD (AFT_KEEL) 100%
	LOAD (FORE_KEEL) 100%
	LOAD (DECK_TANKS) 100%
	LOAD (BOW_TANK) 100%
	FSMMT (AFT_KEEL) = TRUE
	FSMMT (DECK_TANKS) = TRUE
	FSMMT (BOW_TANK) = TRUE
	FSMMT (FORE_KEEL) = TRUE

	WEIGHT 1.088 6.47a 0 2.24;
	     0 9.51a 0 1.78;
	` WEIGHTS are:
	`	HULL MATERIAL
	`	Batteries 0.232 9.51a 0 1.78;
/

MACRO STATE3
	`Boat is floating at operating draft without AUV
	LOAD (AFT_KEEL) 0%
	LOAD (FORE_KEEL) 0%
	LOAD (DECK_TANKS) 0%
	LOAD (BOW_TANK) 0%
	FSMMT (AFT_KEEL) = TRUE
	FSMMT (DECK_TANKS) = TRUE
	FSMMT (BOW_TANK) = TRUE
	FSMMT (FORE_KEEL) = TRUE

	WEIGHT 1.088 6.47a 0 2.24;
	     0 9.51a 0 1.78;
	` WEIGHTS are:
	`	HULL MATERIAL
	`	Batteries 0.232 9.51a 0 1.78;
/
```

```
MACRO SOLV2
HS 0.6 0.8 ... 4   ``hydrostatics at varying drafts
RA 5 10 15 ... 90 /LIM              ``GZ curve
solve
trim 0
heel 0
solve draft
status
solve
status
/
```

```
MACRO LT_LIMIT
m-rad = 187.9782792 ft-deg
LIMIT (1) AREA FROM 0 TO 30 > 10.3
LIMIT (2) AREA FROM 0 TO 40  OR FLD > 16.9
LIMIT (3) AREA FROM 30 TO 40 OR FLD  > 5.64
LIMIT (4) RA AT 30 > 0.656
LIMIT (5) ANGLE AT MAX > 15
LIMIT (6) GM UPRIGHT > 0.492
/
```

```
```````````````````````````````````````````````````````` MAIN BODY
````````````````````````````````````````````````````````

.LT_LIMIT
.STATE3
.SOLV2
display status
Report preview
```

GHS Analysis of the Loaded State

04/02/16 12:45:37 Memorial Univ. of Newfoundland - Educational Use Page 1
GHS 14.40C **LARVA**

HYDROSTATIC PROPERTIES
No Trim, No Heel

Origin Depth	Displacement Weight (LT)	Center of Buoyancy LCB	TCB	VCB	WPA	LCF	BML	BMT
0.600	0.32	6.45a	0.00	0.47	59	6.80a	84.5	7.70
0.800	0.74	6.72a	0.00	0.61	88	6.89a	58.2	10.48
1.000	1.17	6.75a	0.00	0.71	56	5.41a	17.7	7.86
1.200	1.49	6.48a	0.00	0.79	58	5.60a	15.8	6.27
1.400	1.82	6.34a	0.00	0.89	59	5.80a	14.7	5.20
1.600	2.16	6.27a	0.00	0.98	60	6.00a	14.0	4.41
1.800	2.51	6.25a	0.00	1.08	14	12.54a	1.9	0.72
2.000	2.65	6.42a	0.00	1.12	27	9.30a	8.0	2.04
2.200	2.79	6.57a	0.00	1.17	20	9.75a	8.4	1.36
2.400	2.91	6.72a	0.00	1.22	22	10.26a	8.8	1.33
2.600	3.04	6.88a	0.00	1.27	23	10.60a	8.9	1.30
2.800	3.17	7.03a	0.00	1.33	23	10.67a	8.6	1.25
3.000	3.31	7.18a	0.00	1.40	24	10.74a	8.4	1.20
3.200	3.44	7.32a	0.00	1.46	24	10.80a	8.1	1.16
3.400	3.57	7.44a	0.00	1.53	23	10.72a	7.7	1.11
3.600	3.70	7.55a	0.00	1.60	23	10.54a	7.3	1.06
3.800	3.83	7.65a	0.00	1.67	22	10.34a	6.8	1.01
4.000	3.96	7.73a	0.00	1.74	21	10.09a	6.3	0.97

Distances in FEET.-------Specific Gravity = 1.025.--------------------------

RIGHTING ARMS vs HEEL ANGLE
LCG = 5.97a TCG = 0.00 VCG = 2.41

Origin Depth	Degrees of Trim	Heel	Displacement Weight(LT)	Righting Arms in Trim	in Heel	Area	Flood Pt Height
1.549	1.83f	0.00	1.774	0.00	0.000	0.00	-1.55(1)
1.547	1.88f	5.00s	1.774	0.00	0.326	0.81	-1.55(1)
1.551	1.99f	10.00s	1.774	0.00	0.597	3.14	-1.55(1)
1.557	2.14f	15.00s	1.774	0.00	0.753	6.57	-1.56(1)
1.528	2.11f	20.00s	1.774	0.00	0.819	10.54	-1.53(1)
1.447	1.85f	25.00s	1.774	0.00	0.841	14.71	-1.45(1)
1.401	1.70f	26.89s	1.774	0.00	0.842	16.30	-1.40(1)
1.303	1.39f	30.00s	1.774	0.00	0.839	18.91	-1.30(1)
1.112	0.86f	35.00s	1.774	0.00	0.830	23.09	-1.11(1)
0.888	0.32f	40.00s	1.774	0.00	0.819	27.21	-0.89(1)
0.628	0.26a	45.00s	1.774	0.00	0.810	31.28	-0.63(1)
0.338	0.86a	50.00s	1.774	0.00	0.810	35.33	-0.34(1)
0.025	1.47a	55.00s	1.774	0.00	0.829	39.42	-0.03(1)
0.000	1.52a	55.39s	1.774	0.00	0.832	39.74	-0.00(1)
-0.314	2.11a	60.00s	1.774	0.00	0.878	43.67	0.31(1)
-0.690	2.81a	65.00s	1.774	0.00	0.972	48.28	0.69(1)
-1.097	3.62a	70.00s	1.774	0.00	1.066	53.37	1.10(1)
-1.263	3.93a	72.20s	1.774	0.00	1.079	55.74	1.26(1)
-1.435	4.18a	75.00s	1.774	0.00	1.058	58.74	1.43(1)
-1.550	3.76a	80.00s	1.774	0.00	0.894	63.67	1.55(1)
-1.582	2.94a	85.00s	1.774	0.00	0.688	67.65	1.58(1)
-1.592	1.99a	90.00s	1.774	0.00	0.475	70.56	1.59(1)

Distances in FEET.------Specific Gravity = 1.025.-----------Area in Ft-Deg.

```
04/02/16 12:45:37 Memorial Univ. of Newfoundland - Educational Use      Page 2
GHS 14.40C                          LARVA

           Critical Point-----------------------LCP-----TCP-----VCP
       (1) ORIGIN                     FLOOD    0.00    0.00    0.00
LIM--------------------STABILITY CRITERION------------Min/Max----------Margin
(1) Area from abs 0.000 deg to 30                 >    10.30 Ft-deg   84%
(2) Area from abs 0.000 deg to 40 or Flood        >    16.90 Ft-deg -100%
(3) Area from 30 deg to 40 or Flood               >     5.64 Ft-deg -100%
(4) Righting Arm at 30 deg                        >     0.66 Ft       28%
(5) Absolute Angle at MaxRA                       >    15.00 deg      57 deg
(6)  GM Upright                                   >     0.49 Ft      661%
--------------------Relative angles measured from 0.000 ---------------------
```

04/02/16 12:45:37 Memorial Univ. of Newfoundland - Educational Use *Page 3*
GHS 14.40C **LARVA**

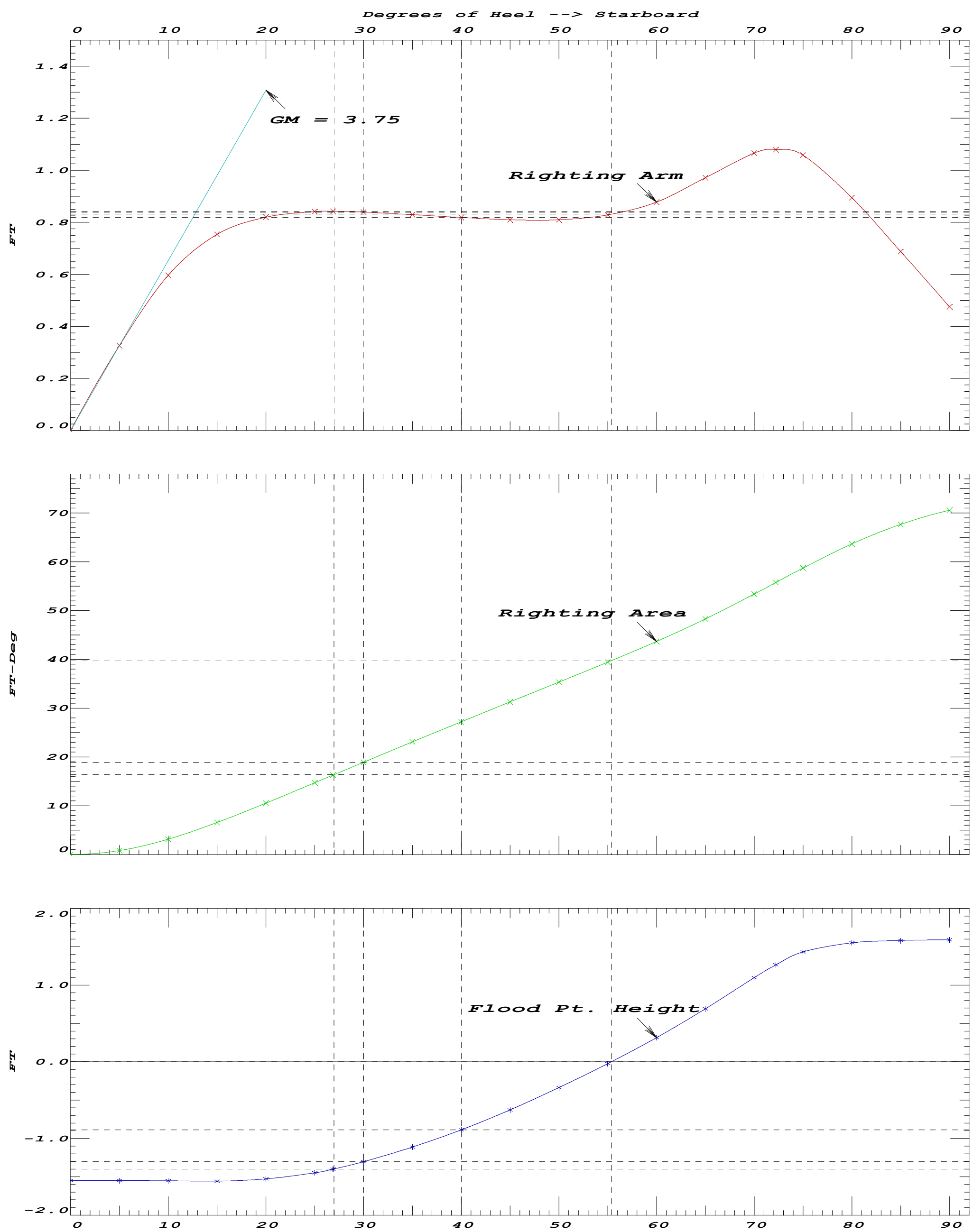

04/02/16 12:45:37 Memorial Univ. of Newfoundland - Educational Use Page 4
GHS 14.40C LARVA

WEIGHT and DISPLACEMENT STATUS
Baseline draft: 1.370
Trim: zero, Heel: zero

Part	SpGr	Weight(LT) / Displ(LT)	LCG / LCB	TCG / TCB	VCG / VCB	RefHt
WEIGHT		1.77	5.97a	0.00	2.41	
KEEL	1.025	1.12	6.66a	0.00	0.70	-1.37
BOW	1.025	0.05	15.76a	0.00	1.09	-1.37
AFT	1.025	0.52	4.26a	0.00	1.18	-1.37
BATT_COMP	1.025	0.08	9.49a	0.00	1.17	-1.37
Total Displacement-->	1.025	1.77	6.35a	0.00	0.87	
Righting Arms:			0.38a	0.00		

Distances in FEET.

WEIGHT and DISPLACEMENT STATUS
Baseline draft: 1.550 @ Origin
Trim: Fwd 1.84 deg., Heel: 0.00 deg.

Part	SpGr	Weight(LT) / Displ(LT)	LCG / LCB	TCG / TCB	VCG / VCB	RefHt
WEIGHT		1.77	5.97a	0.00	2.41	
KEEL	1.025	1.12	6.66a	0.00	0.70	-1.55
BOW	1.025	0.02	15.59a	0.00	0.89	-1.55
AFT	1.025	0.58	3.82a	0.00	1.20	-1.55
BATT_COMP	1.025	0.06	9.44a	0.00	1.11	-1.55
Total Displacement-->	1.025	1.77	5.92a	0.00	0.88	
Righting Arms:			0.00	0.00		

Distances in FEET.

CG - Draft: 1.55 @ 0.00 Trim: fwd 1.84 deg. Heel : 0.00 deg.

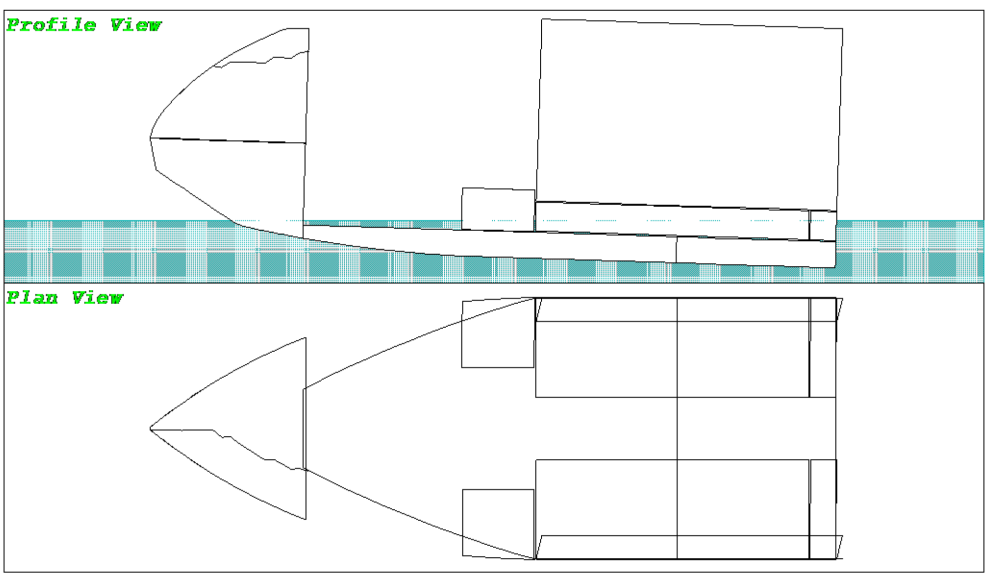

GHS Analysis of the Launching State

04/02/16 12:47:26 Memorial Univ. of Newfoundland - Educational Use *Page 1*
GHS 14.40C **LARVA**

HYDROSTATIC PROPERTIES
No Trim, No Heel

Origin Depth	Displacement Weight(LT)	Center of Buoyancy LCB	TCB	VCB	WPA	LCF	BML	BMT
0.600	0.32	6.45a	0.00	0.47	59	6.80a	84.5	7.70
0.800	0.74	6.72a	0.00	0.61	88	6.89a	58.2	10.48
1.000	1.17	6.75a	0.00	0.71	56	5.41a	17.7	7.86
1.200	1.49	6.48a	0.00	0.79	58	5.60a	15.8	6.27
1.400	1.82	6.34a	0.00	0.89	59	5.80a	14.7	5.20
1.600	2.16	6.27a	0.00	0.98	60	6.00a	14.0	4.41
1.800	2.51	6.25a	0.00	1.08	14	12.54a	1.9	0.72
2.000	2.65	6.42a	0.00	1.12	27	9.30a	8.0	2.04
2.200	2.79	6.57a	0.00	1.17	20	9.75a	8.4	1.36
2.400	2.91	6.72a	0.00	1.22	22	10.26a	8.8	1.33
2.600	3.04	6.88a	0.00	1.27	23	10.60a	8.9	1.30
2.800	3.17	7.03a	0.00	1.33	23	10.67a	8.6	1.25
3.000	3.31	7.18a	0.00	1.40	24	10.74a	8.4	1.20
3.200	3.44	7.32a	0.00	1.46	24	10.80a	8.1	1.16
3.400	3.57	7.44a	0.00	1.53	23	10.72a	7.7	1.11
3.600	3.70	7.55a	0.00	1.60	23	10.54a	7.3	1.06
3.800	3.83	7.65a	0.00	1.67	22	10.34a	6.8	1.01
4.000	3.96	7.73a	0.00	1.74	21	10.09a	6.3	0.97

Distances in FEET.-------Specific Gravity = 1.025.--------------------------

04/02/16 12:47:26 Memorial Univ. of Newfoundland - Educational Use Page 2
GHS 14.40C **LARVA**

RIGHTING ARMS vs HEEL ANGLE
Fixed CG: LCG = 6.47a TCG = 0.00 VCG = 2.24

Origin Depth	Degrees of Trim	Heel	Displacement Weight(LT)	Righting Arms in Trim	in Heel	Flood Pt Area	Height
3.827	0.80f	0.00	3.755	0.00	0.000	0.00	-3.83(1)
3.813	0.79f	5.00s	3.755	0.00	0.097	0.24	-3.81(1)
3.769	0.76f	10.00s	3.755	0.00	0.195	0.97	-3.77(1)
3.694	0.71f	15.00s	3.755	0.00	0.296	2.20	-3.69(1)
3.592	0.65f	20.00s	3.755	0.00	0.401	3.93	-3.59(1)
3.464	0.57f	25.00s	3.755	0.00	0.513	6.22	-3.46(1)
3.318	0.47f	30.00s	3.755	0.00	0.644	9.10	-3.32(1)
3.158	0.36f	35.00s	3.755	0.00	0.799	12.70	-3.16(1)
3.042	0.47f	40.00s	3.755	0.00	0.997	17.17	-3.04(1)
3.087	1.08f	43.75s	3.755	0.00	1.071	21.07	-3.09(1)
3.142	1.45f	45.00s	3.755	0.00	1.068	22.41	-3.14(1)
3.355	2.92f	50.00s	3.755	0.00	1.049	27.74	-3.35(1)
3.551	4.42f	55.00s	3.755	0.00	1.020	32.92	-3.55(1)
3.724	5.91f	60.00s	3.755	0.00	0.982	37.92	-3.72(1)
3.857	7.31f	65.00s	3.755	0.00	0.938	42.73	-3.86(1)
3.937	8.55f	70.00s	3.755	0.00	0.892	47.31	-3.94(1)
3.954	9.60f	75.00s	3.755	0.00	0.846	51.65	-3.95(1)
3.897	10.37f	80.00s	3.755	0.00	0.806	55.78	-3.90(1)
3.742	10.78f	85.00s	3.755	0.00	0.783	59.74	-3.74(1)
3.502	10.84f	90.00s	3.755	0.00	0.777	63.63	-3.50(1)

Distances in FEET.------Specific Gravity = 1.025.-----------Area in Ft-Deg.

Note: The Center of Gravity shown above is for the Fixed Weight of 1.09 LT. As the tank load centers shift with heel and trim, the total Center of Gravity varies. The righting arms shown above include the effect of the C.G. variation.

Critical Point		LCP	TCP	VCP
(1) ORIGIN	FLOOD	0.00	0.00	0.00

LIM	STABILITY CRITERION		Min/Max	Margin
(1)	Area from abs 0.000 deg to 30	>	10.30 Ft-deg	-12%
(2)	Area from abs 0.000 deg to 40 or Flood	>	16.90 Ft-deg	-100%
(3)	Area from 30 deg to 40 or Flood	>	5.64 Ft-deg	-100%
(4)	Righting Arm at 30 deg	>	0.66 Ft	-2%
(5)	Absolute Angle at MaxRA	>	15.00 deg	29 deg
(6)	GM Upright	>	0.49 Ft	125%

--------------------Relative angles measured from 0.000 ---------------------

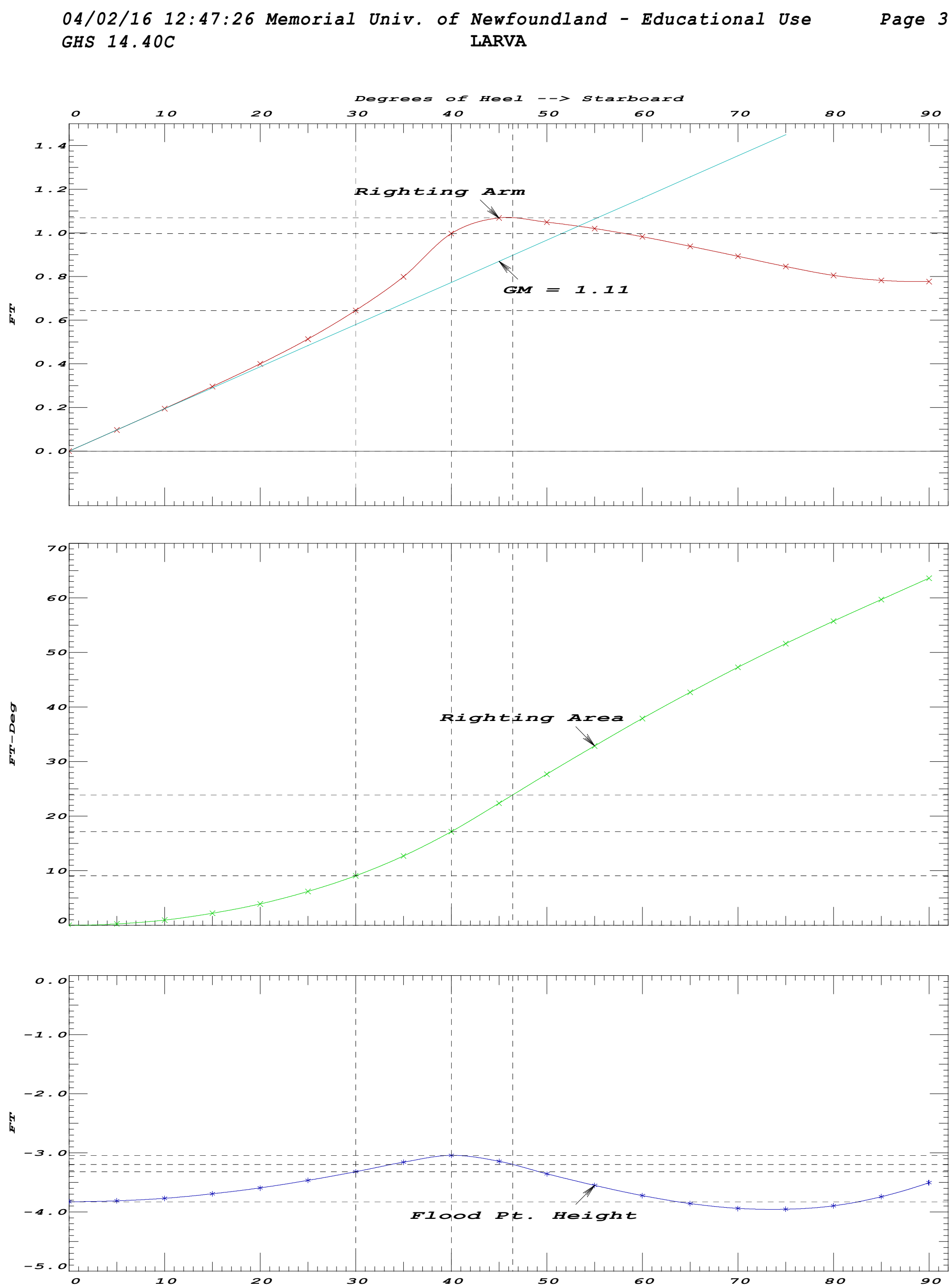
04/02/16 12:47:26 Memorial Univ. of Newfoundland - Educational Use
Page 3
GHS 14.40C
LARVA
Degrees of Heel --> Starboard
Righting Arm
GM = 1.11
FT
Righting Area
FT-Deg
Flood Pt. Height
FT

```
04/02/16 12:47:26 Memorial Univ. of Newfoundland - Educational Use      Page 4
GHS 14.40C                          LARVA

                       WEIGHT and DISPLACEMENT STATUS
                            Baseline draft: 3.681
                           Trim: zero,  Heel: zero
Part-----------------------------Weight(LT)----LCG-----TCG-----VCG
FIXED WEIGHT                          1.09    6.47a   0.00    2.24
                Load-----SpGr-----Weight(LT)----LCG-----TCG-----VCG------RefHt
DECK_TANKS     1.000    1.025         1.00    4.63a   0.00    1.39
AFT_KEEL       1.000    1.025         0.38    2.25a   0.00    0.69
BOW_TANK       1.000    1.025         0.55   16.35a   0.00    2.34
FORE_KEEL      1.000    1.025         0.73    8.96a   0.00    0.70
  Total Tanks--------->               2.67    7.91a   0.00    1.30
  Total Weight-------->               3.76    7.49a   0.00    1.57
                                   Displ(LT)----LCB-----TCB-----VCB
KEEL                    1.025         1.12    6.66a   0.00    0.70      -3.68
BOW                     1.025         0.70   16.39a   0.00    2.58      -3.68
AFT                     1.025         1.68    4.26a   0.00    1.87      -3.68
BATT_COMP               1.025         0.25    9.51a   0.00    1.56      -3.68
  Total Displacement--> 1.025         3.76    7.59a   0.00    1.63
------------------------------------------------------------------------------
               Righting Arms:                 0.10a   0.00
Distances in FEET.------------------------------------------------------------

                       WEIGHT and DISPLACEMENT STATUS
                       Baseline draft: 3.829 @ Origin
                      Trim: Fwd 0.81 deg.,  Heel: zero
Part-----------------------------Weight(LT)----LCG-----TCG-----VCG
FIXED WEIGHT                          1.09    6.47a   0.00    2.24
                Load-----SpGr-----Weight(LT)----LCG-----TCG-----VCG------RefHt
DECK_TANKS     1.000    1.025         1.00    4.63a   0.00    1.39
AFT_KEEL       1.000    1.025         0.38    2.25a   0.00    0.69
BOW_TANK       1.000    1.025         0.55   16.35a   0.00    2.34
FORE_KEEL      1.000    1.025         0.73    8.96a   0.00    0.70
  Total Tanks--------->               2.67    7.91a   0.00    1.30
  Total Weight-------->               3.76    7.49a   0.00    1.57
                                   Displ(LT)----LCB-----TCB-----VCB
KEEL                    1.025         1.12    6.66a   0.00    0.70      -3.83
BOW                     1.025         0.67   16.38a   0.00    2.53      -3.83
AFT                     1.025         1.71    4.24a   0.00    1.90      -3.83
BATT_COMP               1.025         0.25    9.51a   0.00    1.56      -3.83
  Total Displacement--> 1.025         3.76    7.49a   0.00    1.63
------------------------------------------------------------------------------
               Righting Arms:                 0.00    0.00
Distances in FEET.------------------------------------------------------------
```

04/02/16 12:47:26 Memorial Univ. of Newfoundland - Educational Use Page 5
GHS 14.40C LARVA

Condition Graphic - Draft: 3.83 @ 0.00 Trim: fwd 0.81 deg. Heel: zero

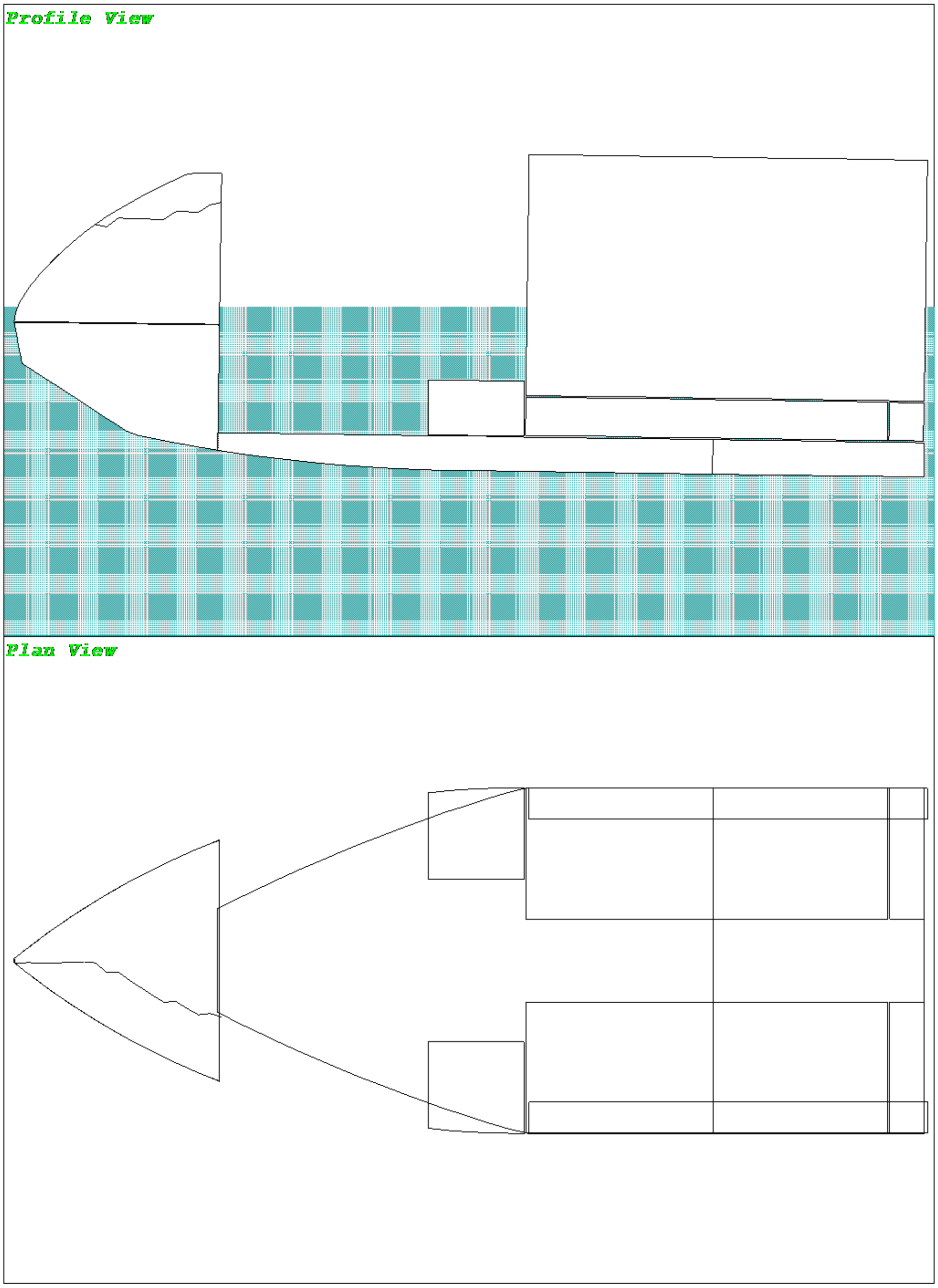

GHS Analysis of the Unloaded State

04/02/16 12:52:04 Memorial Univ. of Newfoundland - Educational Use Page 1
GHS 14.40C **LARVA**

HYDROSTATIC PROPERTIES
No Trim, No Heel

Origin Depth	Displacement Weight (LT)	Center of Buoyancy LCB	TCB	VCB	WPA	LCF	BML	BMT
0.600	0.32	6.45a	0.00	0.47	59	6.80a	84.5	7.70
0.800	0.74	6.72a	0.00	0.61	88	6.89a	58.2	10.48
1.000	1.17	6.75a	0.00	0.71	56	5.41a	17.7	7.86
1.200	1.49	6.48a	0.00	0.79	58	5.60a	15.8	6.27
1.400	1.82	6.34a	0.00	0.89	59	5.80a	14.7	5.20
1.600	2.16	6.27a	0.00	0.98	60	6.00a	14.0	4.41
1.800	2.51	6.25a	0.00	1.08	14	12.54a	1.9	0.72
2.000	2.65	6.42a	0.00	1.12	27	9.30a	8.0	2.04
2.200	2.79	6.57a	0.00	1.17	20	9.75a	8.4	1.36
2.400	2.91	6.72a	0.00	1.22	22	10.26a	8.8	1.33
2.600	3.04	6.88a	0.00	1.27	23	10.60a	8.9	1.30
2.800	3.17	7.03a	0.00	1.33	23	10.67a	8.6	1.25
3.000	3.31	7.18a	0.00	1.40	24	10.74a	8.4	1.20
3.200	3.44	7.32a	0.00	1.46	24	10.80a	8.1	1.16
3.400	3.57	7.44a	0.00	1.53	23	10.72a	7.7	1.11
3.600	3.70	7.55a	0.00	1.60	23	10.54a	7.3	1.06
3.800	3.83	7.65a	0.00	1.67	22	10.34a	6.8	1.01
4.000	3.96	7.73a	0.00	1.74	21	10.09a	6.3	0.97

Distances in FEET.-------Specific Gravity = 1.025.--------------------------

RIGHTING ARMS vs HEEL ANGLE
LCG = 6.47a TCG = 0.00 VCG = 2.24

Origin Depth	Degrees of Trim	Heel	Displacement Weight (LT)	Righting Arms in Trim	in Heel	Flood Pt Area	Height
1.019	0.62f	0.00	1.088	0.00	0.000	0.00	-1.02(1)
0.977	0.34f	5.00s	1.088	0.00	0.513	1.28	-0.98(1)
0.876	0.11a	10.00s	1.088	0.00	0.842	4.75	-0.88(1)
0.730	0.62a	15.00s	1.088	0.00	1.041	9.51	-0.73(1)
0.556	1.14a	20.00s	1.088	0.00	1.155	15.03	-0.56(1)
0.359	1.71a	25.00s	1.088	0.00	1.206	20.96	-0.36(1)
0.274	1.96a	27.06s	1.088	0.00	1.209	23.44	-0.27(1)
0.149	2.31a	30.00s	1.088	0.00	1.202	26.99	-0.15(1)
-0.000	2.71a	33.39s	1.088	0.00	1.183	31.04	0.00(1)
-0.073	2.90a	35.00s	1.088	0.00	1.170	32.94	0.07(1)
-0.311	3.47a	40.00s	1.088	0.00	1.120	38.66	0.31(1)
-0.563	4.02a	45.00s	1.088	0.00	1.062	44.12	0.56(1)
-0.831	4.53a	50.00s	1.088	0.00	1.001	49.28	0.83(1)
-1.114	5.02a	55.00s	1.088	0.00	0.943	54.13	1.11(1)
-1.415	5.49a	60.00s	1.088	0.00	0.894	58.72	1.41(1)
-1.735	5.94a	65.00s	1.088	0.00	0.865	63.11	1.74(1)
-2.079	6.40a	70.00s	1.088	0.00	0.876	67.45	2.08(1)
-2.447	6.87a	75.00s	1.088	0.00	0.952	71.99	2.45(1)
-2.826	7.38a	80.00s	1.088	0.00	1.058	77.00	2.83(1)
-3.191	7.91a	85.00s	1.088	0.00	1.134	82.49	3.19(1)
-3.528	8.36a	90.00s	1.088	0.00	1.175	88.28	3.53(1)

Distances in FEET.------Specific Gravity = 1.025.-----------Area in Ft-Deg.

```
04/02/16 12:52:04 Memorial Univ. of Newfoundland - Educational Use      Page 2
GHS 14.40C                          LARVA

           Critical Point-----------------------LCP-----TCP-----VCP
       (1) ORIGIN                     FLOOD    0.00    0.00    0.00
LIM--------------------STABILITY CRITERION------------Min/Max----------Margin
(1) Area from abs 0.000 deg to 30                >    10.30 Ft-deg  162%
(2) Area from abs 0.000 deg to 40 or Flood       >    16.90 Ft-deg -100%
(3) Area from 30 deg to 40 or Flood              >     5.64 Ft-deg -100%
(4) Righting Arm at 30 deg                       >     0.66 Ft       83%
(5) Absolute Angle at MaxRA                      >    15.00 deg      12 deg
(6)  GM Upright                                  >     0.49 Ft      911%
--------------------Relative angles measured from 0.000 ---------------------
```

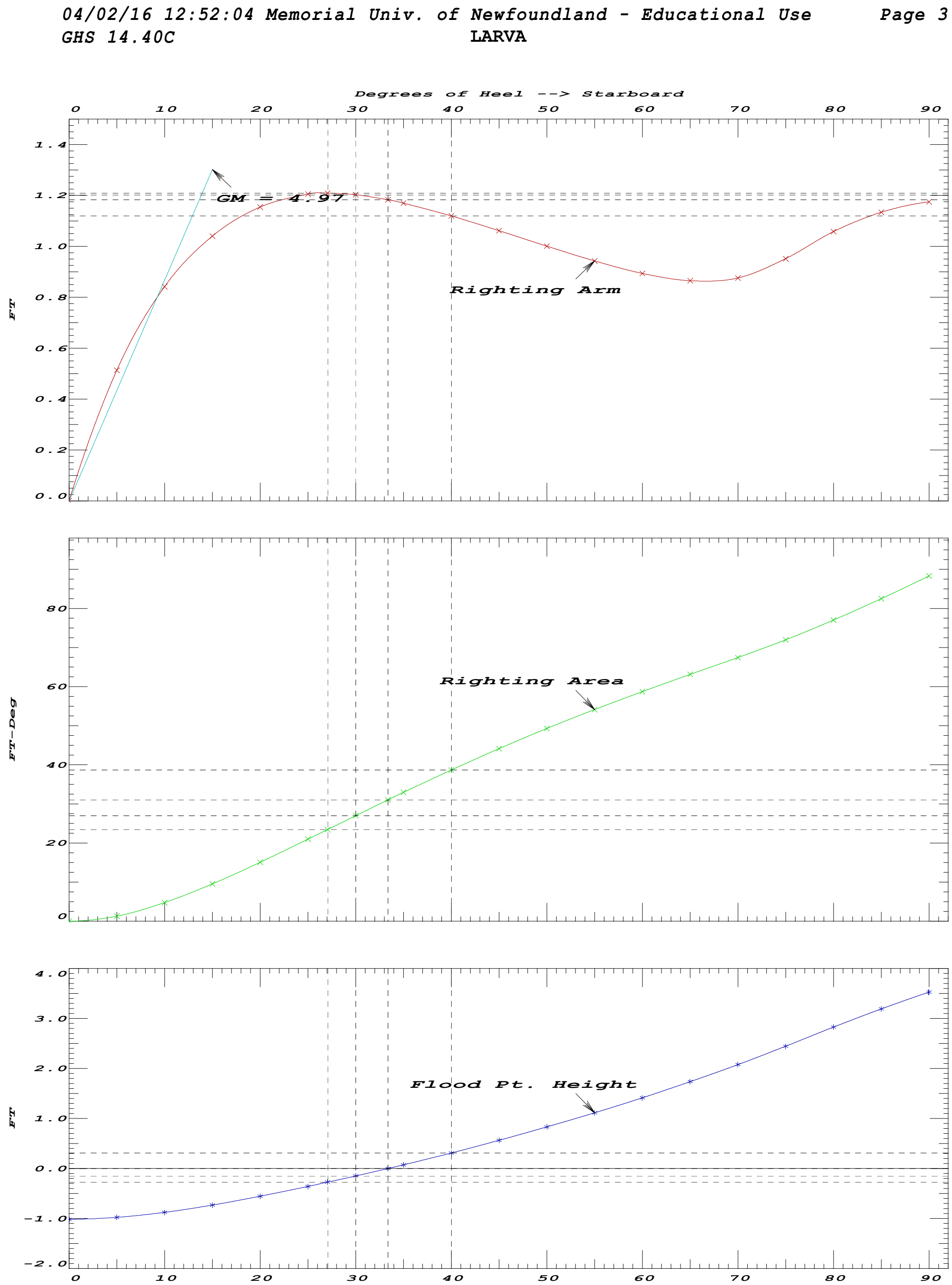
04/02/16 12:52:04 Memorial Univ. of Newfoundland - Educational Use
Page 3
GHS 14.40C
LARVA
Degrees of Heel --> Starboard
GM = 4.97
Righting Arm
FT
Righting Area
FT-Deg
Flood Pt. Height
FT

```
04/02/16 12:52:04 Memorial Univ. of Newfoundland - Educational Use        Page 4
GHS 14.40C                         LARVA

                      WEIGHT and DISPLACEMENT STATUS
                           Baseline draft: 0.929
                          Trim: zero,  Heel: zero
Part------------------------------Weight(LT)----LCG-----TCG-----VCG
WEIGHT                                 1.09    6.47a   0.00    2.24
                        SpGr------Displ(LT)----LCB-----TCB-----VCB------RefHt
KEEL                    1.025          1.08    6.66a   0.00    0.69      -0.93
BOW                     1.025          0.01   15.54a   0.00    0.82      -0.93
AFT                     1.025          0.00
BATT_COMP               1.025          0.00
  Total Displacement--> 1.025          1.09    6.76a   0.00    0.69
------------------------------------------------------------------------------
               Righting Arms:                  0.29a   0.00
Distances in FEET.------------------------------------------------------------

                      WEIGHT and DISPLACEMENT STATUS
                      Baseline draft: 1.019 @ Origin
                   Trim: Fwd 0.62 deg.,  Heel: 0.00 deg.
Part------------------------------Weight(LT)----LCG-----TCG-----VCG
WEIGHT                                 1.09    6.47a   0.00    2.24
                        SpGr------Displ(LT)----LCB-----TCB-----VCB------RefHt
KEEL                    1.025          1.07    6.45a   0.00    0.69      -1.02
BOW                     1.025          0.01   15.45a   0.00    0.77      -1.02
AFT                     1.025          0.01    1.21a   0.02p   0.99      -1.02
BATT_COMP               1.025          0.00
  Total Displacement--> 1.025          1.09    6.45a   0.00    0.69
------------------------------------------------------------------------------
               Righting Arms:                  0.00    0.00
Distances in FEET.------------------------------------------------------------
```

CG - Draft: 1.02 @ 0.00   Trim: fwd 0.62 deg. Heel : 0.00 deg.

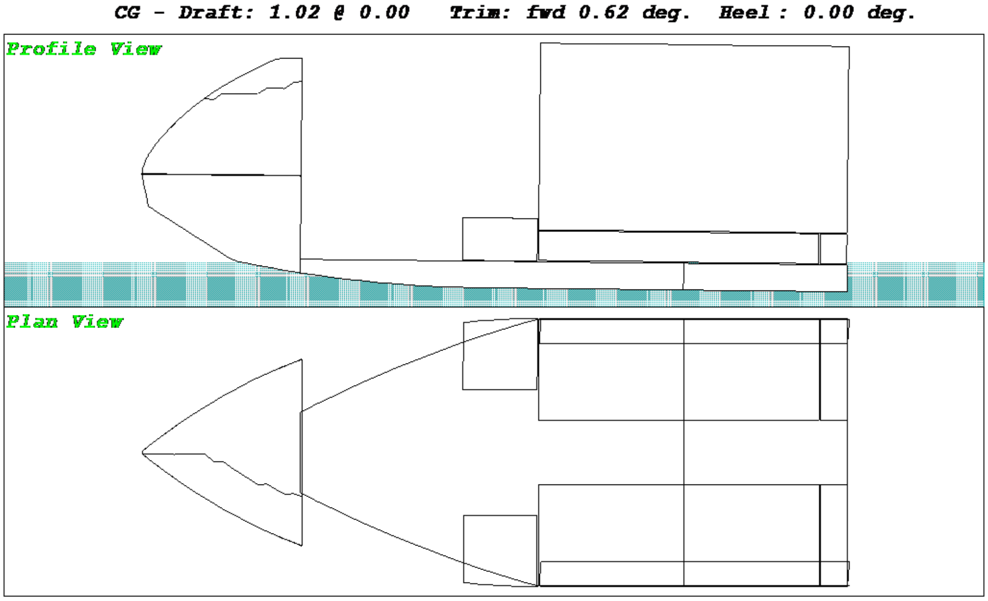

Appendix B: GUI Analysis of LARVA Reponse in the Following State

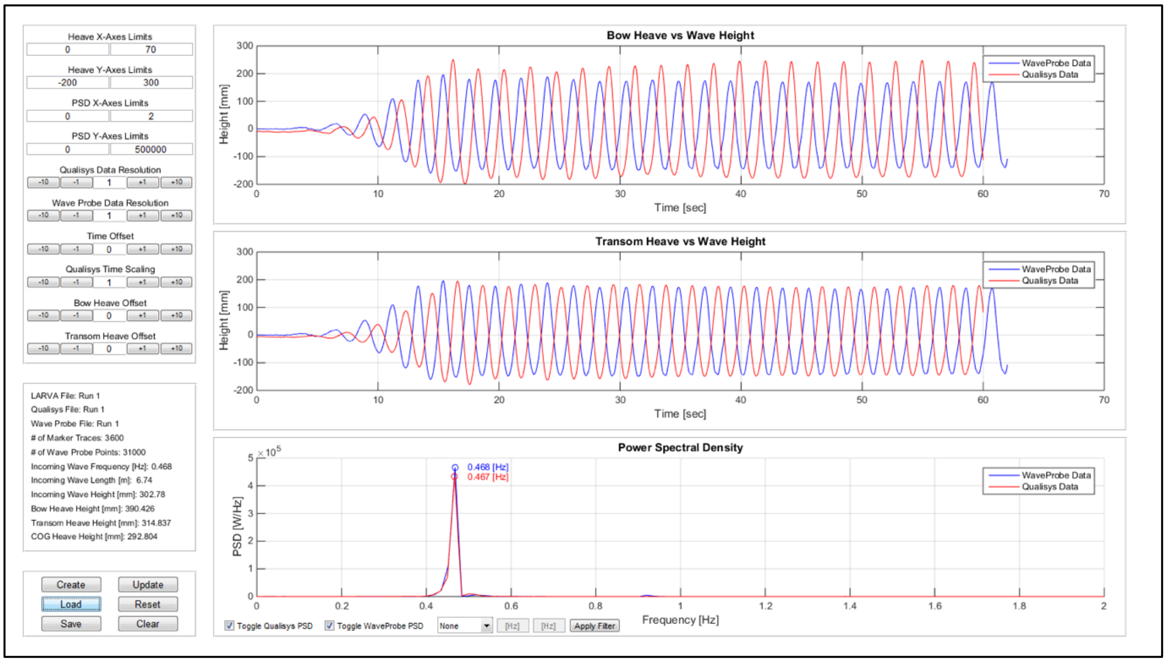

Analysis of LARVA response in the following state to an incoming wave set with a frequency of 0.46Hz and a height of 302mm.

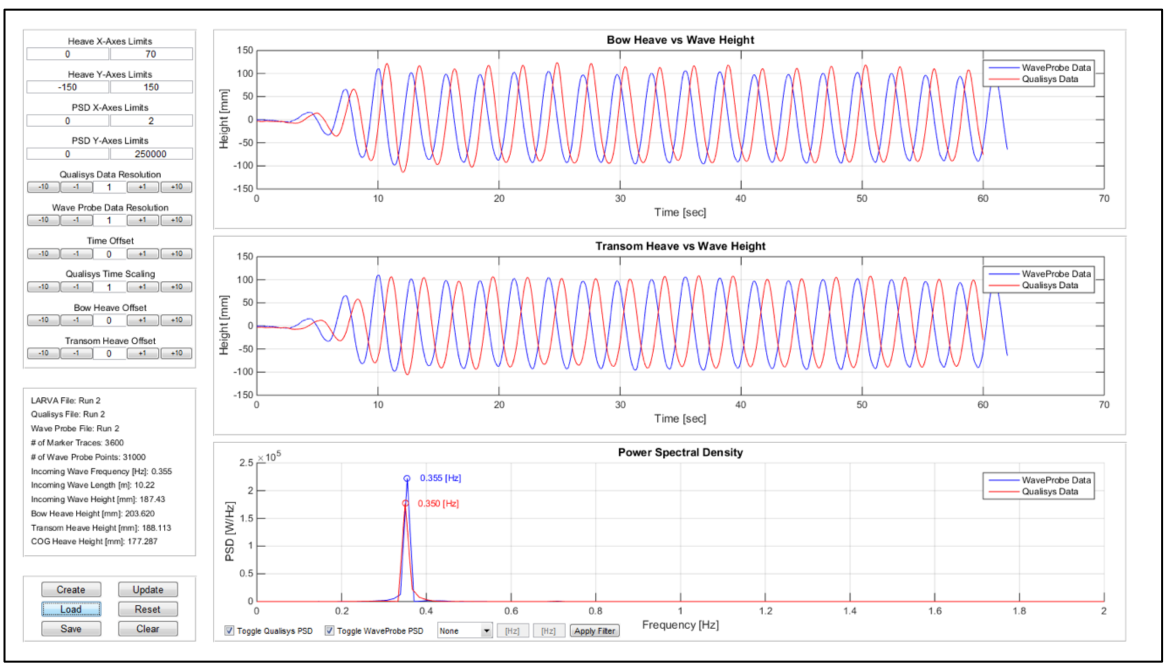

Analysis of LARVA response in the following state to an incoming wave set with a frequency of 0.36Hz and a height of 187mm.

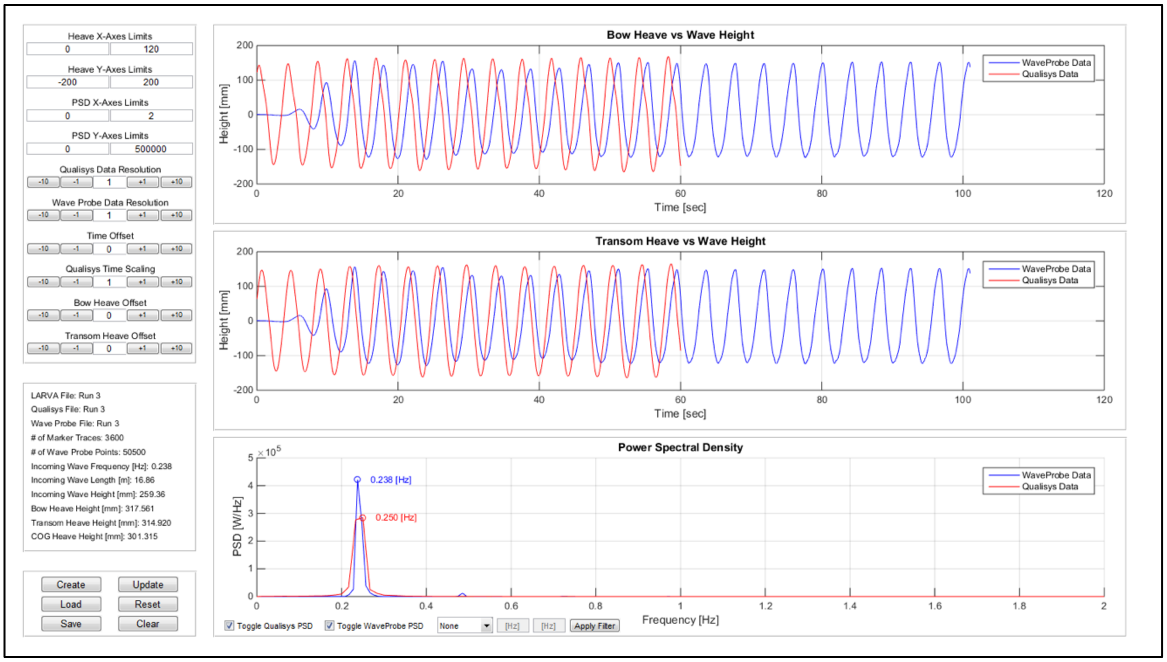

Analysis of LARVA response in the following state to an incoming wave set with a frequency of 0.24Hz and a height of 259mm.

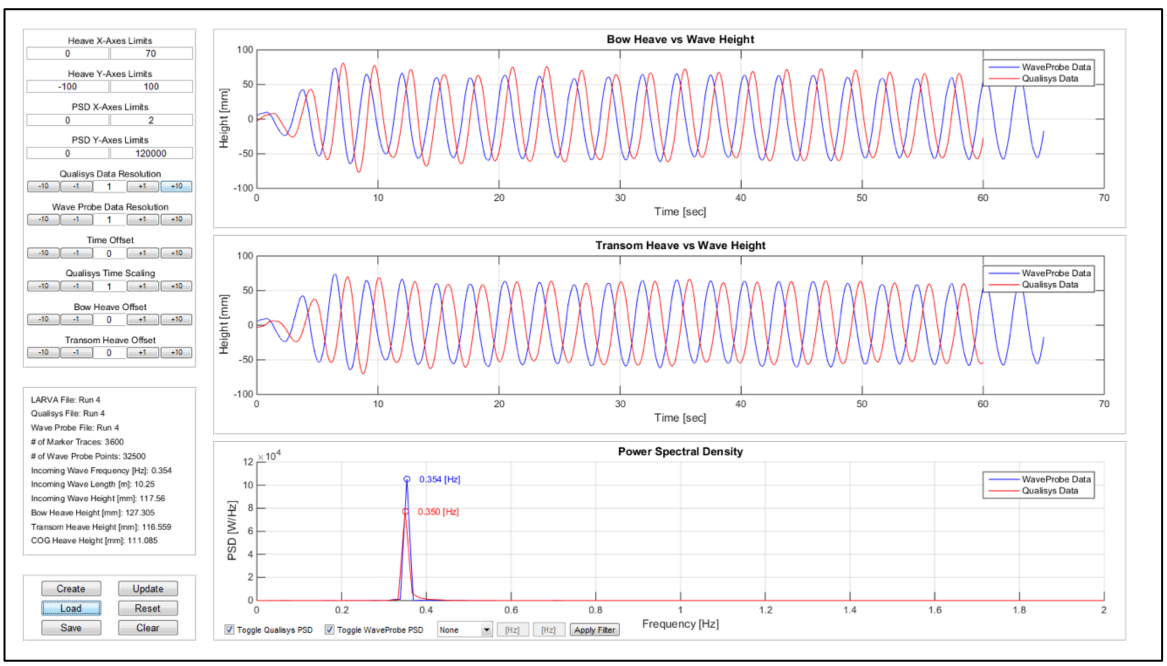

Analysis of LARVA response in the following state to an incoming wave set with a frequency of 0.35Hz and a height of 118mm.

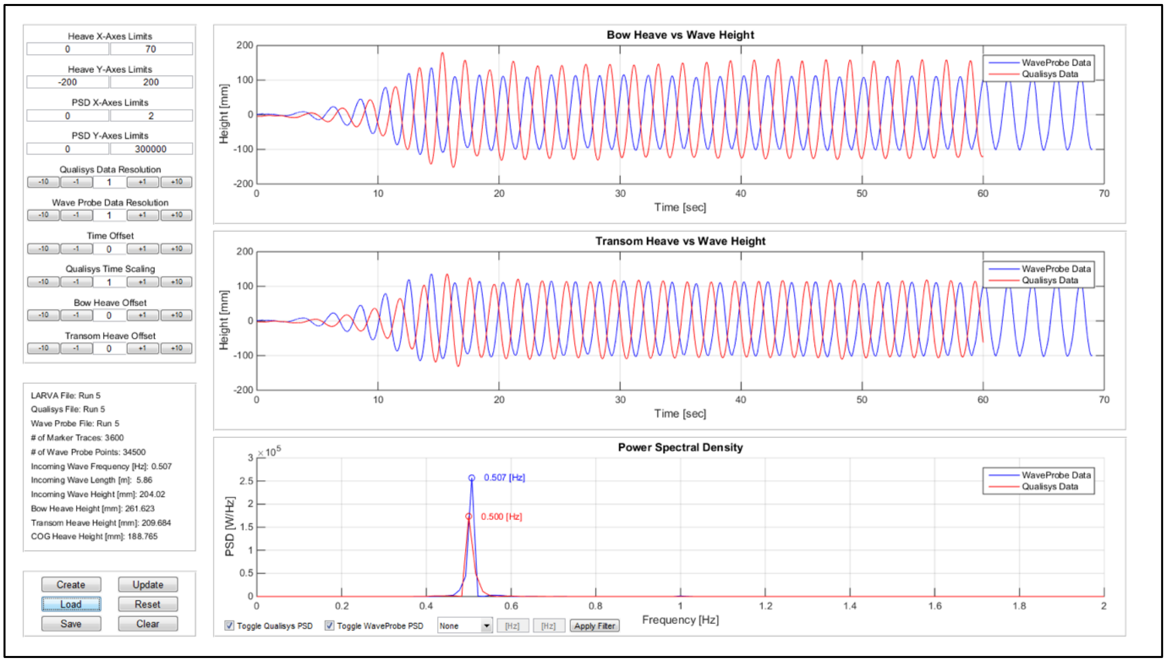

Analysis of LARVA response in the following state to an incoming wave set with a frequency of 0.51Hz and a height of 204mm.

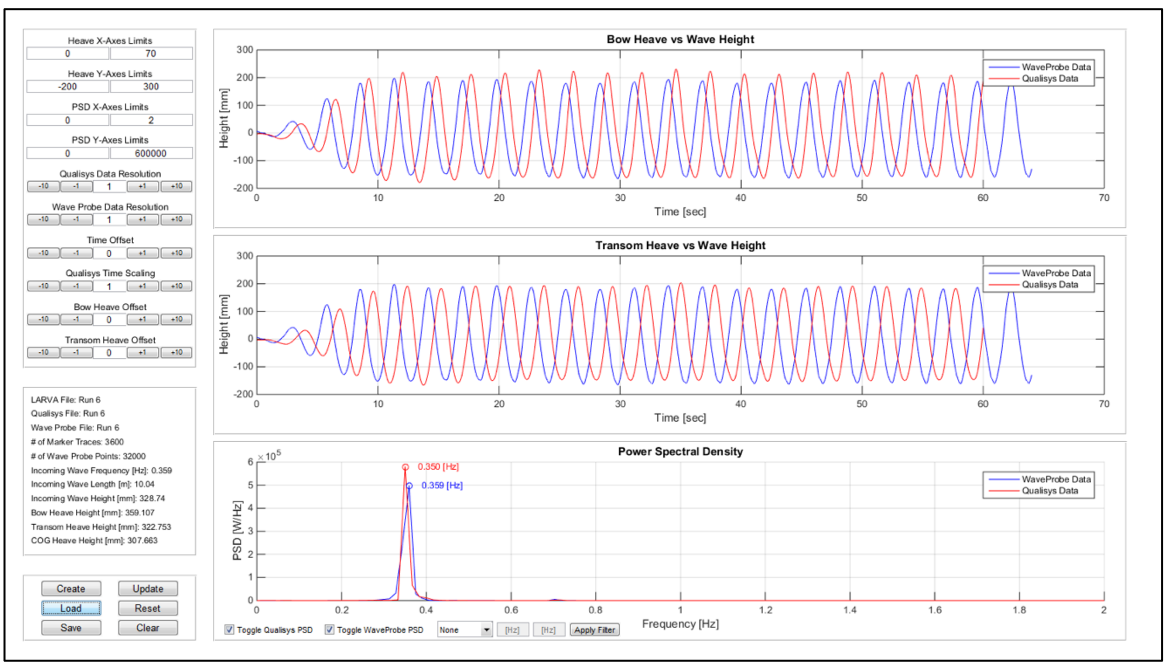

Analysis of LARVA response in the following state to an incoming wave set with a frequency of 0.36Hz and a height of 329mm.

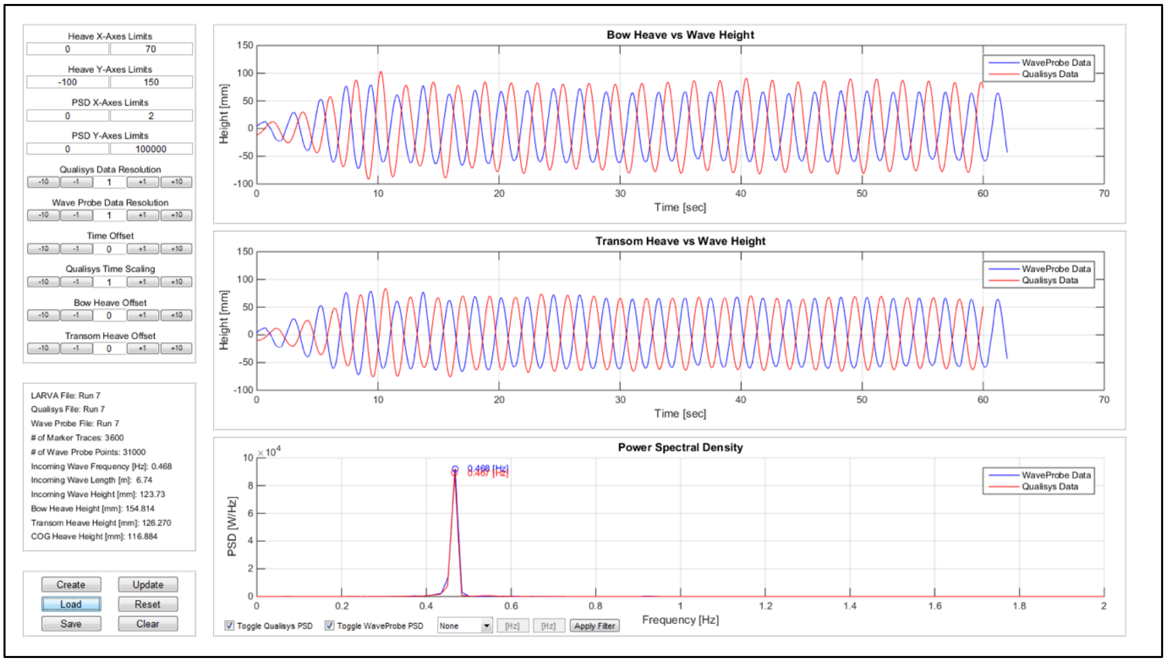

Analysis of LARVA response in the following state to an incoming wave set with a frequency of 0.46 Hz and a height of 124mm.

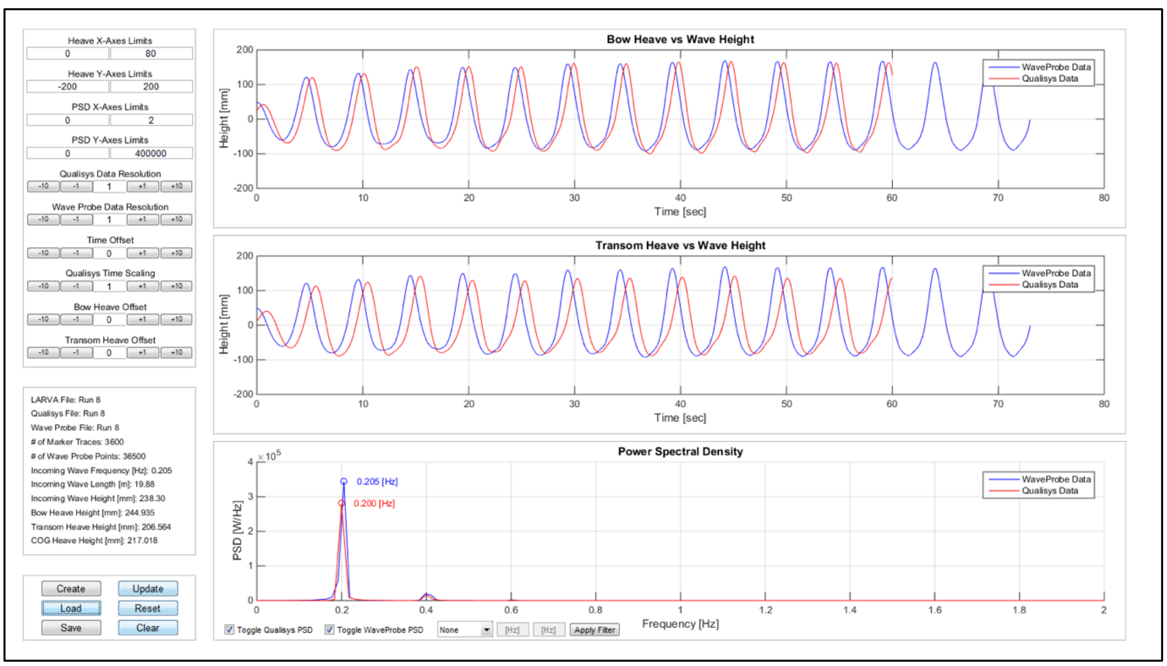

Analysis of LARVA response in the following state to an incoming wave set with a frequency of 0.21Hz and a height of 238mm.

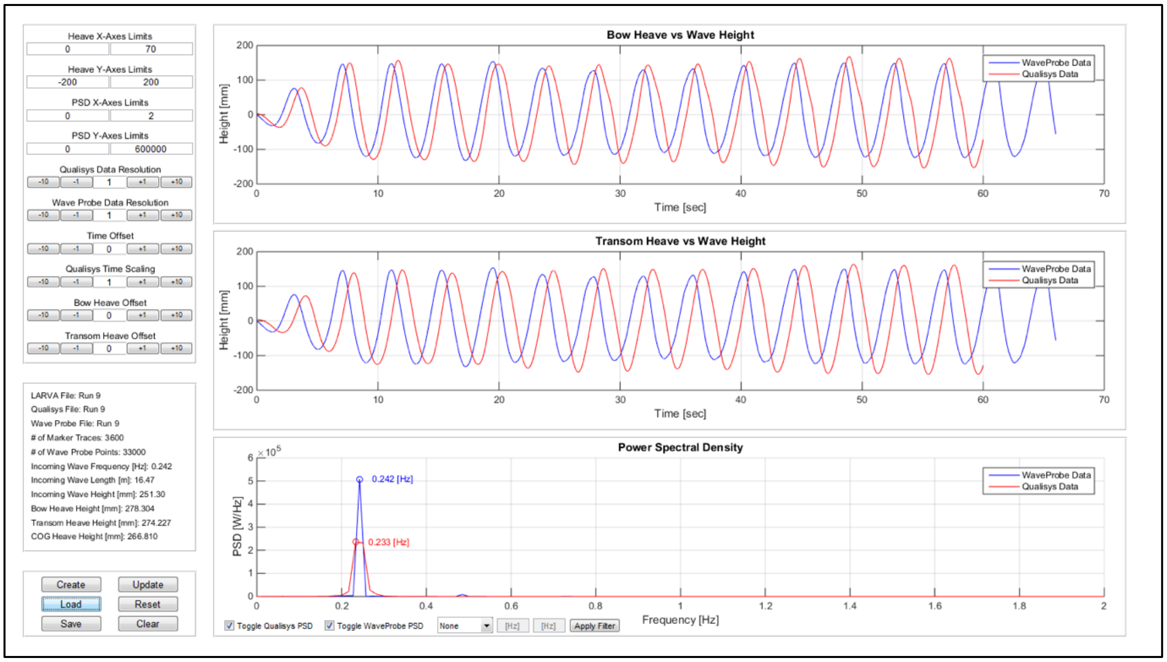

Analysis of LARVA response in the following state to an incoming wave set with a frequency of 0.24Hz and a height of 251mm.

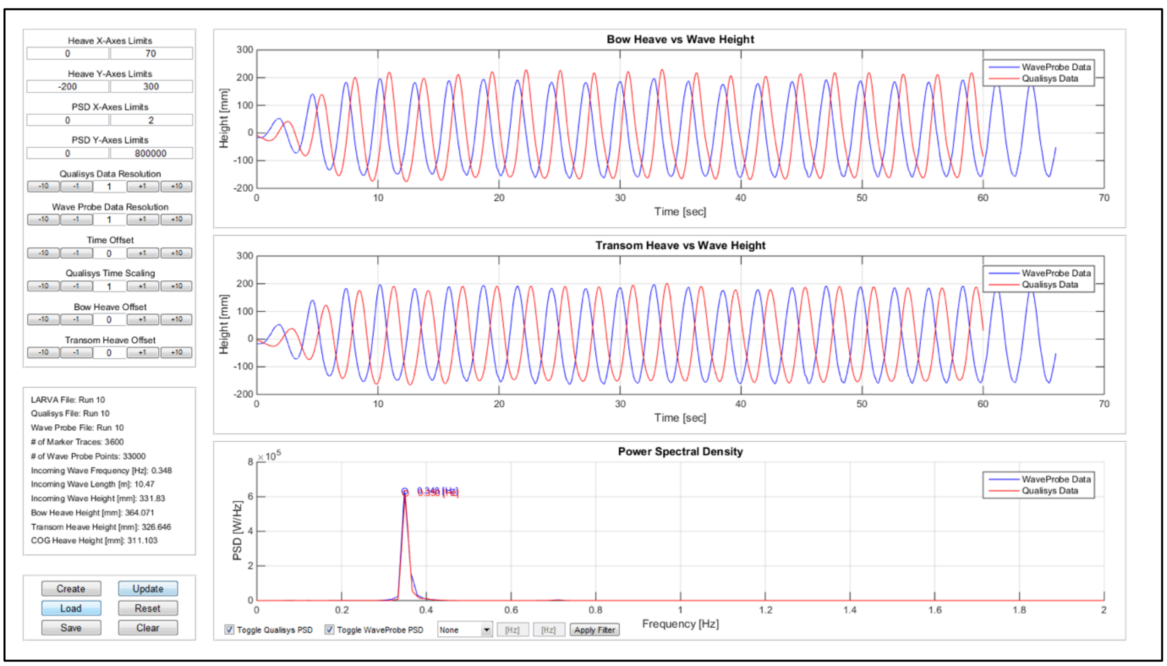

Analysis of LARVA response in the following state to an incoming wave set with a frequency of 0.35Hz and a height of 332mm.

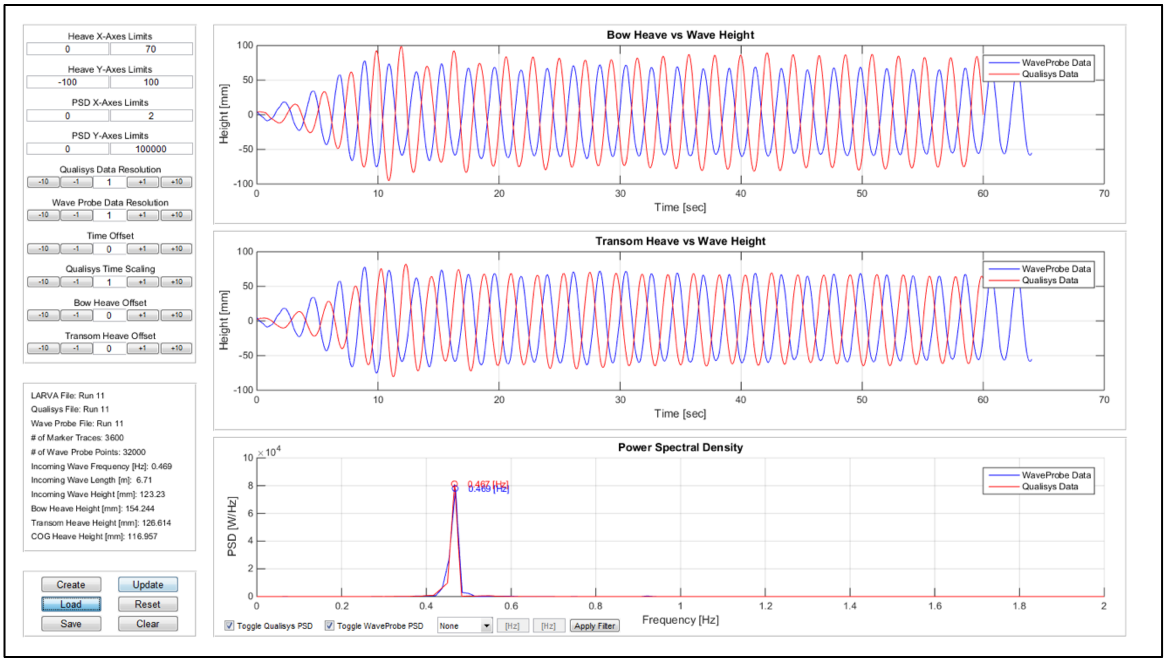

Analysis of LARVA response in the following state to an incoming wave set with a frequency of 0.47Hz and a height of 123mm.

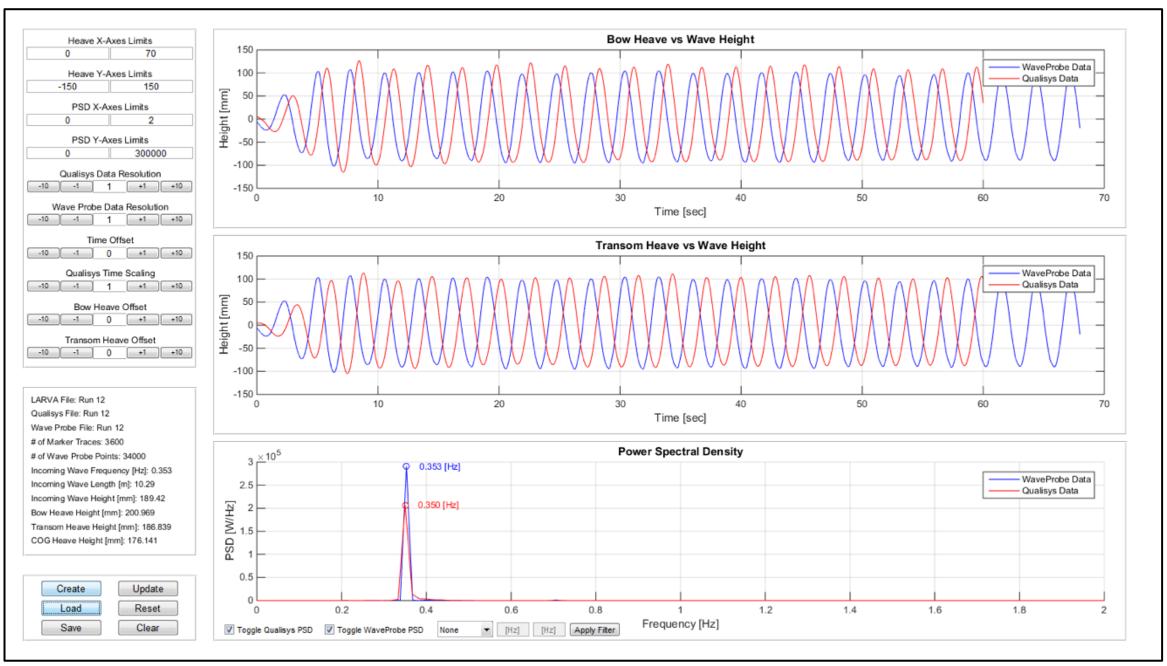

Analysis of LARVA response in the following state to an incoming wave set with a frequency of 0.35Hz and a height of 189mm.

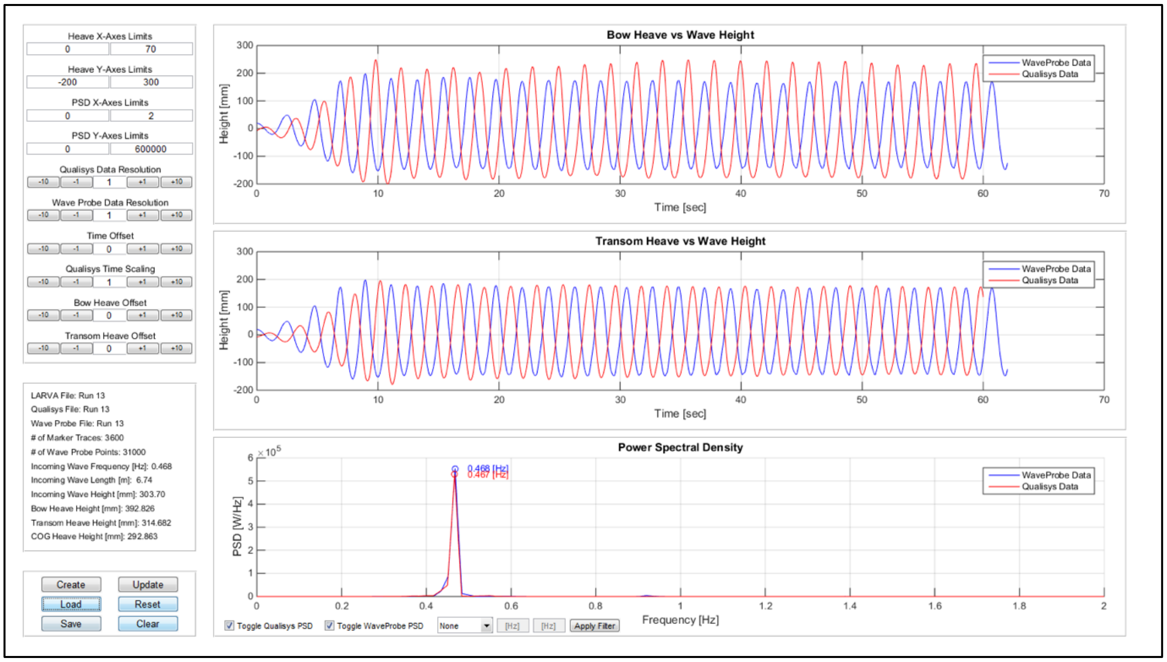

Analysis of LARVA response in the following state to an incoming wave set with a frequency of 0.46Hz and a height of 304mm.

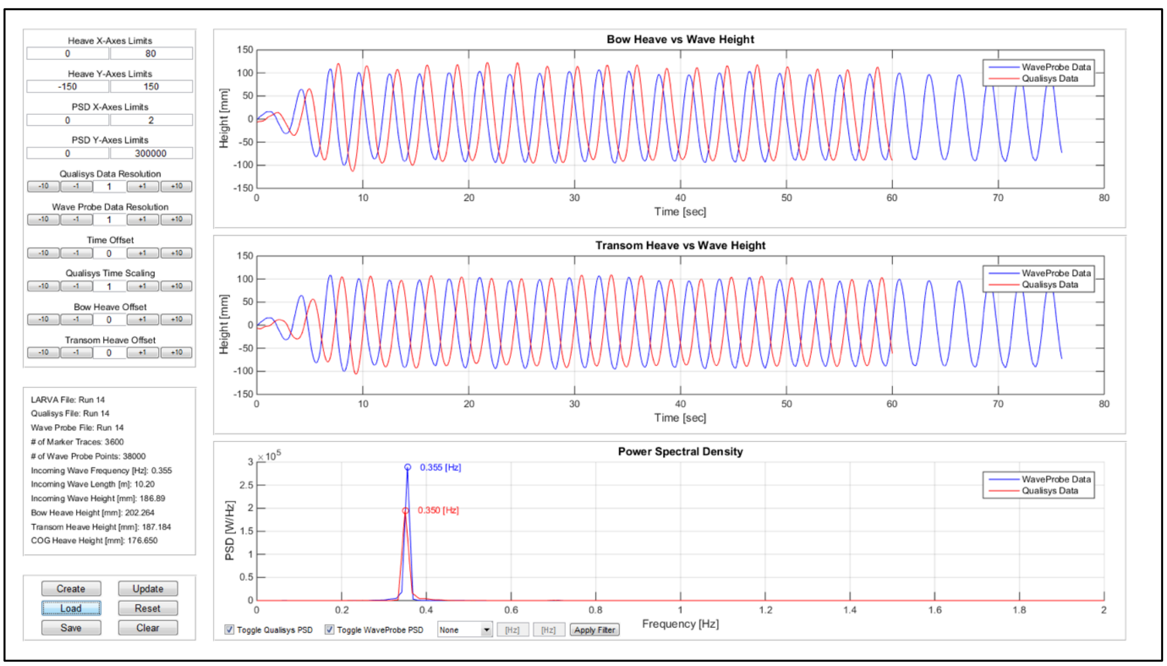

Analysis of LARVA response in the following state to an incoming wave set with a frequency of 0.37Hz and a height of 187mm.

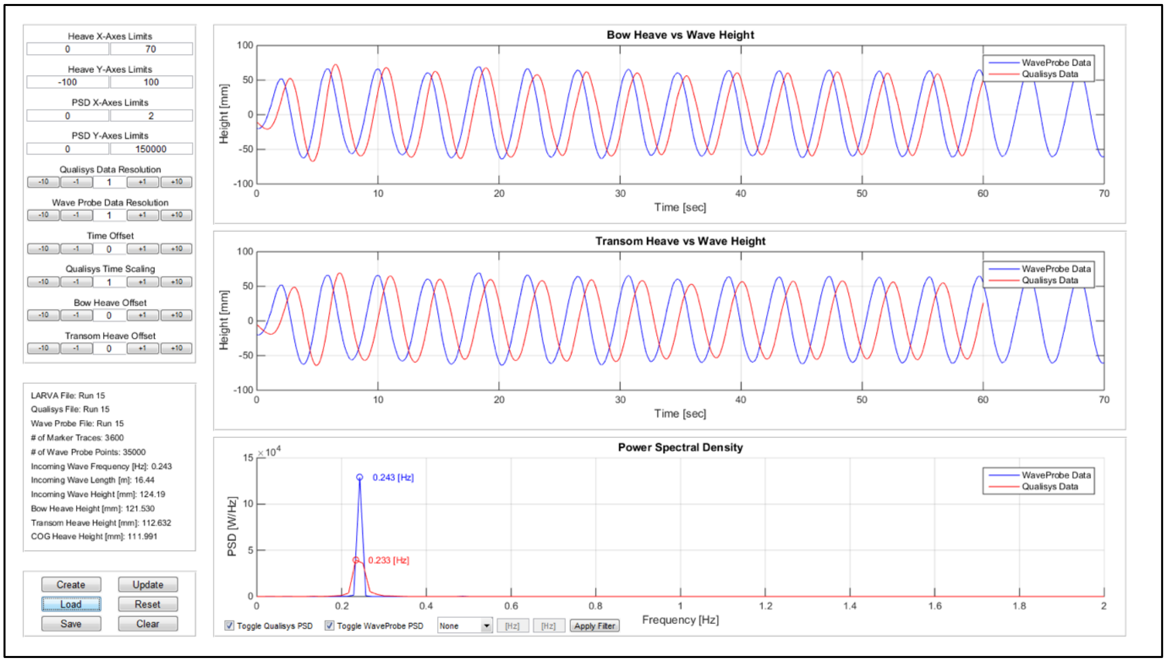

Analysis of LARVA response in the following state to an incoming wave set with a frequency of 0.24Hz and a height of 124mm.

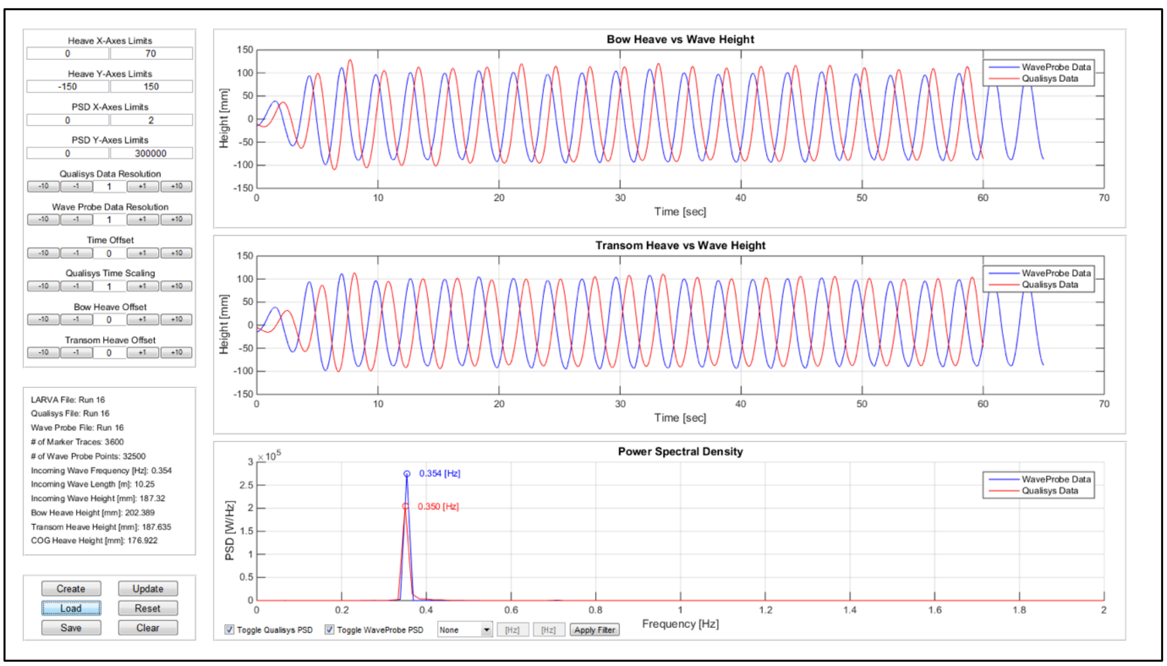

Analysis of LARVA response in the following state to an incoming wave set with a frequency of 0.35Hz and a height of 187mm.

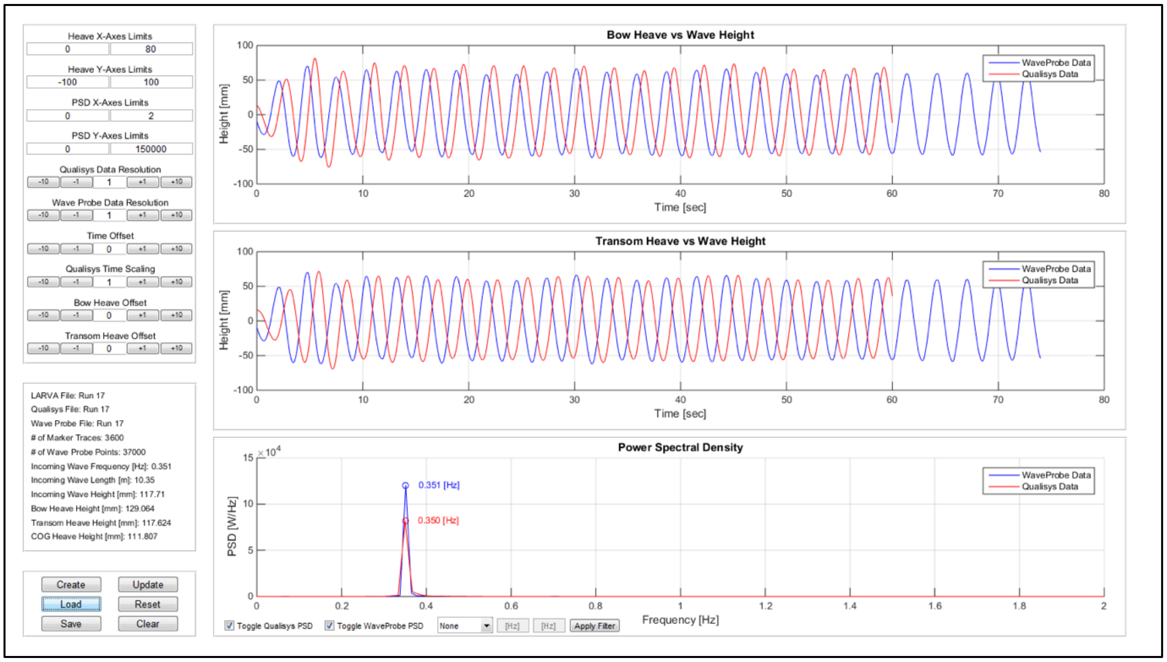

Analysis of LARVA response in the following state to an incoming wave set with a frequency of 0.35Hz and a height of 117mm.

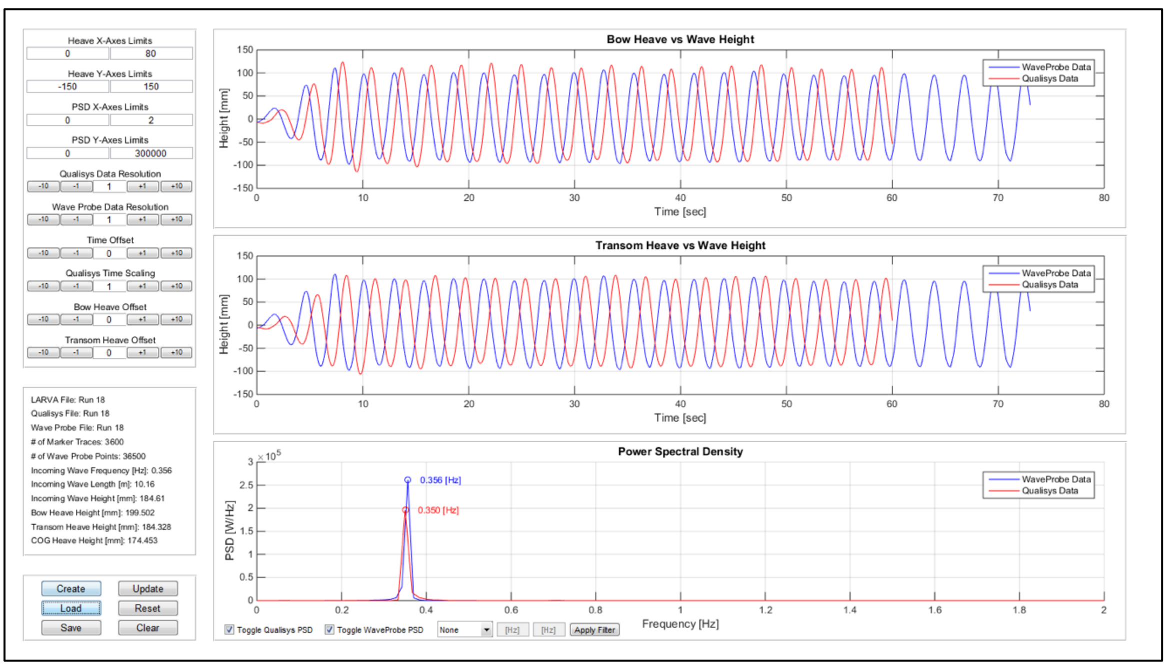

Analysis of LARVA response in the following state to an incoming wave set with a frequency of 0.36Hz and a height of 184mm.

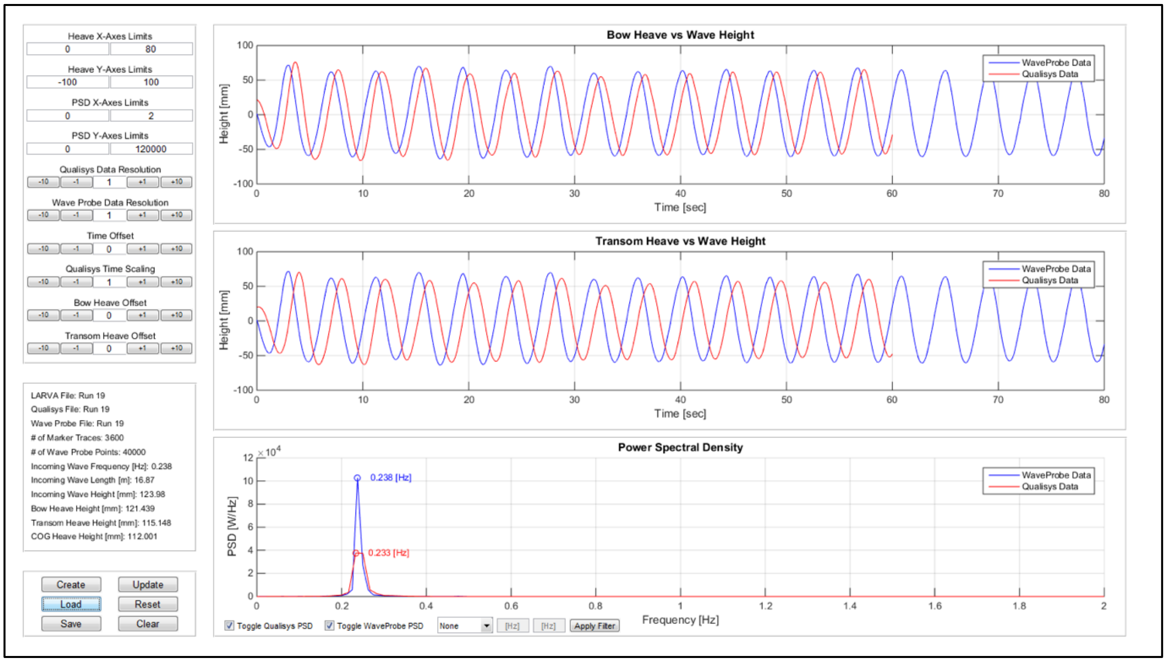

Analysis of LARVA response in the following state to an incoming wave set with a frequency of 0.24Hz and a height of 124mm.

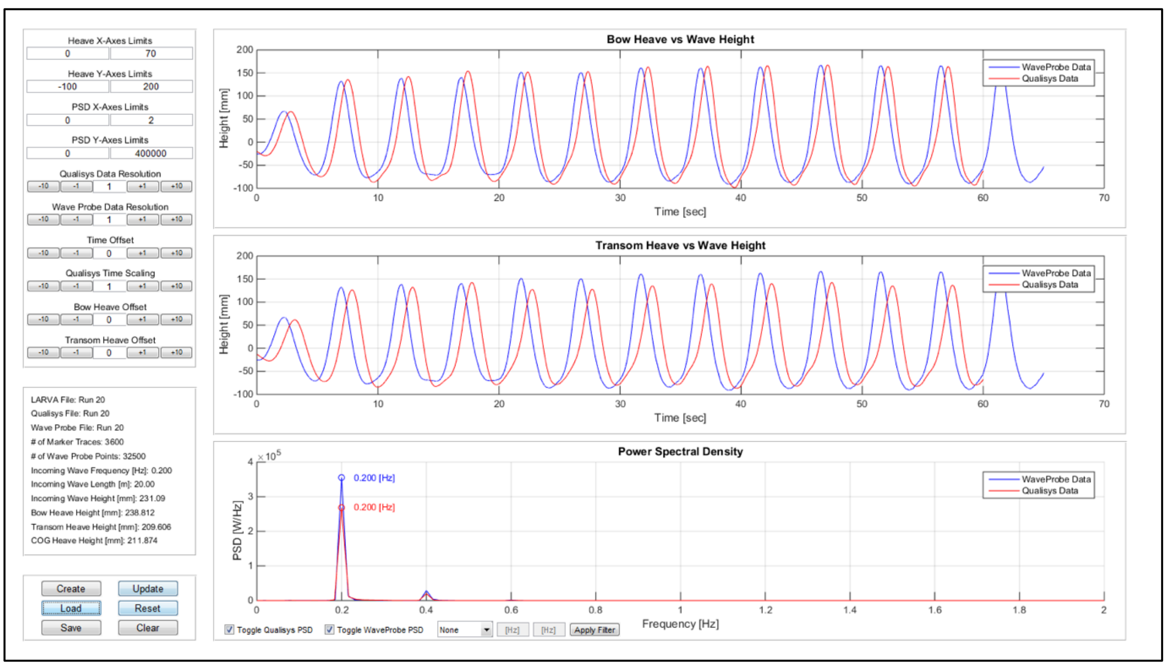

Analysis of LARVA response in the following state to an incoming wave set with a frequency of 0.20Hz and a height of 231mm.

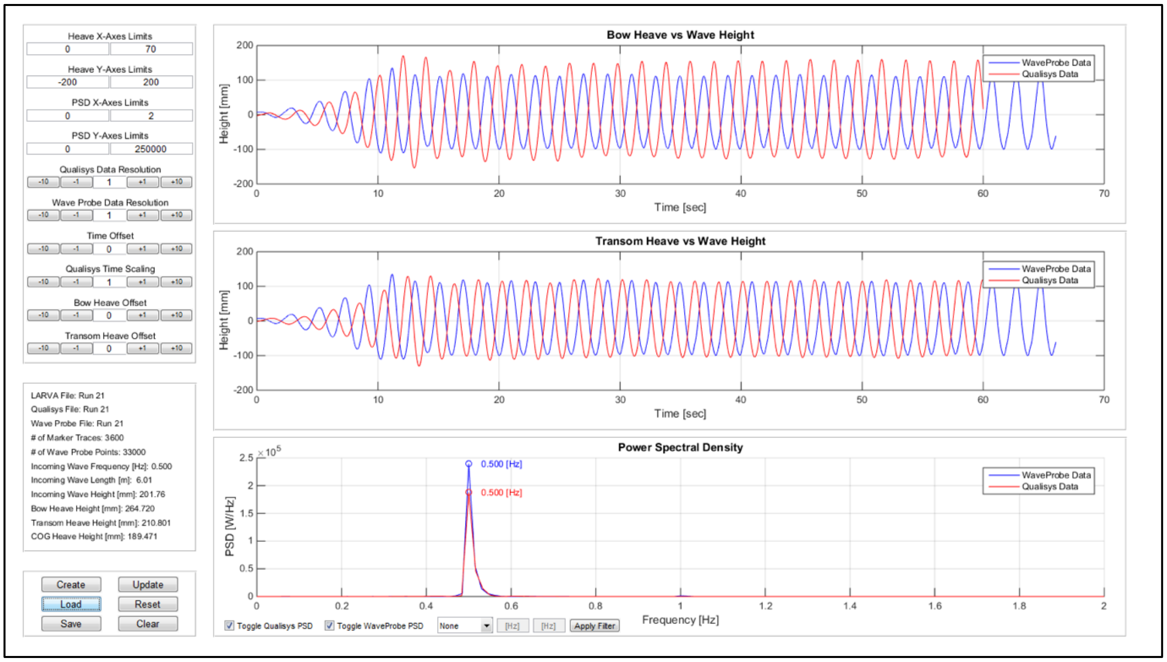

Analysis of LARVA response in the following state to an incoming wave set with a frequency of 0.50Hz and a height of 202mm.

Appendix C: GUI Analysis of LARVA Reponse in the Launching State

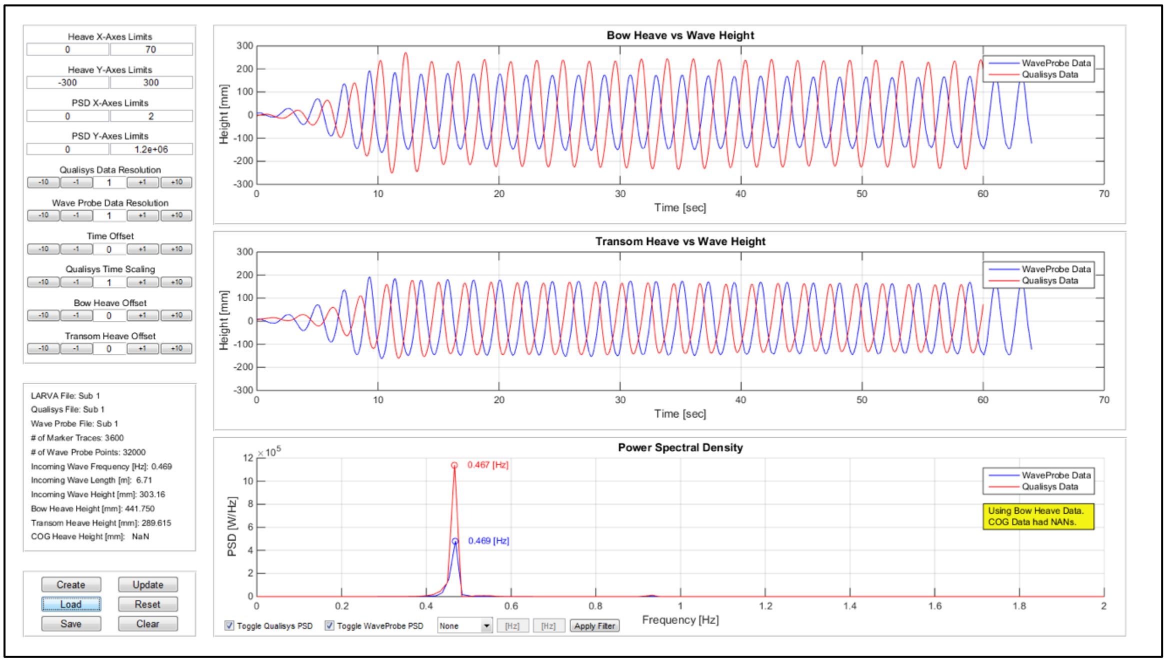

Analysis of LARVA response in the launching state to an incoming wave set with a frequency of 0.47Hz and a height of 303mm.

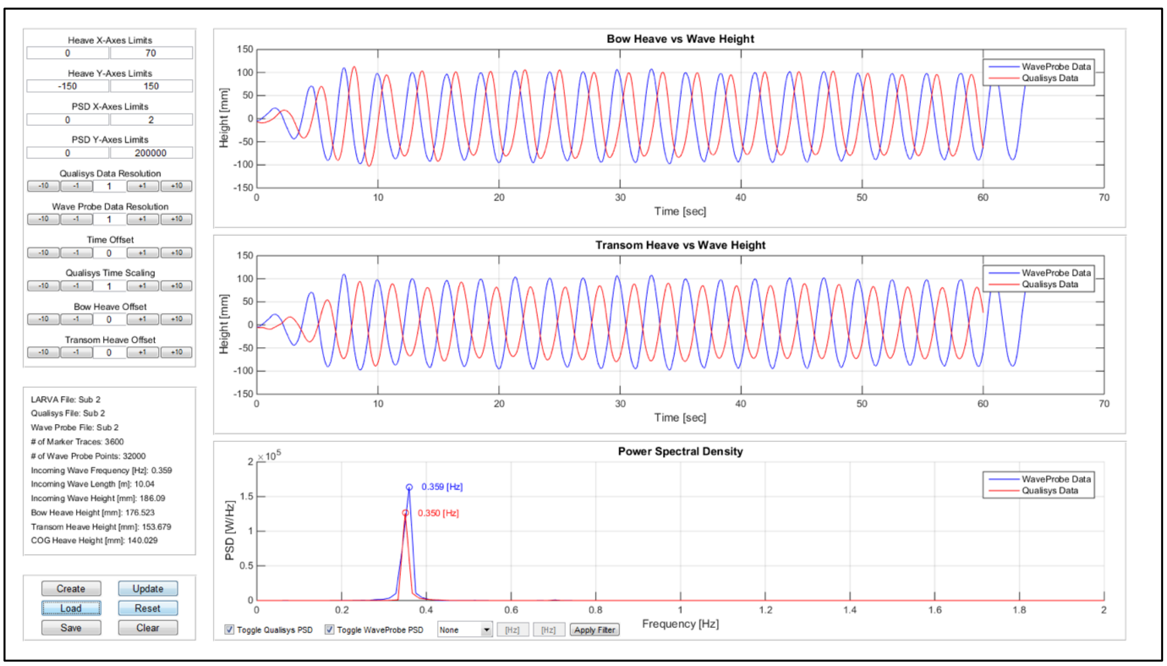

Analysis of LARVA response in the launching state to an incoming wave set with a frequency of 0.36Hz and a height of 186mm.

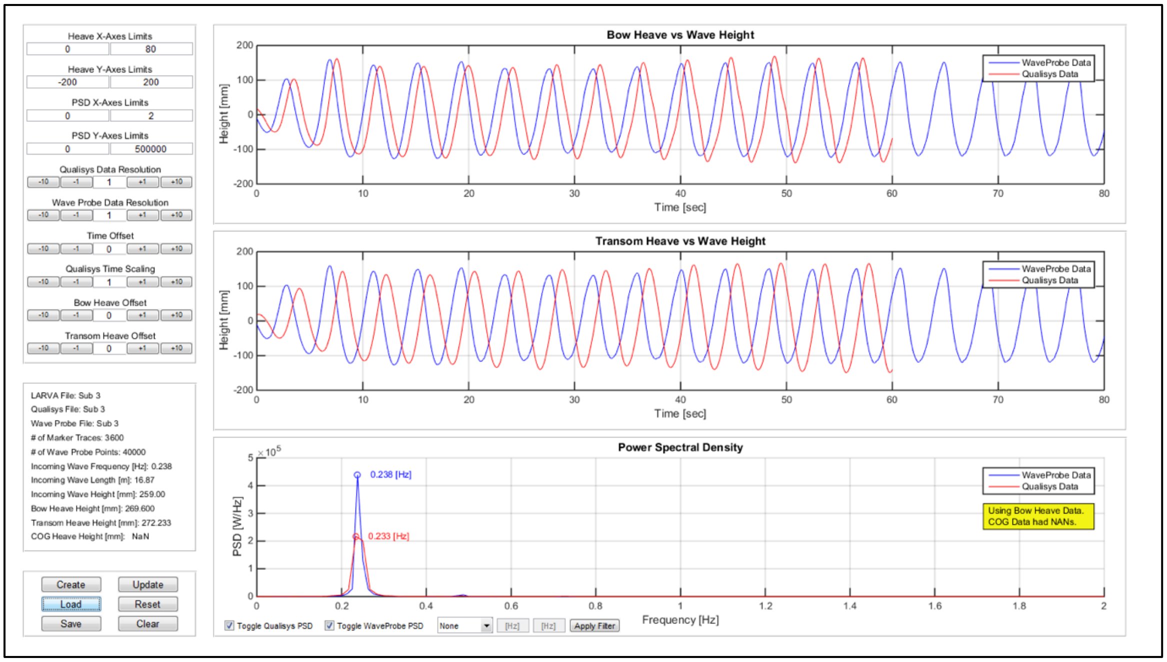

Analysis of LARVA response in the launching state to an incoming wave set with a frequency of 0.24Hz and a height of 259mm.

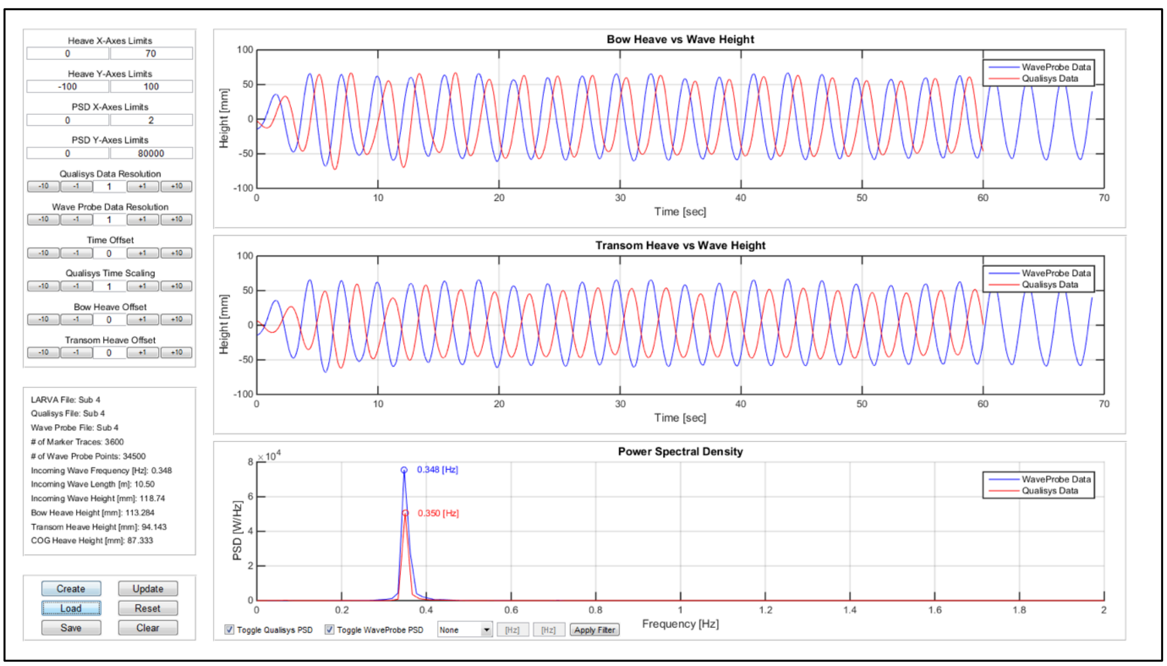

Analysis of LARVA response in the launching state to an incoming wave set with a frequency of 0.35Hz and a height of 119mm.

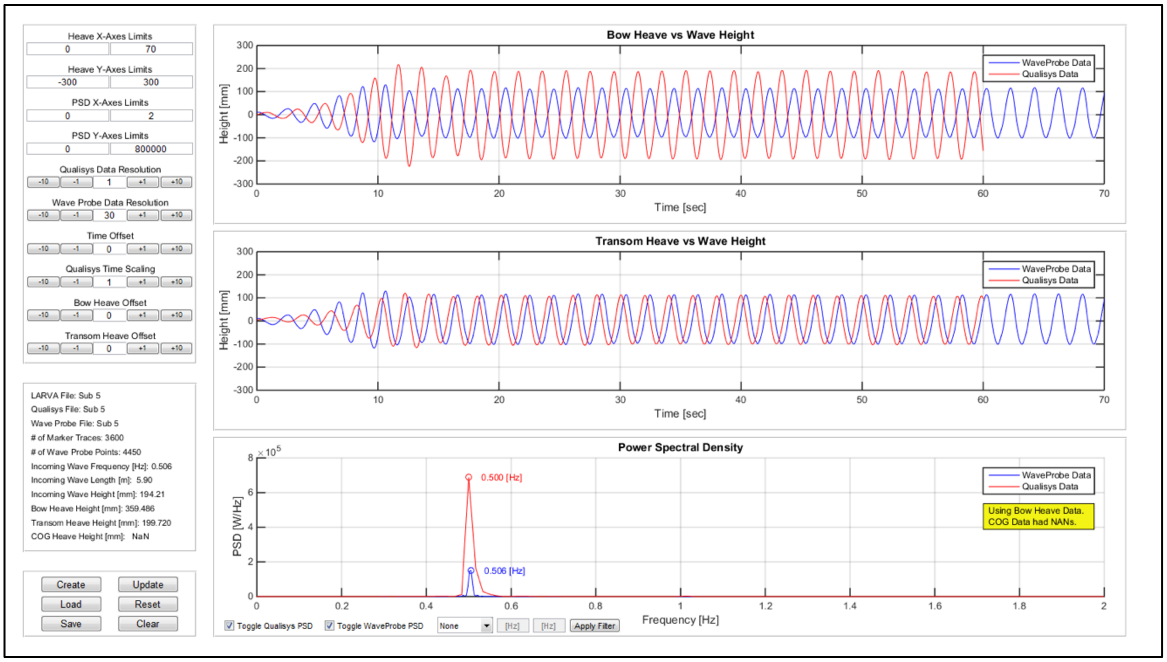

Analysis of LARVA response in the launching state to an incoming wave set with a frequency of 0.51Hz and a height of 194mm.

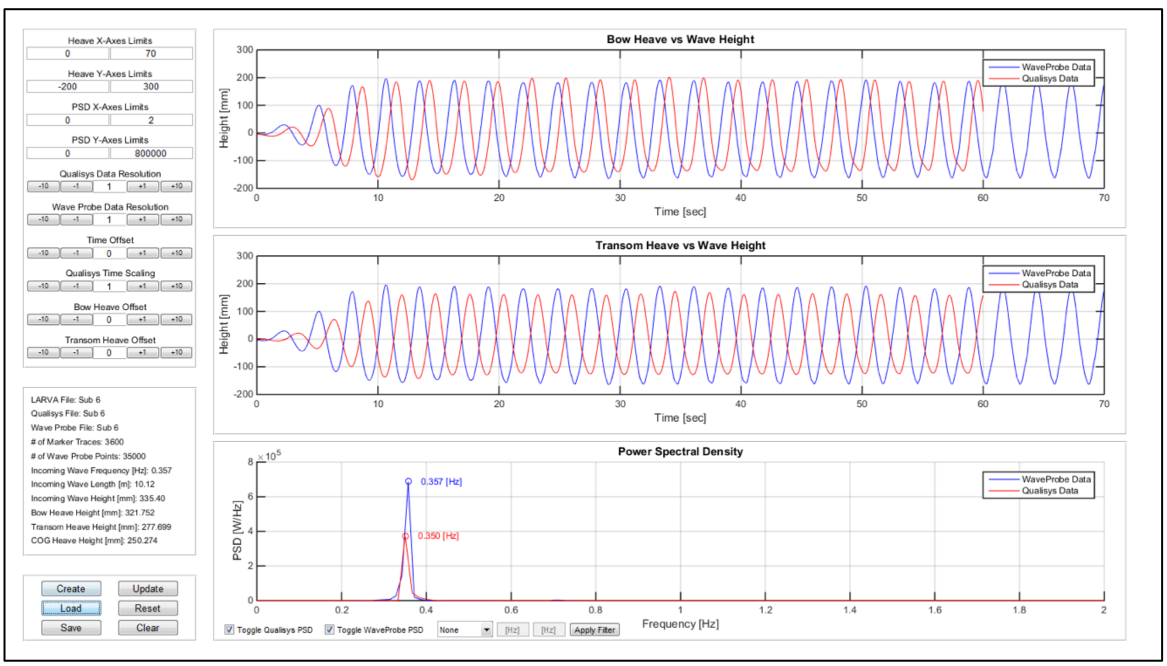

Analysis of LARVA response in the launching state to an incoming wave set with a frequency of 0.36Hz and a height of 335mm.

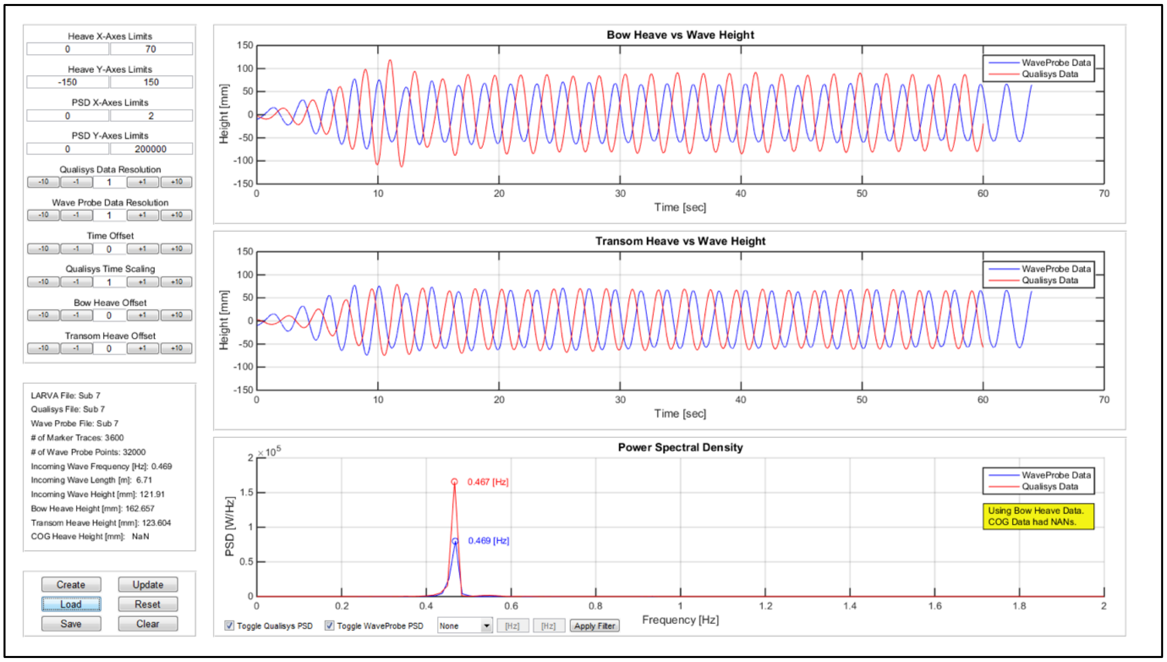

Analysis of LARVA response in the launching state to an incoming wave set with a frequency of 0.47Hz and a height of 122mm.

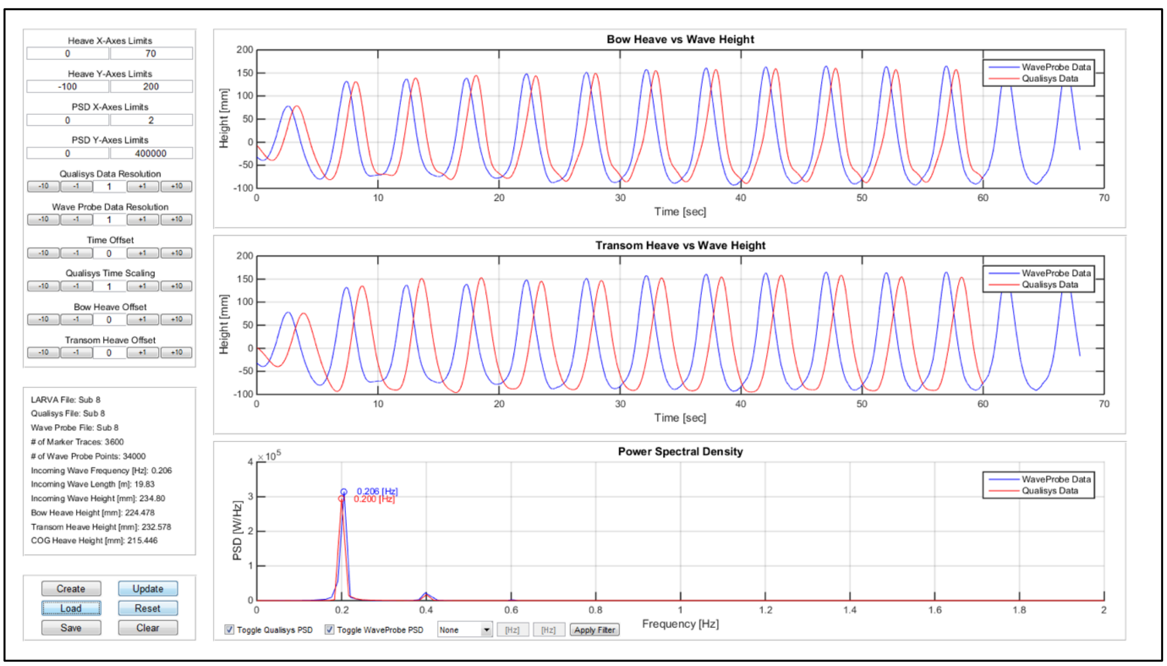

Analysis of LARVA response in the launching state to an incoming wave set with a frequency of 0.21Hz and a height of 235mm.

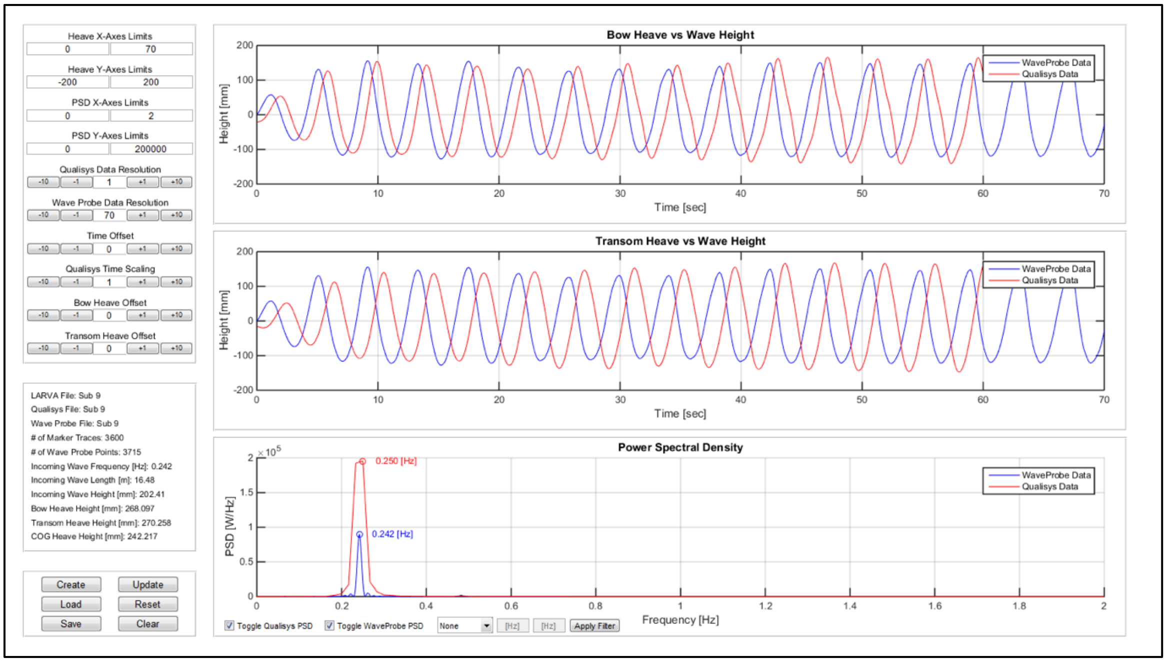

Analysis of LARVA response in the launching state to an incoming wave set with a frequency of 0.24Hz and a height of 202mm.

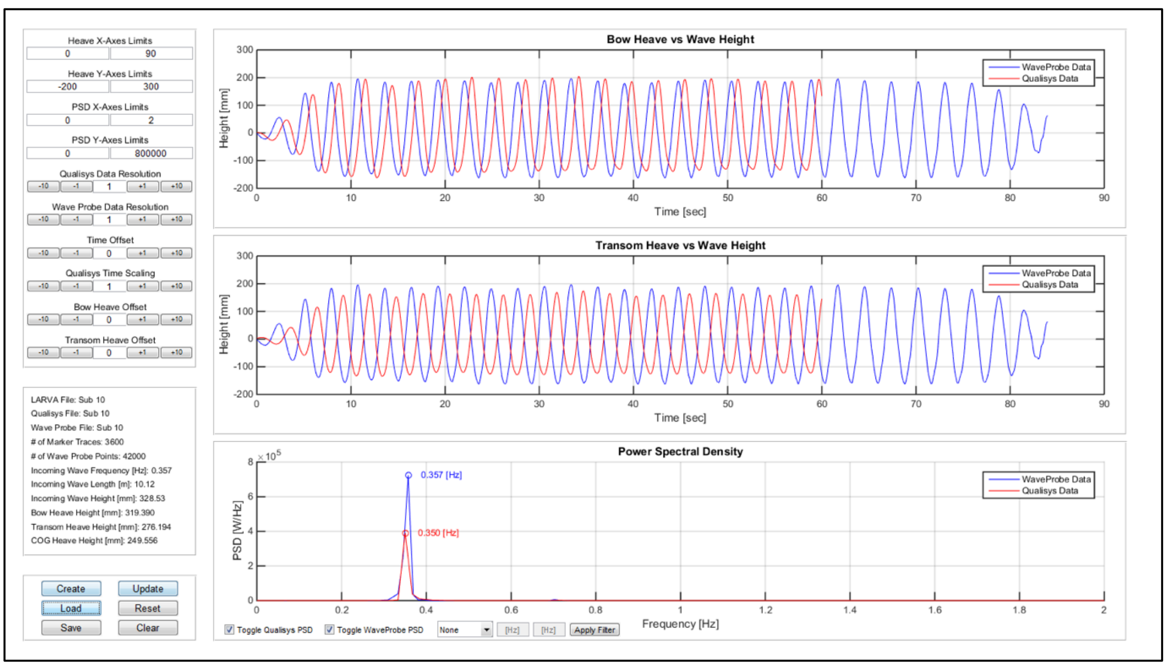

Analysis of LARVA response in the launching state to an incoming wave set with a frequency of 0.36Hz and a height of 329mm.

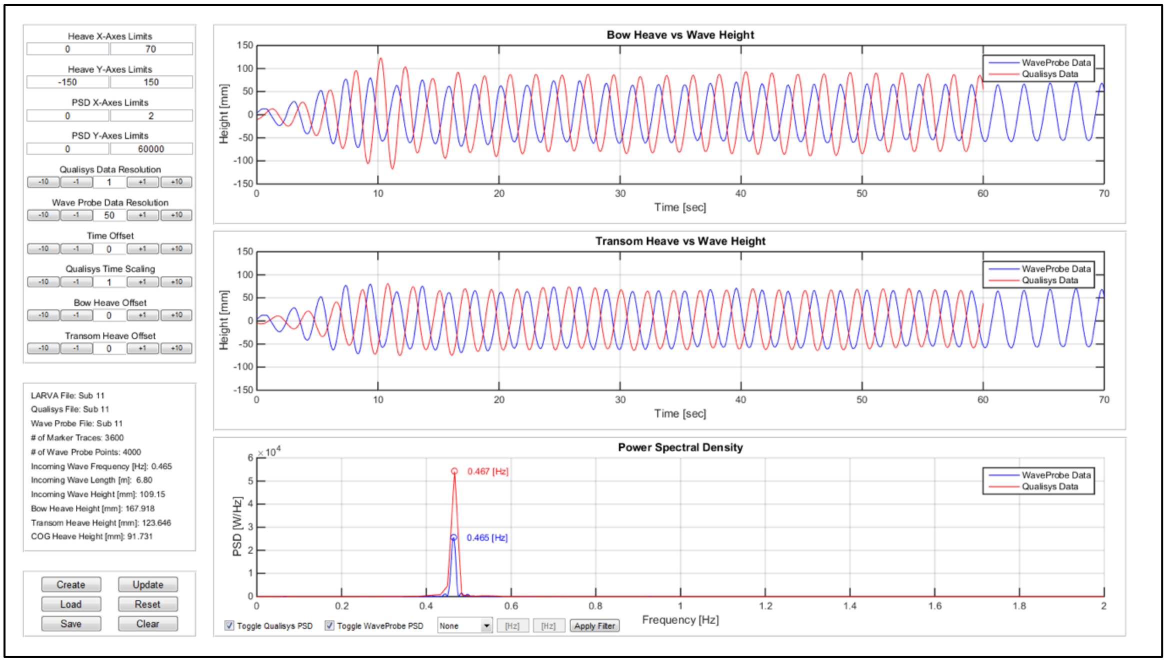

Analysis of LARVA response in the launching state to an incoming wave set with a frequency of 0.47Hz and a height of 109mm.

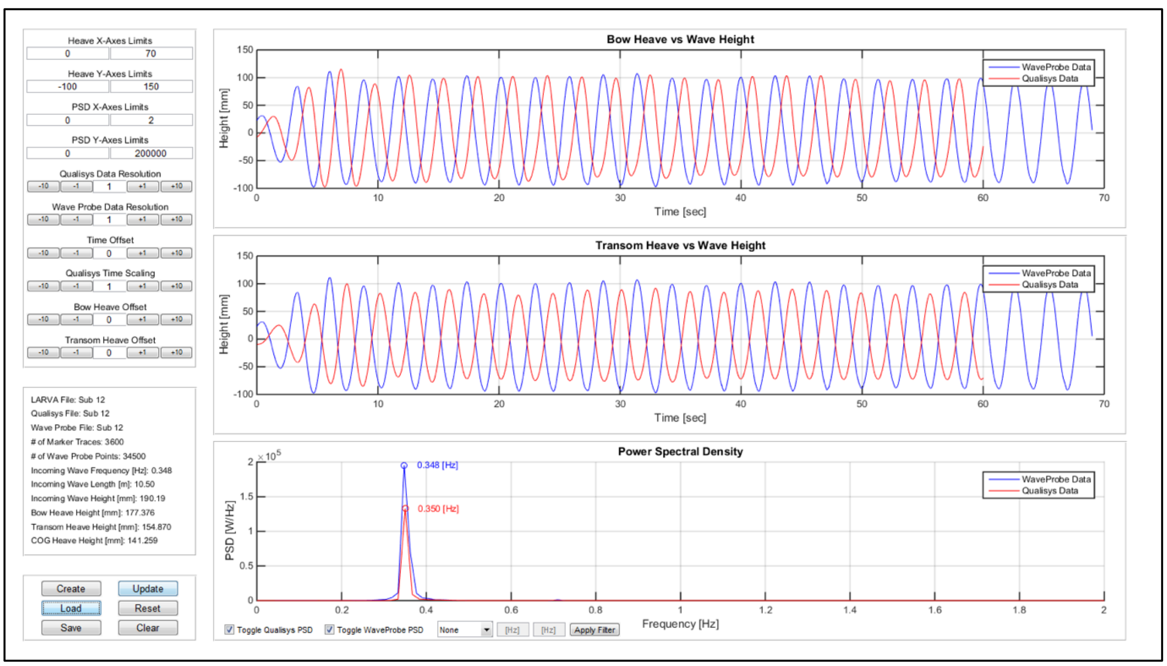

Analysis of LARVA response in the launching state to an incoming wave set with a frequency of 0.35Hz and a height of 190mm.

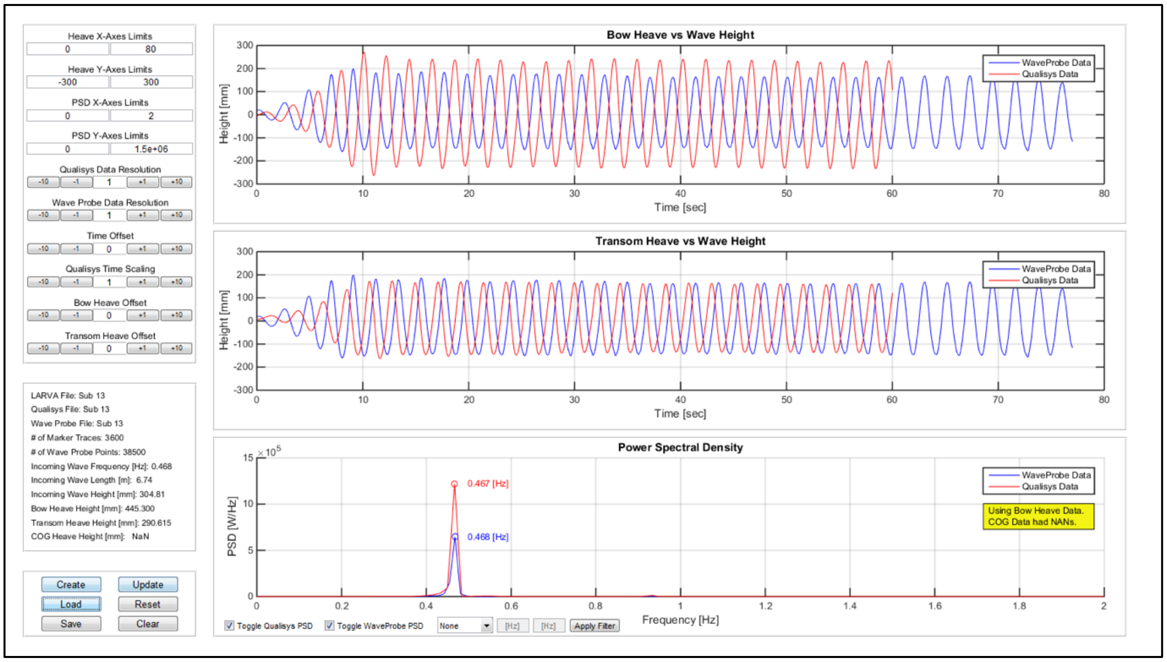

Analysis of LARVA response in the launching state to an incoming wave set with a frequency of 0.47Hz and a height of 305mm.

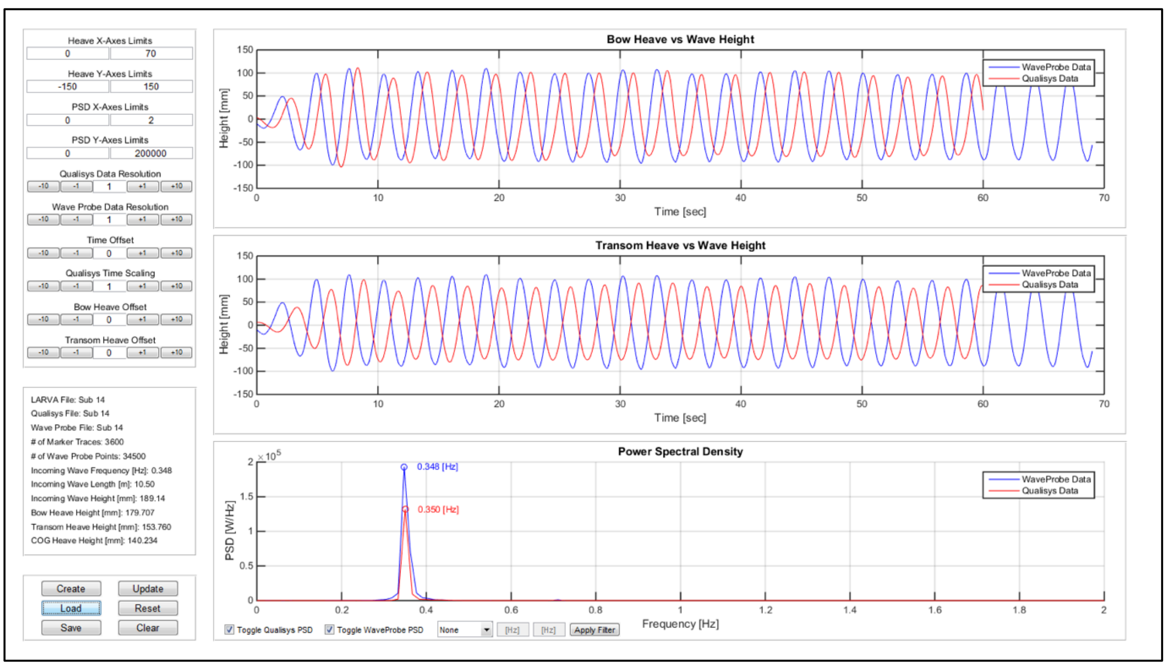

Analysis of LARVA response in the launching state to an incoming wave set with a frequency of 0.35Hz and a height of 189mm.

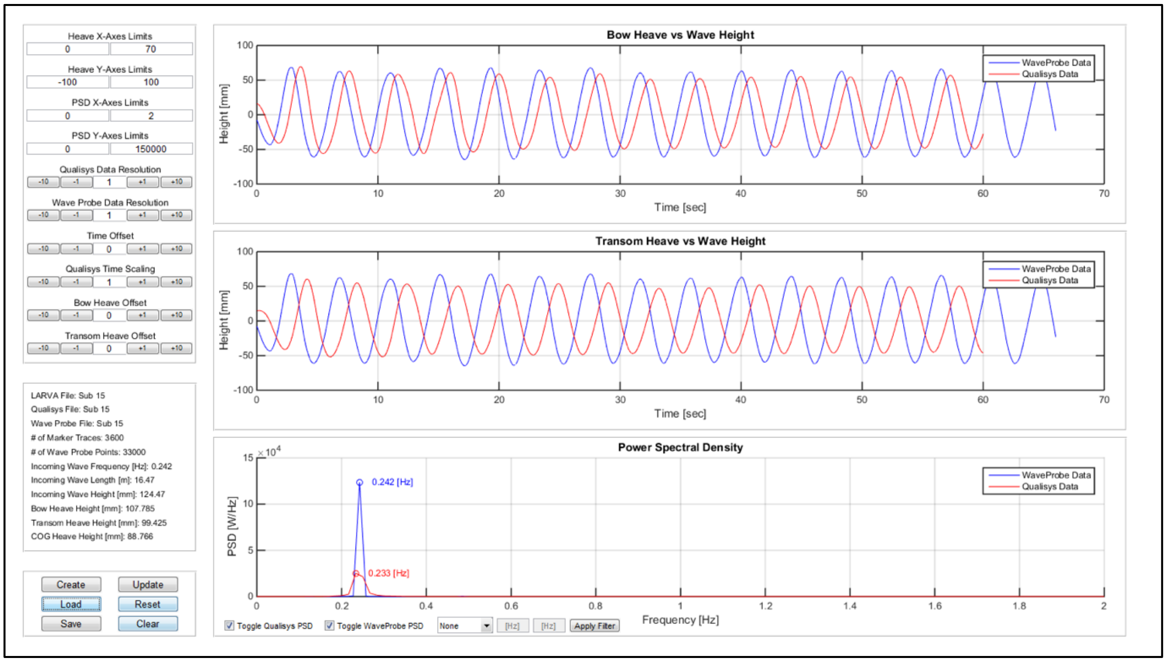

Analysis of LARVA response in the launching state to an incoming wave set with a frequency of 0.24Hz and a height of 125mm.

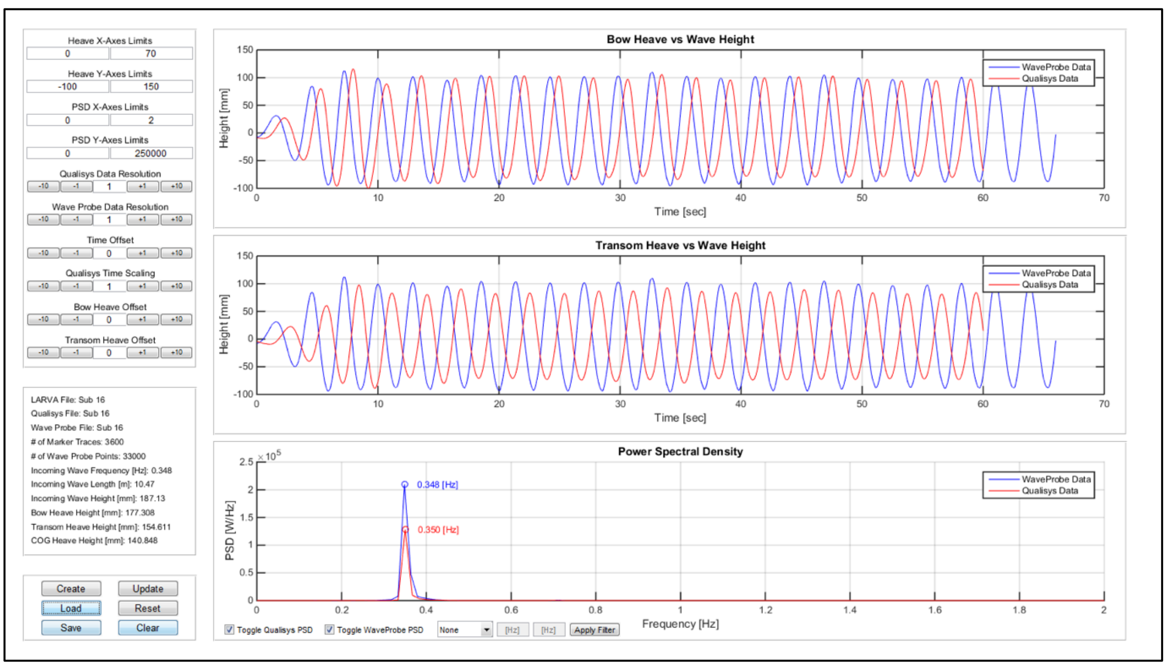

Analysis of LARVA response in the launching state to an incoming wave set with a frequency of 0.35Hz and a height of 187mm.

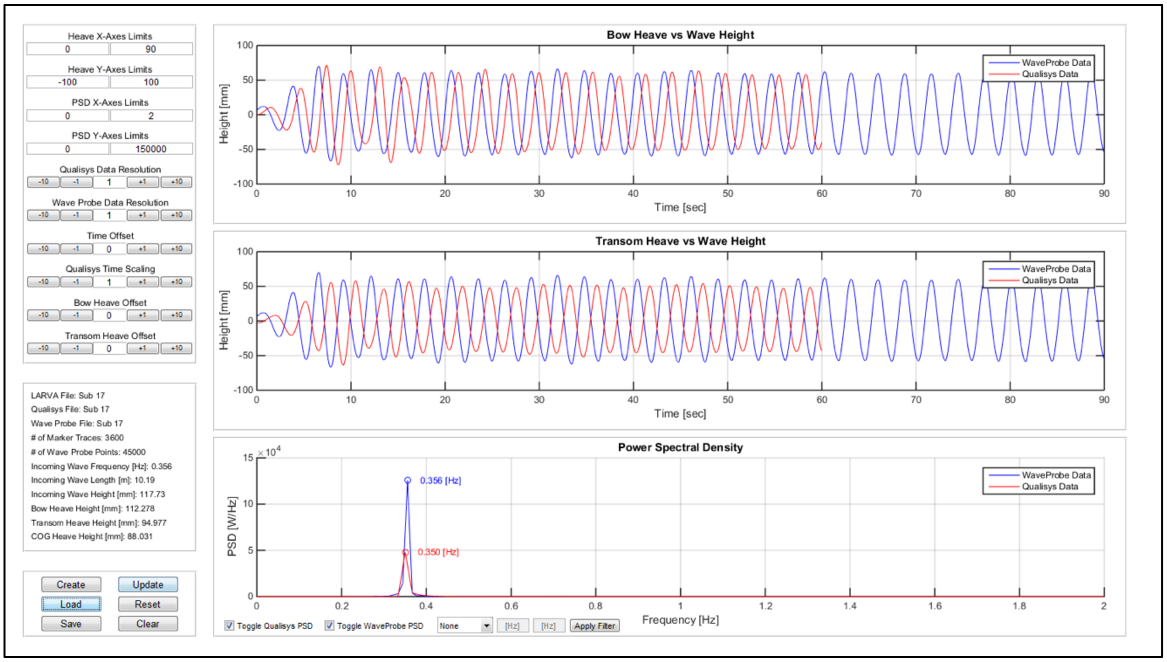

Analysis of LARVA response in the launching state to an incoming wave set with a frequency of 0.36Hz and a height of 118mm.

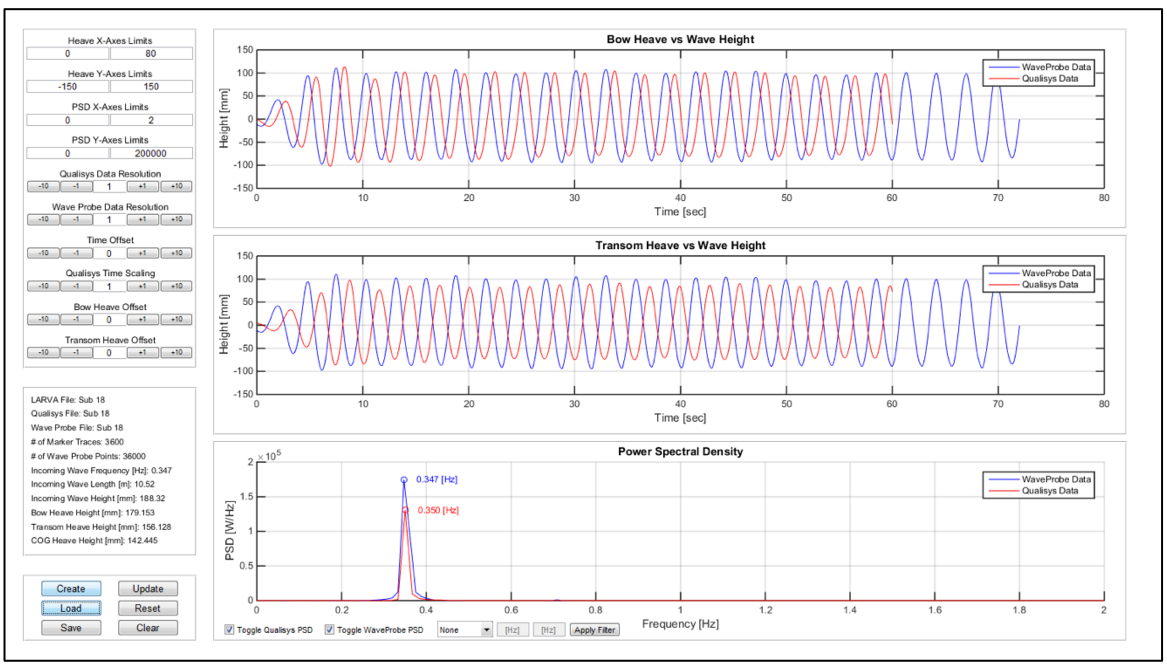

Analysis of LARVA response in the launching state to an incoming wave set with a frequency of 0.35Hz and a height of 118mm.

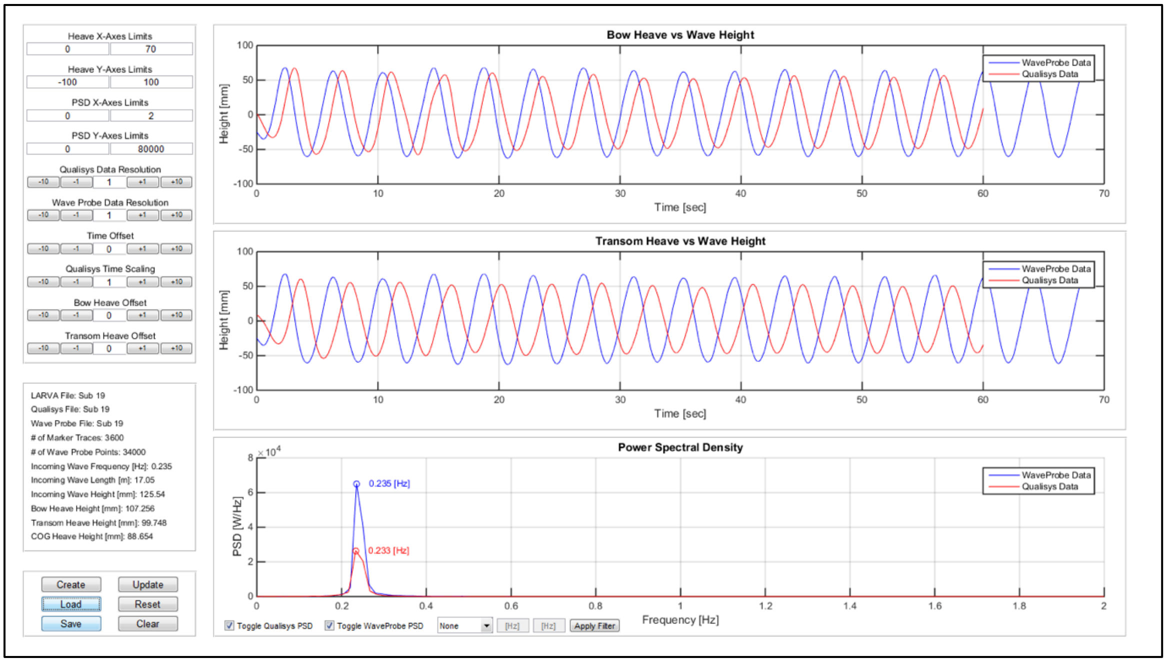

Analysis of LARVA response in the launching state to an incoming wave set with a frequency of 0.24Hz and a height of 126mm.

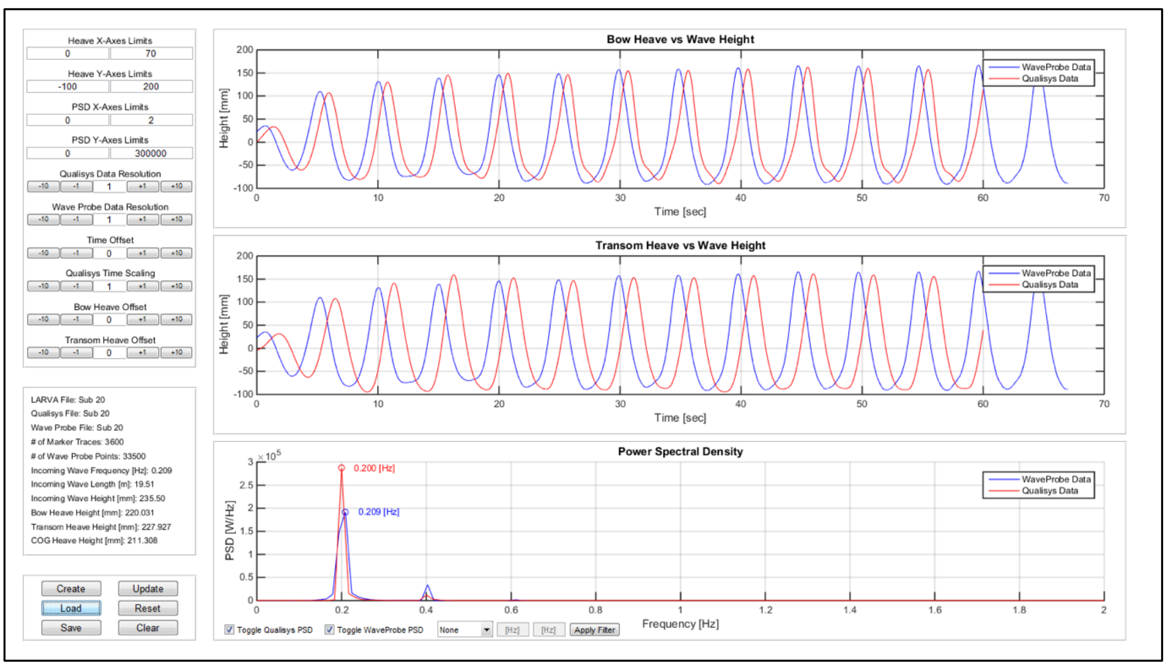

Analysis of LARVA response in the launching state to an incoming wave set with a frequency of 0.21Hz and a height of 236mm.

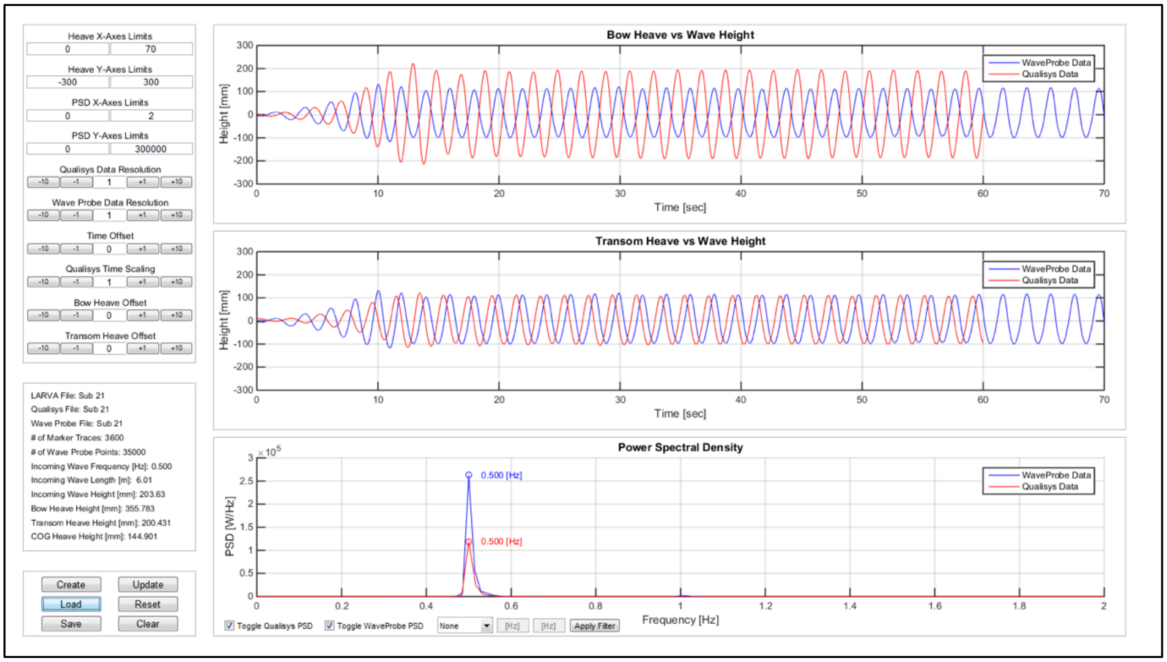

Analysis of LARVA response in the launching state to an incoming wave set with a frequency of 0.50Hz and a height of 204mm.

Appendix D: ANOVA Analysis of Relative Heaving in the Launching State

Bow Relative Heaving

When initially analyzing the data, the normal plot of the residuals (Figure D.1) and the Box-Cox plot (Figure D.2) indicated that the data needed to be transformed. Figure D.3 shows that after applying a log transform to the data, the residuals are more normally distributed and Figure D.4 shows the Box-Cox plot after applying the transform.

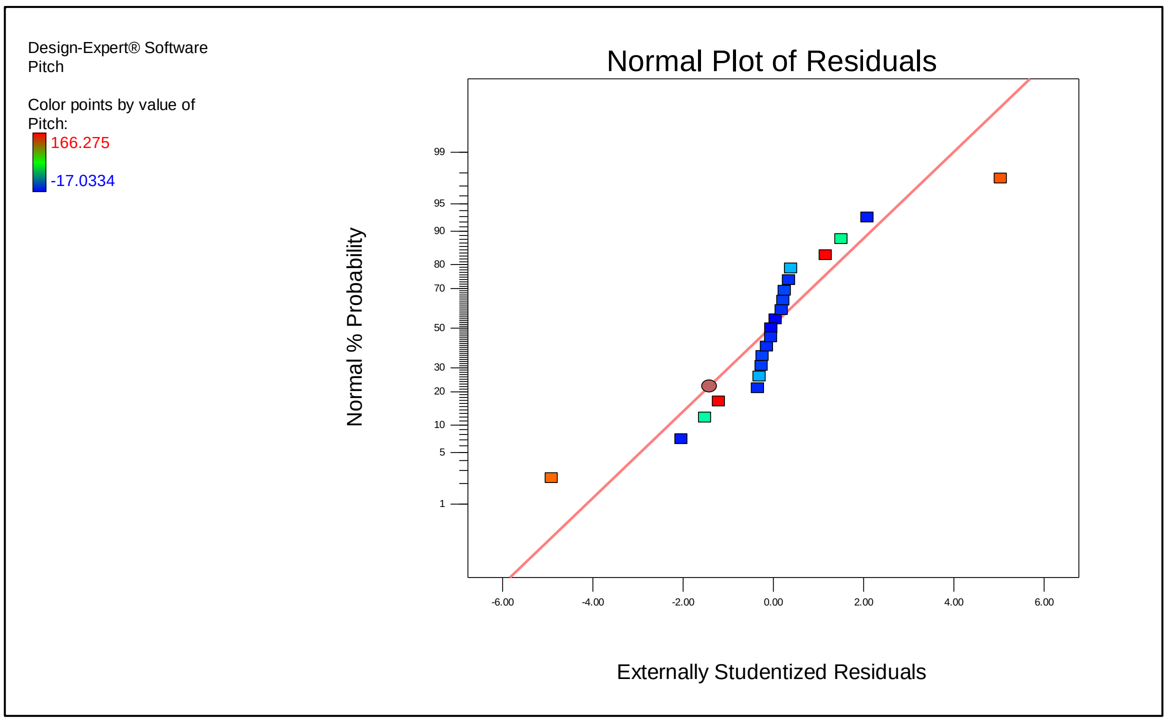

Figure D.1: Normal plot of relative bow heaving residuals showing that a transform of the data is required.

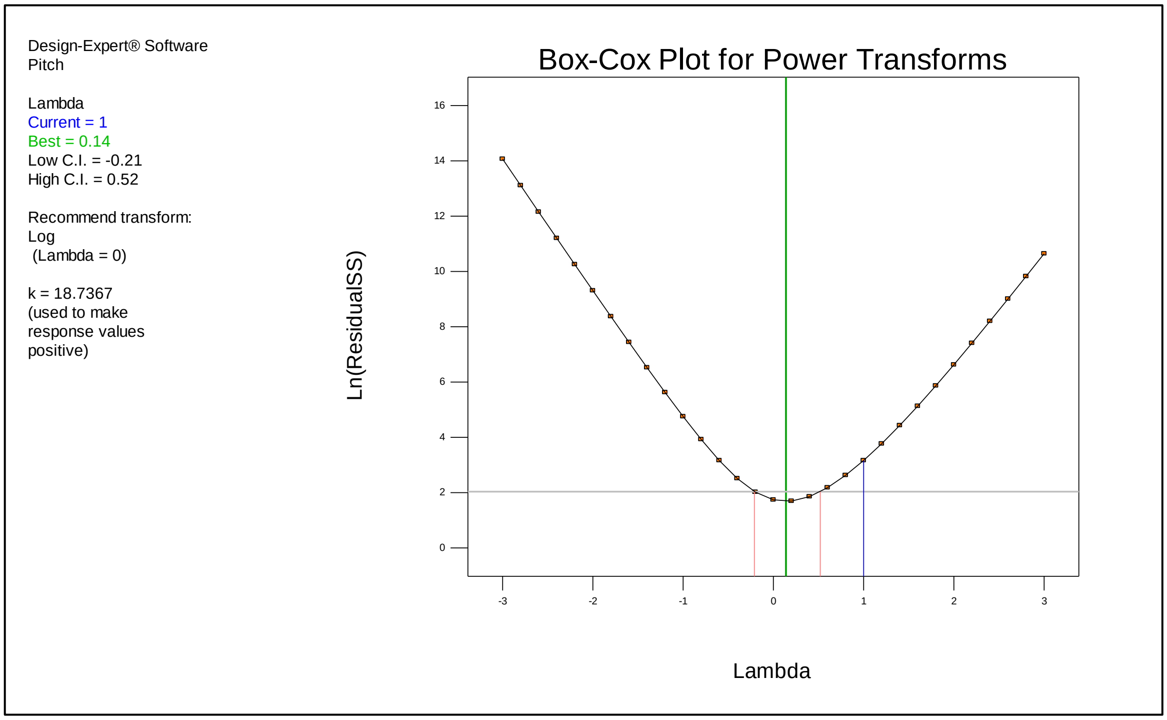

Figure D.2: Box-Cox plot indicating a log transform with a constant of 18.7367 is required.

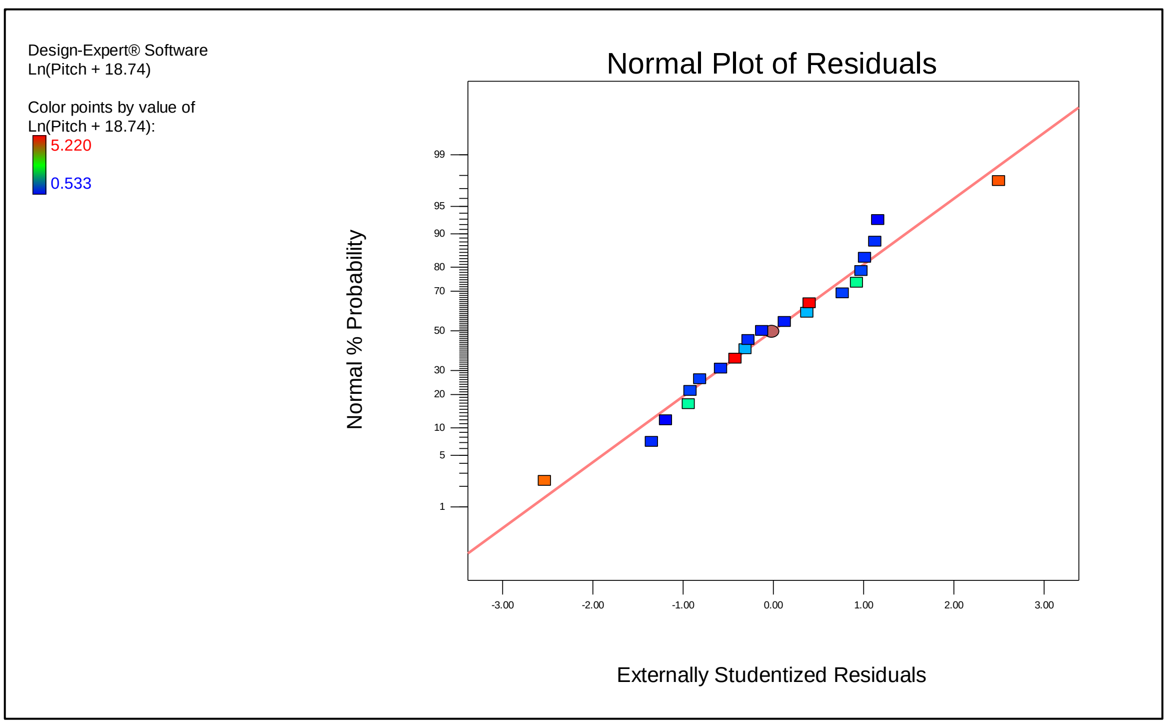

Figure D.3: Normal plot of residuals for relative bow heaving after applying the log transform.

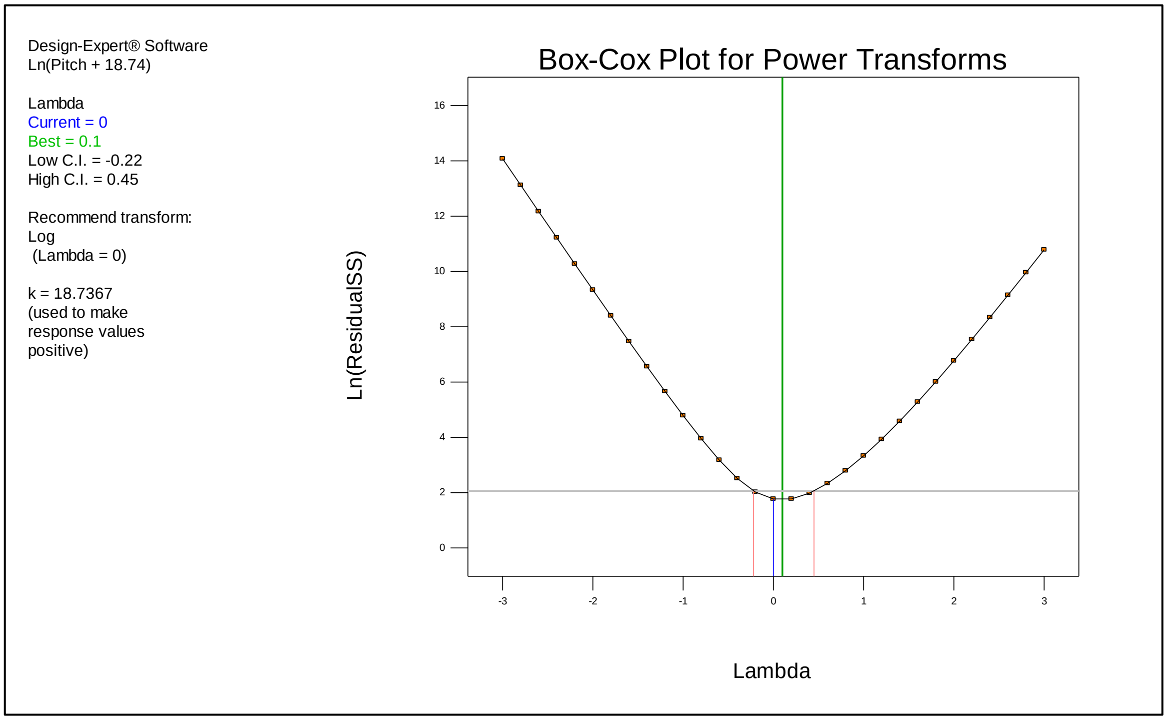

Figure D.4: Box-Cox plot after applying the log transformation.

Table D.1: ANOVA results for the relative bow heaving in the launching state. Natural log transform applied with a constant of K=18.7367.

ANOVA for Response Surface Reduced Cubic model Analysis of variance table [Partial sum of squares - Type III]						
Source	Sum of Squares	df	Mean Square	F Value	p-value Prob > F	
Model	40.30	8	5.04	3967.88	< 0.0001	significant
A-Frequency	*1.00*	*1*	*1.00*	*790.78*	*< 0.0001*	
B-Height	*0.56*	*1*	*0.56*	*444.75*	*< 0.0001*	
AB	*0.065*	*1*	*0.065*	*51.02*	*< 0.0001*	
A^2	*6.54*	*1*	*6.54*	*5147.06*	*< 0.0001*	
B^2	*0.035*	*1*	*0.035*	*27.25*	*0.0002*	
A^2B	*1.44*	*1*	*1.44*	*1133.85*	*< 0.0001*	
AB^2	*1.97*	*1*	*1.97*	*1553.15*	*< 0.0001*	
A^3	*2.22*	*1*	*2.22*	*1745.36*	*< 0.0001*	
Residual	0.015	12	1.270E-003			
Lack of Fit	*0.011*	*10*	*1.074E-003*	*0.48*	*0.8259*	*not significant*
Pure Error	*4.496E-003*	*2*	*2.248E-003*			
Cor Total	40.32	20				

Table D.2: Polynomial fit summary for the relative bow heaving in the launching state.

Std. Dev.	0.036	R-Squared	0.9996
Mean	2.98	Adj R-Squared	0.9994
C.V. %	1.20	Pred R-Squared	0.9988
PRESS	0.050	Adeq Precision	200.294

Table D.1 shows the ANOVA results for the relative heaving in the launching state. It shows that both higher order terms and factor interaction are significant to the model. The "Lack of Fit p-value" of 0.8259 implies that the model lack of fit is not significant relative to the pure error. Table D.2 shows the fit summary of the polynomial to the data. The "Pred R-Squared" value of 0.9988 is in reasonable agreement with the "Adj R-Squared" value of 0.9994. Additionally, the "Adeq Precision" measures the signal to noise ratio, and with a ratio of 200.94, the model can be used to navigate the design space.

Table D.3: Final equations in terms of both coded and actual factors for the relative bow heaving in the launching state.

	Coded Terms	Actual Terms
Response	Ln(Relative Heave + 18.74)	Ln(Relative Heave + 18.74)
Intercept	2.13	-105.36
A	-2.22	696.7
B	-0.25	0.47
AB	-0.12	-1.69
A2	0.85	-1584.42
B2	0.056	-7.79
A2B	0.74	0.95
AB2	1.14	0.002
A3	1.65	1.38E+03

Table D.3 shows the coefficients of the fitted polynomial in terms of both coded and actual factors where *A* represents the frequency factor and *B* represents the wave height factor. The high levels of the factors are coded as +1 and the low levels of the factors are coded as -1. This format is useful for identifying the relative impact of the factors by comparing the factor coefficients. As actual terms, the levels of each factor are scaled to accommodate the units of each factor. In this form, it is easy to predict the relative heave when given the incoming frequency and wave height in Hz and millimeters.

The assumptions made during the ANOVA testing are 1) the residuals are normally distributed, 2) there is constant variance of the residuals, and 3) independency between experimental runs. Figure D.5 shows the normal plot of residuals and indicates the first assumption of normality is valid. Figure D.6 shows the externally studentized residuals versus the predicted value and since there is no discernable pattern, this indicates that the second assumption of constant variance is valid. Finally, Figure D.7 shows the externally studentized residuals vs the run number and since there is no discernable pattern, this indicates that the third assumption of independence is valid.

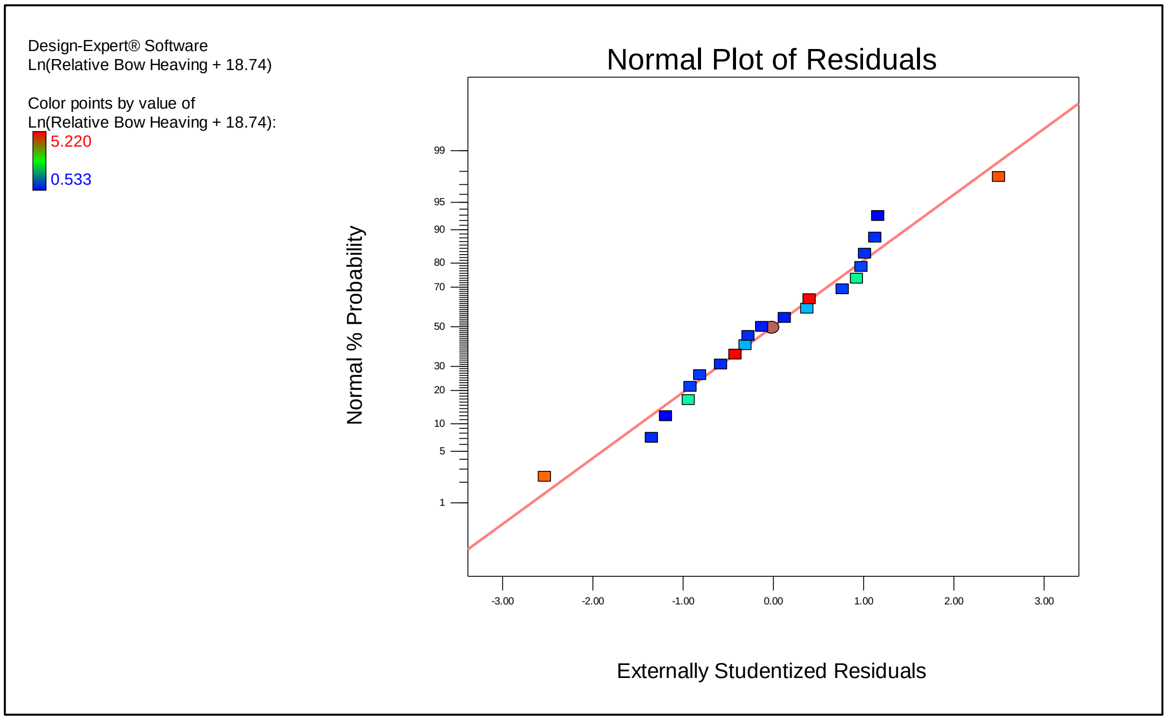

Figure D.5: Normal plot of residuals for the relative bow heaving in the launching state used for testing the first assumption of normality.

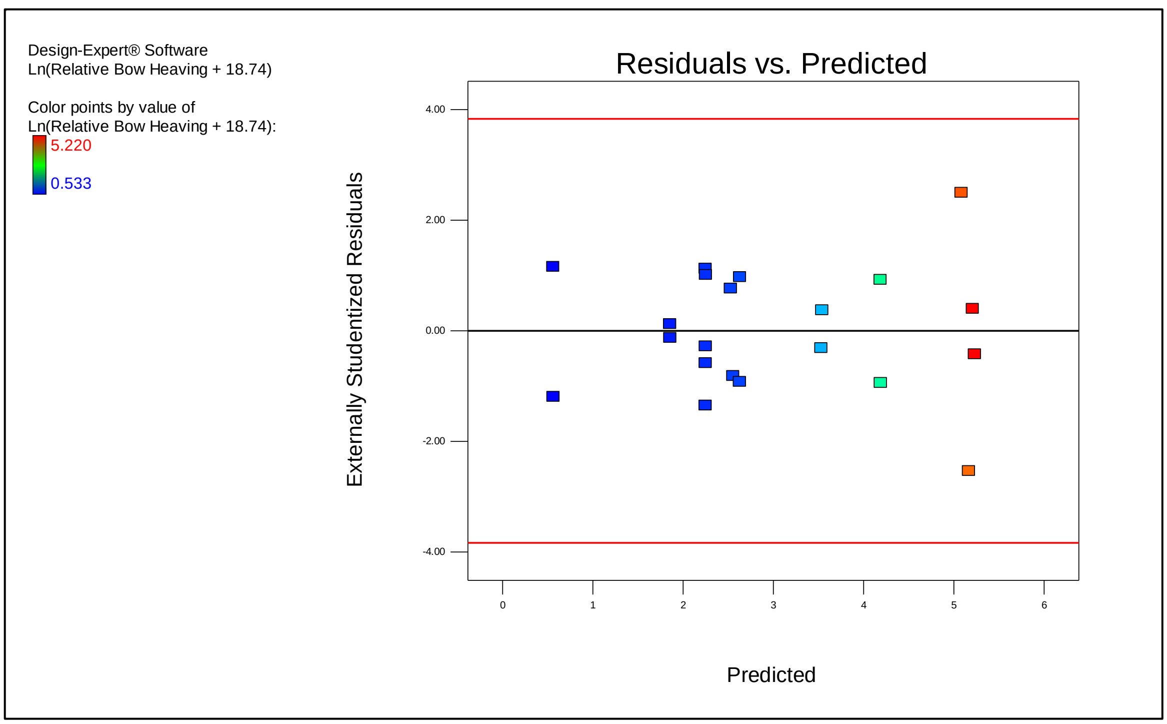

Figure D.6: Residuals vs predicted values for the relative bow heaving in the launching state used for testing the second assumption of constant variance.

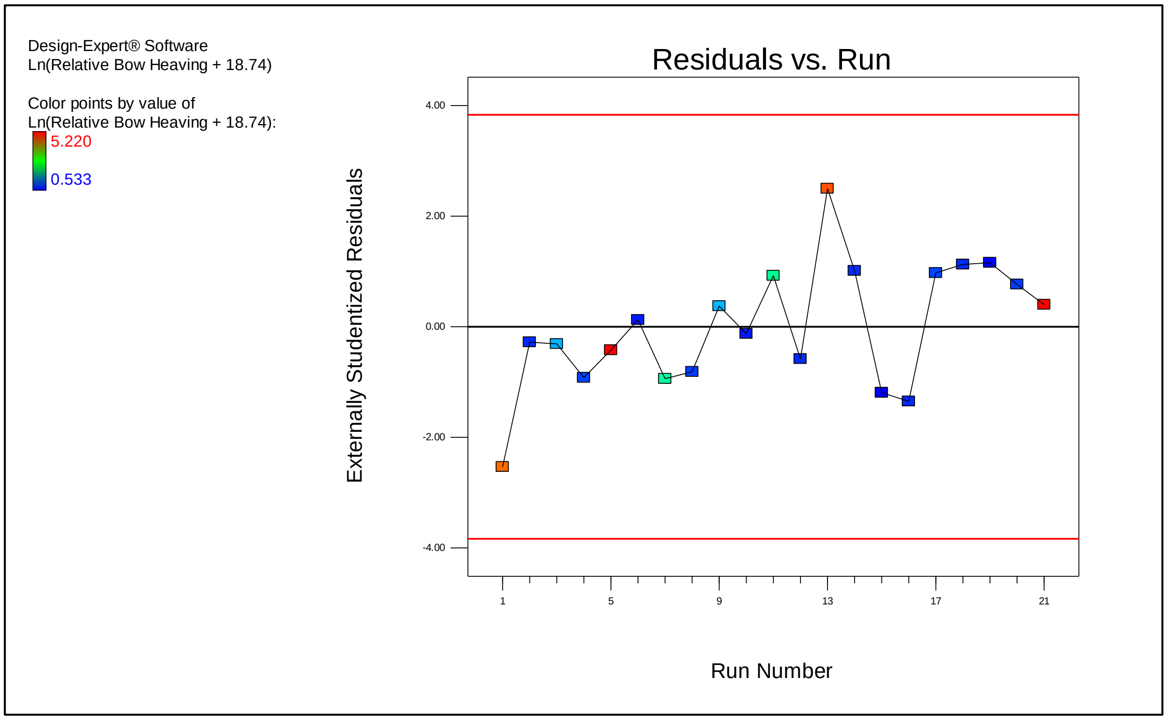

Figure D.7: Residuals vs run number for the relative bow heaving in the launching state used for testing the third assumption of independence.

7.1.1. COG Relative Heaving

Unlike the bow relative heave data, the COG data did not need to be transformed which is evident from the Box-Cox plot (Figure D.8) and normal plot of residuals (Figure D.9). Using the ANOVA technique, a cubic polynomial was fitted to the data (ANOVA results shown in Table D.4). Values of "Prob > F" of less than 0.05 indicate model terms that are statistically significant. In this case, A, B, AB, A^2, B^2, AB^2, A^3, and B^3 are all significant terms where A is the incoming wave frequency and B is the incoming wave height. The "Lack of Fit F-value" of 1.01 implies the Lack of Fit of the model is not significant relative to the pure error.

Additionally, Table D.5 shows the fit summary of the cubic polynomial which indicates that the cubic polynomial is a good fit to the data. The "Pred R-Squared" value of 0.9985 is in reasonable agreement with the "Adj R-Squared" value of 0.9993 (i.e. the difference is less than 0.2). The "Adeq Precision" value represents a measure of the signal to noise ratio in which a value greater than four is desired. In this case, a ratio of 195.228 indicates an adequate signal and thus the model can be used to navigate the design space.

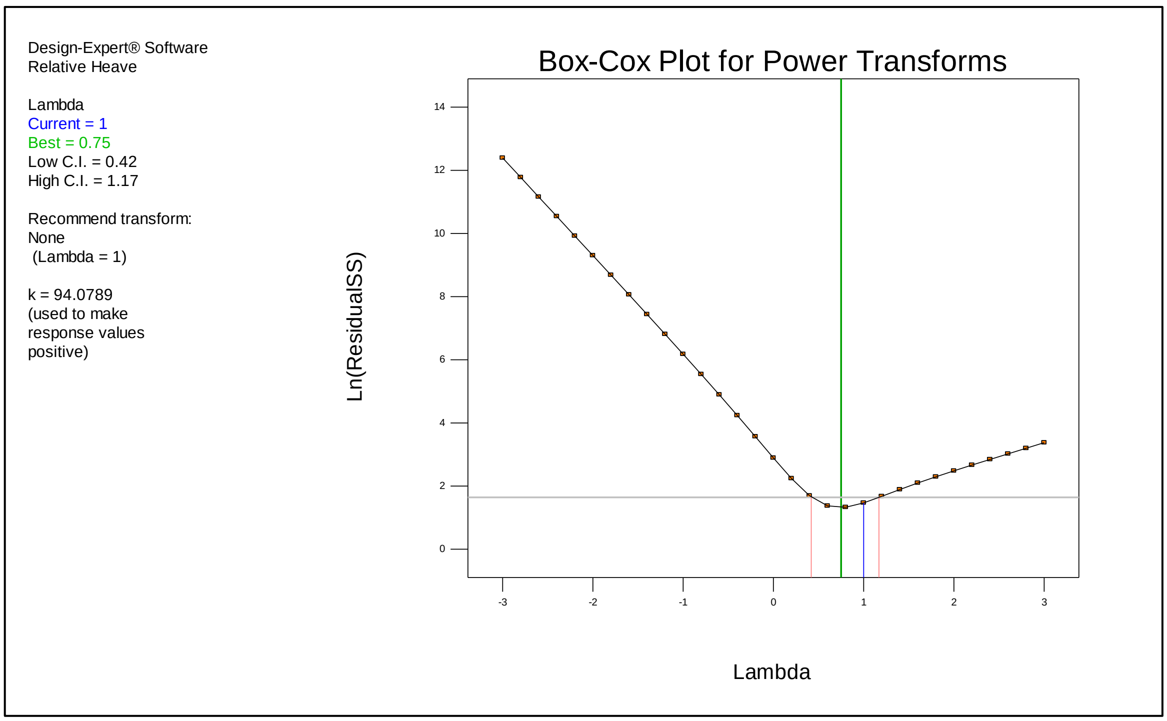

Figure D.8: Box-Cox plot for the COG relative heaving in the launching state indicating a transformation of the data is not required.

Table D.4: ANOVA results for the fitted cubic polynomial for the COG relative heaving in the launching state.

ANOVA for Response Surface Reduced Cubic model Analysis of variance table [Partial sum of squares - Type III]						
Source	Sum of Squares	df	Mean Square	F Value	p-value Prob > F	
Model	10984.92	8	1373.11	3793.38	< 0.0001	significant
A-Frequency	*57.63*	*1*	*57.63*	*159.21*	*< 0.0001*	
B-Height	*30.37*	*1*	*30.37*	*83.91*	*< 0.0001*	
AB	*239.24*	*1*	*239.24*	*660.93*	*< 0.0001*	
A^2	*3.06*	*1*	*3.06*	*8.44*	*0.0132*	
B^2	*108.84*	*1*	*108.84*	*300.69*	*< 0.0001*	
AB^2	*22.23*	*1*	*22.23*	*61.41*	*< 0.0001*	
A^3	*24.05*	*1*	*24.05*	*66.45*	*< 0.0001*	
B^3	*138.92*	*1*	*138.92*	*383.79*	*< 0.0001*	
Residual	4.34	12	0.36			
Lack of Fit	*3.63*	*10*	*0.36*	*1.01*	*0.5938*	*not significant*
Pure Error	*0.72*	*2*	*0.36*			
Cor Total	10989.26	20				

Table D.5: Polynomial fit summary for the relative COG heaving in the launching state.

Std. Dev.	0.60	R-Squared	0.9996
Mean	-43.74	Adj R-Squared	0.9993
C.V. %	1.38	Pred R-Squared	0.9985
PRESS	16.29	Adeq Precision	195.228

Table D.6: Final equations in terms of both coded and actual factors for the COG relative heaving in the launching state.

	Coded Terms	Actual Terms
Response	Relative Heave	Relative Heave
Intercept	-41.58	-344.67
A	-34.45	3822.05
B	12.61	-1.76
AB	-8.97	-7.88
A2	1.02	-9044.75
B2	-2.44	0.016
AB2	7.53	0.015
A3	10.38	8700.04
B3	-10.88	-3.32E-05

Table D.6 shows the coefficients of the fitted polynomial in terms of both coded and actual factors where *A* represents the frequency factor and *B* represents the wave height factor. The high levels of the factors are coded as +1 and the low levels of the factors are coded as -1. This format is useful for identifying the relative impact of the factors by comparing the factor coefficients. As actual terms, the levels of each factor are scaled to accommodate the units of each factor. In this form, it is easy to predict the relative heave when given the incoming frequency and wave height in Hz and millimeters.

The assumptions made during the ANOVA testing are 1) the residuals are normally distributed, 2) there is constant variance of the residuals, and 3) independency between experimental runs. Figure D.9 shows the normal plot of residuals and indicates the first assumption of normality is valid. Figure D.10 shows the externally studentized residuals versus the predicted value and since there is no discernable pattern, this indicates that the second assumption of constant variance is valid. Finally, Figure D.11 shows the externally studentized residuals vs the run number and since there is no discernable pattern, this indicates that the third assumption of independence is valid.

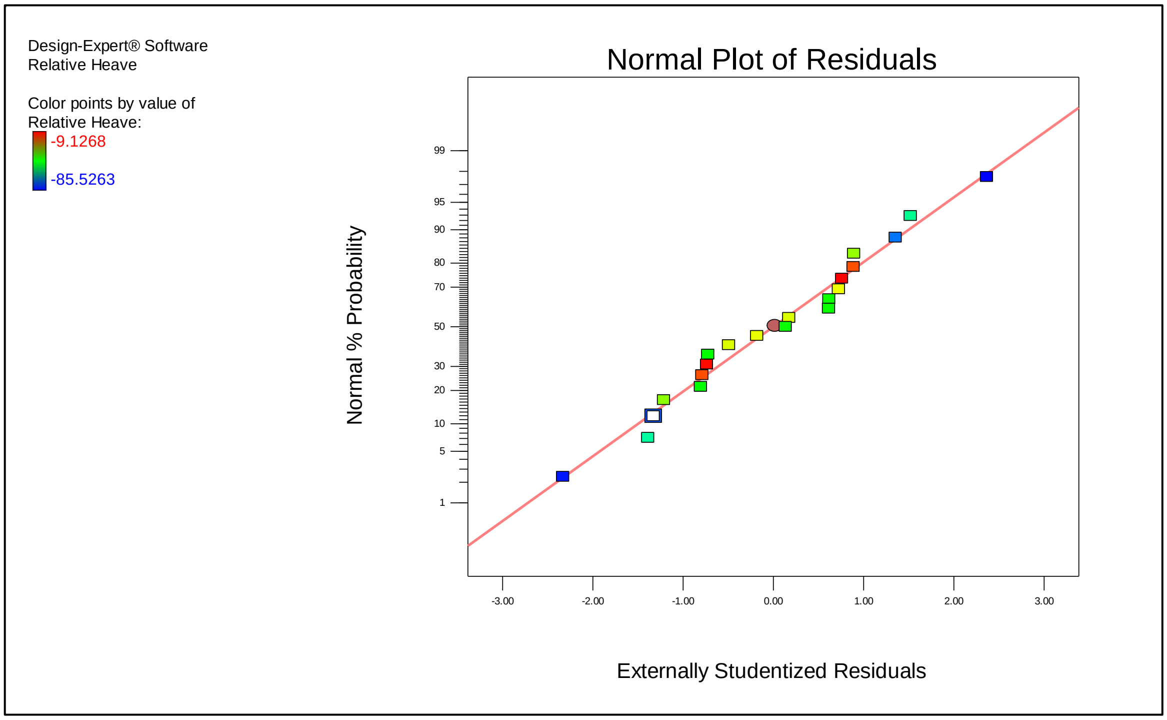

Figure D.9: Normal plot of residuals for the COG relative heaving in the launching state used for testing the first assumption of normality.

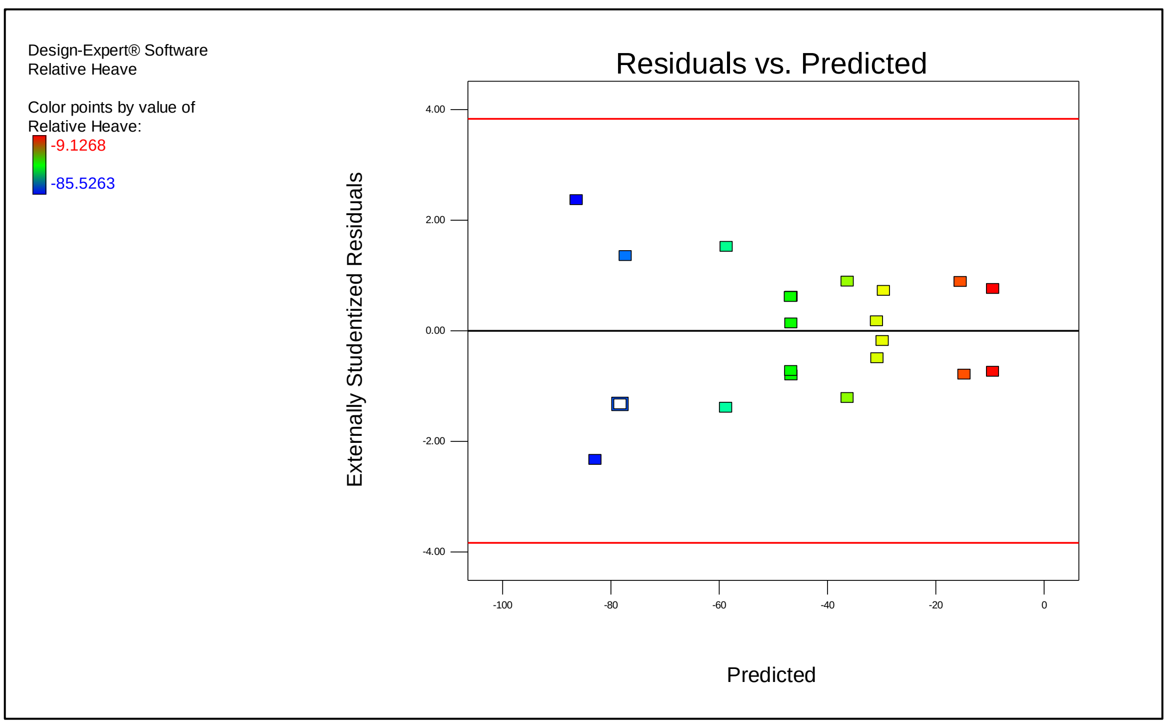

Figure D.10: Residuals vs predicted values for the relative COG heaving in the launching state used for testing the second assumption of constant variance.

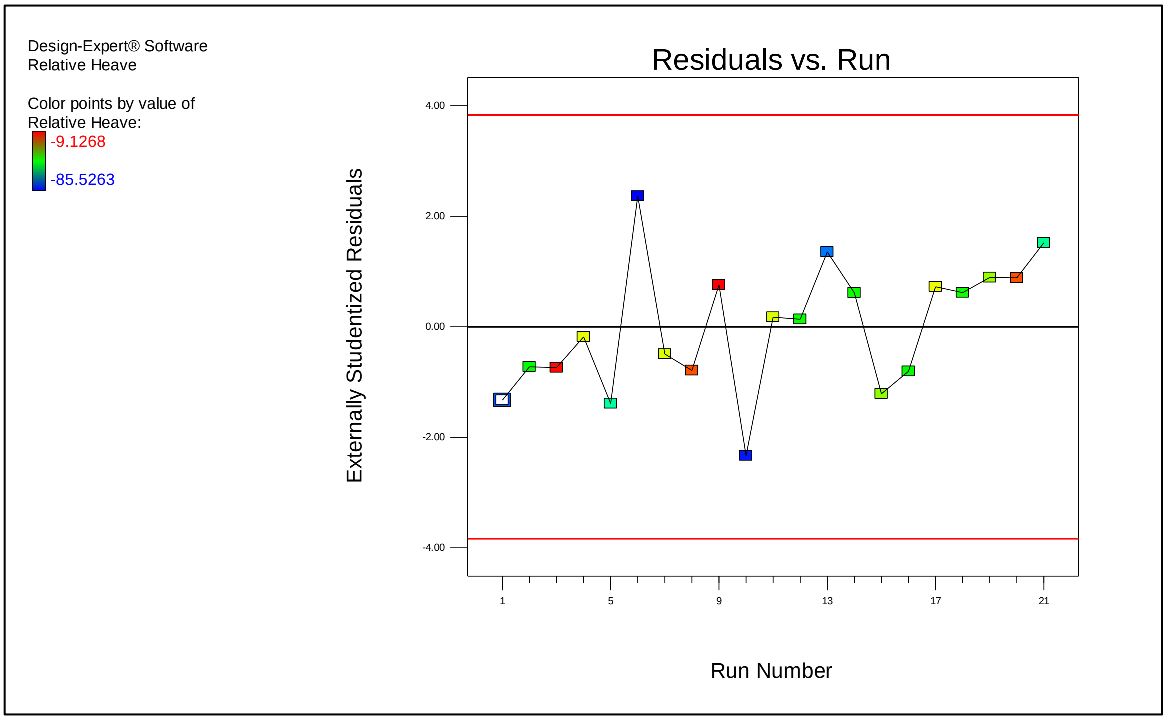

Figure D.11: Residuals vs run number for the relative COG heaving in the launching state used for testing the third assumption of independence.

7.1.2. Transom Relative Heaving

As with the COG relative heave, the transom relative heave did not require a transformation of the data which is evident from the Box-Cox plot in Figure D.12 and the normal plot of residuals in Figure D.13. Using the ANOVA technique, a cubic polynomial was fitted to the data (ANOVA results shown in Table D.7). Values of “Prob > F” of less than 0.05 indicate model terms that are statistically significant. In this case, A, A^2, B^2, AB^2, A^3, and B^3 are all significant terms where A is the incoming wave frequency and B is the incoming wave height. The insignificant terms of B, and AB are kept in the model to maintain hierarchy. Without these terms, the measures of goodness of fit and the predicted response values may be affected by the coding transformation. The “Lack of Fit

F-value" of 0.66 implies the Lack of Fit of the model is not significant relative to the pure error.

Additionally, Table D.8 shows the fit summary of the cubic polynomial which indicates that the cubic polynomial is a good fit to the data. The "Pred R-Squared" value of 0.9958 is in reasonable agreement with the "Adj R-Squared" value of 0.9980 (i.e. the difference is less than 0.2). The "Adeq Precision" value represents a measure of the signal to noise ratio in which a value greater than four is desired. In this case, a ratio of 124.111 indicates an adequate signal and thus the model can be used to navigate the design space

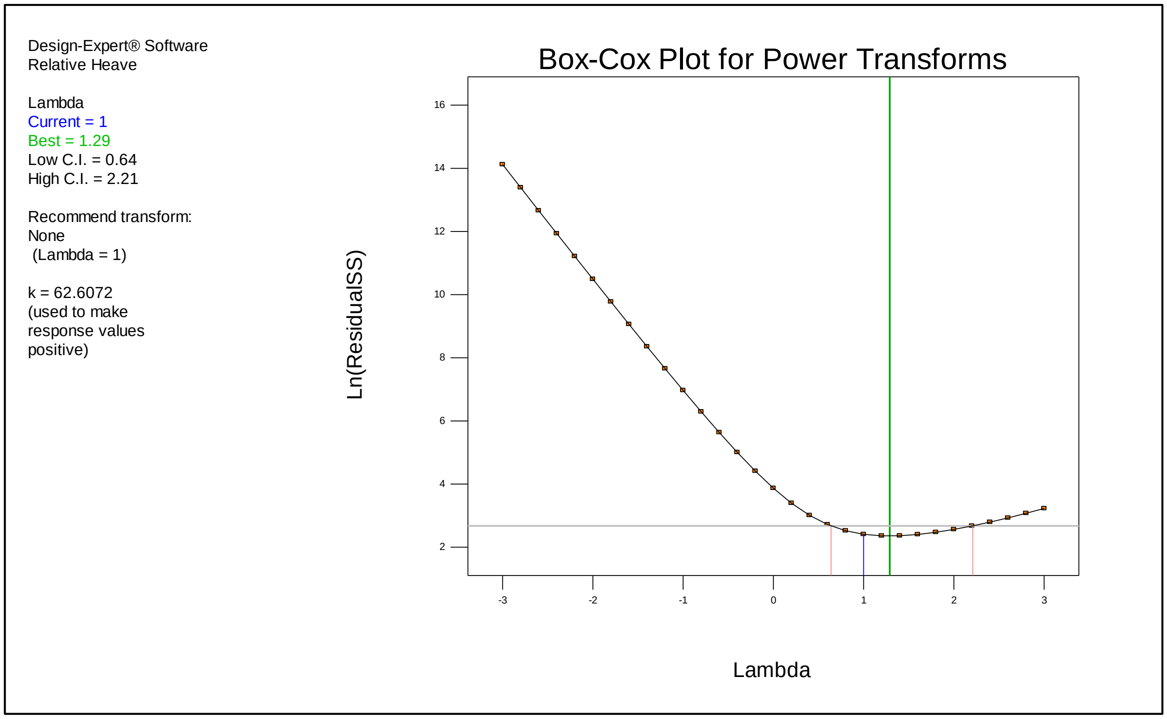

Figure D.12: Box-Cox plot for the transom relative heaving in the launching state indicating a transformation of the data is not required.

Table D.7: ANOVA results for the fitted cubic polynomial for the transom relative heaving in the launching state.

ANOVA for Response Surface Reduced Cubic model Analysis of variance table [Partial sum of squares - Type III]						
Source	**Sum of Squares**	**df**	**Mean Square**	**F Value**	**p-value Prob > F**	
Model	9312.83	8	1164.10	1254.67	< 0.0001	significant
A-Frequency	*320.02*	*1*	*320.02*	*344.92*	*< 0.0001*	
B-Height	*2.26*	*1*	*2.26*	*2.43*	*0.1448*	
AB	*0.92*	*1*	*0.92*	*1.00*	*0.3378*	
A^2	*656.21*	*1*	*656.21*	*707.27*	*< 0.0001*	
B^2	*62.70*	*1*	*62.70*	*67.58*	*< 0.0001*	
AB^2	*344.66*	*1*	*344.66*	*371.47*	*< 0.0001*	
A^3	*347.18*	*1*	*347.18*	*374.19*	*< 0.0001*	
B^3	*28.33*	*1*	*28.33*	*30.53*	*0.0001*	
Residual	11.13	12	0.93			
Lack of Fit	*9.79*	*11*	*0.89*	*0.66*	*0.7553*	*not significant*
Pure Error	*1.34*	*1*	*1.34*			
Cor Total	9323.96	20				

Table D.8: Polynomial fit summary for the relative transom heaving in the launching state.

Std. Dev.	0.96	R-Squared	0.9988
Mean	-16.61	Adj R-Squared	0.9980
C.V. %	5.80	Pred R-Squared	0.9958
PRESS	39.58	Adeq Precision	124.111

Table D.9: Final equations in terms of both coded and actual factors for the transom relative heaving in the launching state.

	Coded Terms	Actual Terms
Response	Relative Heave	Relative Heave
Intercept	-30.40	-1978
A	-86.73	14,149
B	3.67	7.13
AB	-0.51	-26.75
A^2	15.67	-35,684
B^2	-1.93	-0.01

AB^2	30.03	0.06
A^3	42.14	35,312
B^3	-5.31	-1.62E-05

Table D.9 shows the coefficients of the fitted polynomial in terms of both coded and actual factors where *A* represents the frequency factor and *B* represents the wave height factor. The high levels of the factors are coded as +1 and the low levels of the factors are coded as -1. This format is useful for identifying the relative impact of the factors by comparing the factor coefficients. As actual terms, the levels of each factor are scaled to accommodate the units of each factor. In this form, it is easy to predict the relative heave when given the incoming frequency and wave height in Hz and millimeters.

The assumptions made during the ANOVA testing are 1) the residuals are normally distributed, 2) there is constant variance of the residuals, and 3) independency between experimental runs. Figure D.13 shows the normal plot of residuals and indicates the first assumption of normality is valid. Figure D.14 shows the externally studentized residuals versus the predicted value and since there is no discernable pattern, this indicates that the second assumption of constant variance is valid. Finally, Figure D.15 shows the externally studentized residuals vs the run number and since there is no discernable pattern, this indicates that the third assumption of independence is valid.

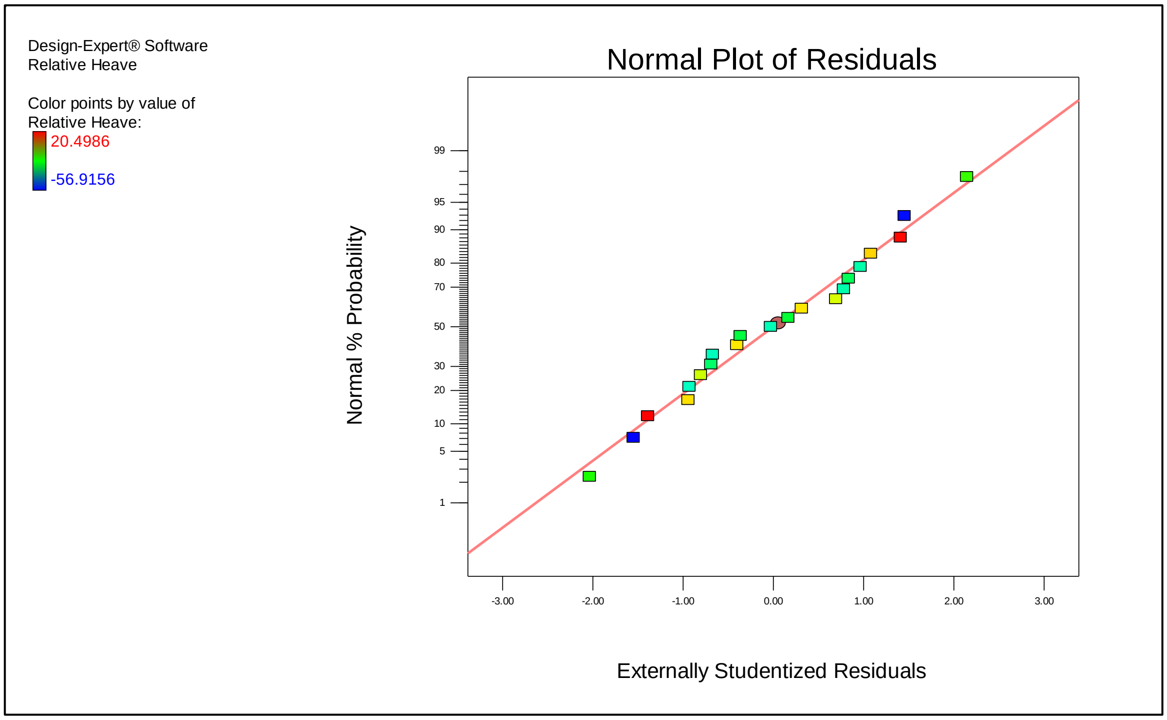

Figure D.13: Normal plot of residuals for the transom relative heaving in the launching state used for testing the first assumption of normality.

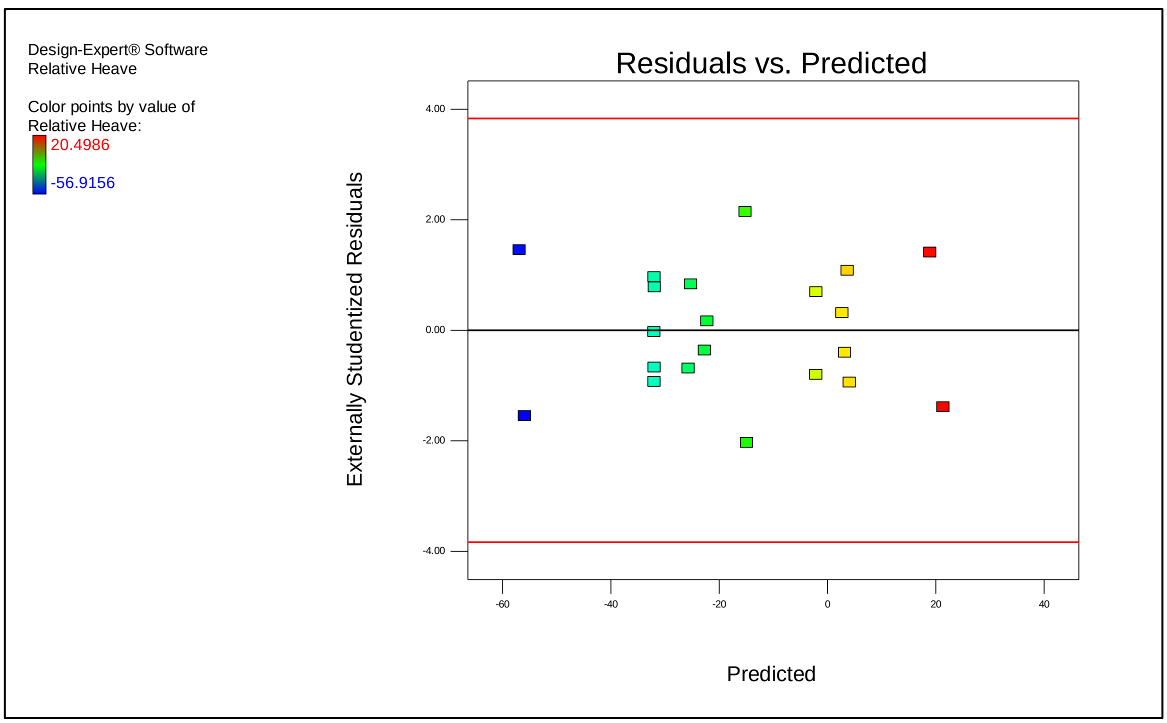

Figure D.14: Residuals vs predicted values for the relative transom heaving in the launching state used for testing the second assumption of constant variance.

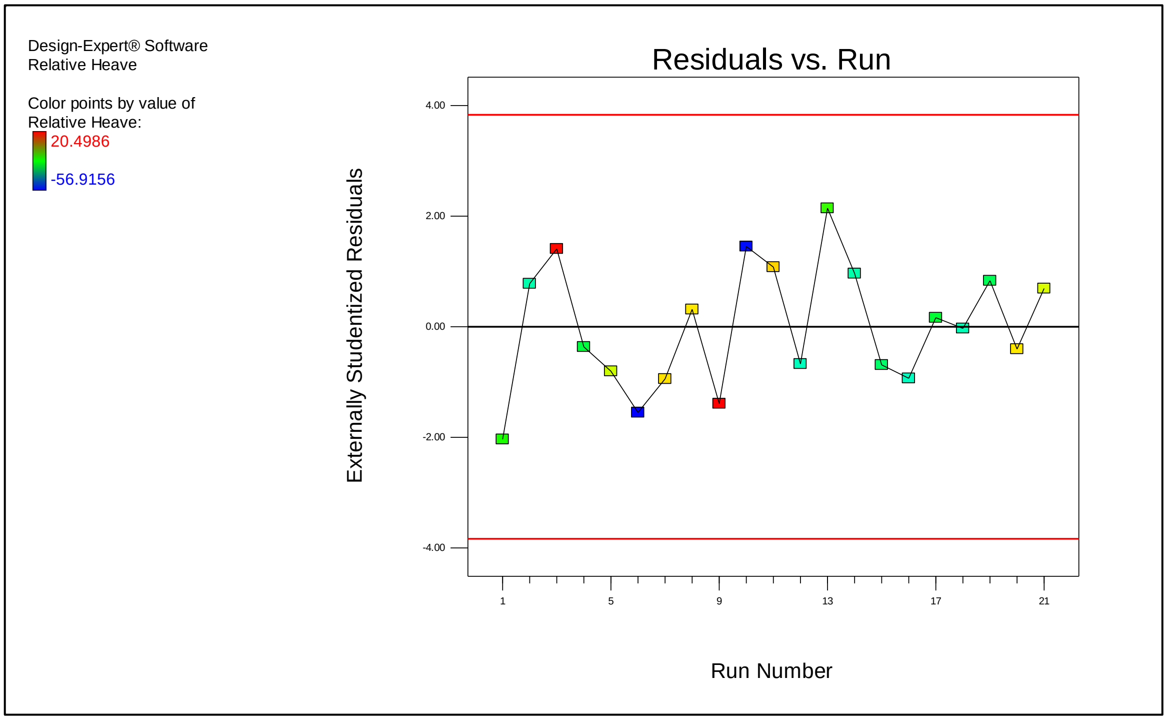

Figure D.15: Residuals vs run number for the relative transom heaving in the launching state used for testing the third assumption of independence.